Polyphase Deformation and Metamorphism in the

Penobscot Bay Area, Coastal Maine

by

John Paul Kaszuba

Thesis submitted to the Faculty of the

Virginia Polytechnic Institute and State University

in partial fulfillment of the requirements for the degree of

Master of Science

in

Department of Geological Sciences

APPROVED:

C. Simpson, Chairman

D. A. Hewitt

L. Glover, III

May 1986

Blacksburg, Virginia

Polyphase Deformation and Metamorphism in the Penobscot Bay Area, Coastal Maine

by

John Paul Kaszuba

C. Simpson, Chairman

Department of Geological Sciences

(ABSTRACT)

Metasediments from portions of two of the six lithologic terranes in the Penobscot Bay area of coastal Maine, the Late Precambrian (?) to Ordovician (?) Copeland Formation and the Rider Bluff member of the Copeland Formation at the eastern margin of the Passagassawakeag (PGW) terrane and the Silurian (?) to Devonian (?) Bucksport Formation of the adjacent Bucksport terrane, shared a common history of four phases of ductile deformation (D_1, D_2 , D_3, and D_4) and interdeformational metamorphism and granitic plutonism. D_1 (early Acadian ?) produced tight to isoclinal folds and an axial plane foliation that deform all three metasedimentary units and contacts between these units. These units and therefore the PGW and Bucksport terranes must have been together by the time of D_1 at the latest. No observed structural or metamorphic gradient coincides with this terrane boundary in the Penobscot Bay area, but in southeast Maine it is mapped as a pre-metamorphic thrust fault. Intrusion of the 412 ± 14 Ma Stricklen Ridge granite and amphibolite facies metamorphism occurred between D_1 and D_2 . D_2 (Acadian) produced open, upright folds and a strong, hinge-parallel mineral elongation lineation under upper greenschist to lower amphibolite conditions. D_3 ductile strike-slip shear zones formed under upper greenschist to lower amphibolite conditions, and D_4 open, steeply-reclined folds formed under greenschist facies conditions. D_3 and D_4 are probably related to the same stress system as the dextral strike-slip Norumbega Fault Zone (Alleghanian) and probably represent a continuum of deformation. Brittle faults exploit D_3 shear zones and may also be related to the same stress system.

ACKNOWLEDGEMENTS

Financial support for this project was provided by a National Science Foundation Graduate Fellowship. Additional support in the form of a part-time assistantship and tuition waivers from the Department of Geological Sciences is gratefully acknowledged. Technical assistance was expertly furnished by Llyn Sharp (photography), Melody Watson and Kathy Hawkins (drafting), and Todd Solberg and Mark Miller (electron microprobe data). Steve Ela, Joe Jurinski, and Terra Dog provided able assistance and companionship in the field. I thank Carol Simpson, my major advisor, for her support, advice, critical review of this manuscript, and the occasional kick-in-the-pants. I also thank David A. Hewitt and Lynn Glover III for advice, helpful discussion, and review of this manuscript. Everyone connected with this department deserves some measure of thanks for the success of this project. They were role models, sources of motivation, professional peers, and friends during my scientific apprenticeship. Among this group, I especially thank structural geologists Rich Gibson, Randy Cumbest, and Alec Gates; petrologists Alex Speer, Roy Chaudet, Diana Solie, and Charlotte Allen; and fellow Maine-iacs John and Karen Hogan and Marc Loiselle for all of their help. I take full responsibility for the interpretations and ideas put forward.

On the personal side, I thank Jeff, Alec, Annette, Margie, and especially Charlotte for their friendship and emotional support. I owe my parents quite a bit too. This project started because of the ideas and energy of the late Dave Wones and has taken many different twists from what we first envisioned. Dave loved geology and Maine, but above all he loved people and brought his personal touch to the science. This thesis is dedicated to him.

TABLE OF CONTENTS

LIST OF ILLUSTRATIONS

LIST OF TABLES

LIST OF PLATES

INTRODUCTION

The geology of the Maine coastal region is composed of six discrete lithologic terranes (Stewart and Wones, 1974) (Fig. 1b). Each terrane contains its own complex history of sedimentation, metamorphism, plutonism, volcanism, and deformation. The boundaries between these terranes (Fig. 1b) have been variously interpreted as strike-slip, normal, thrust, or reverse faults and as unconformities (Stewart and Wones, 1974; Wones, 1976, 1978; Wones and Stewart, 1976; Loiselle and Wones, 1983; Gates and others, 1984; Osberg and others, 1985). Predominantly Lower and Middle Paleozoic movements were interpreted for the faults because they bound Lower and Middle Paleozoic rocks (Stewart and Wones, 1974) and are intruded by various Devonian and younger plutons (Fig. 1b) (Wones, 1974). Carboniferous through Triassic and Jurassic fault reactivations were postulated for the faults because they truncate some Devonian granitic plutons (Fig. 1b) and because Triassic and Jurassic sedimentary basins were interpreted as forming during fault movements (Wones, 1978). Although this framework is generally accepted by New England geologists, specific details are unknown. Intra-terrane correlations are often tenuous, the nature of the terrane boundaries is still uncertain, and specific ages of sediment deposition and metamorphism are largely unknown.

The boundary between the Passagassawakeag (PGW) and Bucksport terranes (Fig. 1b) has been described both as tectonic (Stewart and Wones, 1974; Kaszuba and Wones, 1985; Osberg and others, 1985) and lithologic (Wones, 1976). This paper presents the results of a detailed structural and metamorphic analysis of an area at the eastern boundary between these terranes (Fig. 2) and describes how and when these terranes were assembled. A brief review of the geology of the Penobscot Bay area and a description of the local stratigraphy in the study area are followed by the results of a

Figure 1. Geology of Maine. a. index map of Maine. BH, Bronson Hill Anticlinorium; MS, Merrimack Synclinorium. Outlined area containing diagonal lines is enlarged in b. b. regional geology of coastal Maine (after Osberg and others, 1985; Stewart and others, 1986). Ages of units comprising lithologic terranes shown in Table 1. C, Canada; FT, Fredericton Trough; NFZ, Norumbega Fault Zone; TFZ, Turtle Head Fault Zone; L, Lucerne pluton; W, Mount Waldo pluton; PB, Penobscot Bay; SB, Sheepscot Bay area. Area outlined is enlarged in Figure 2.

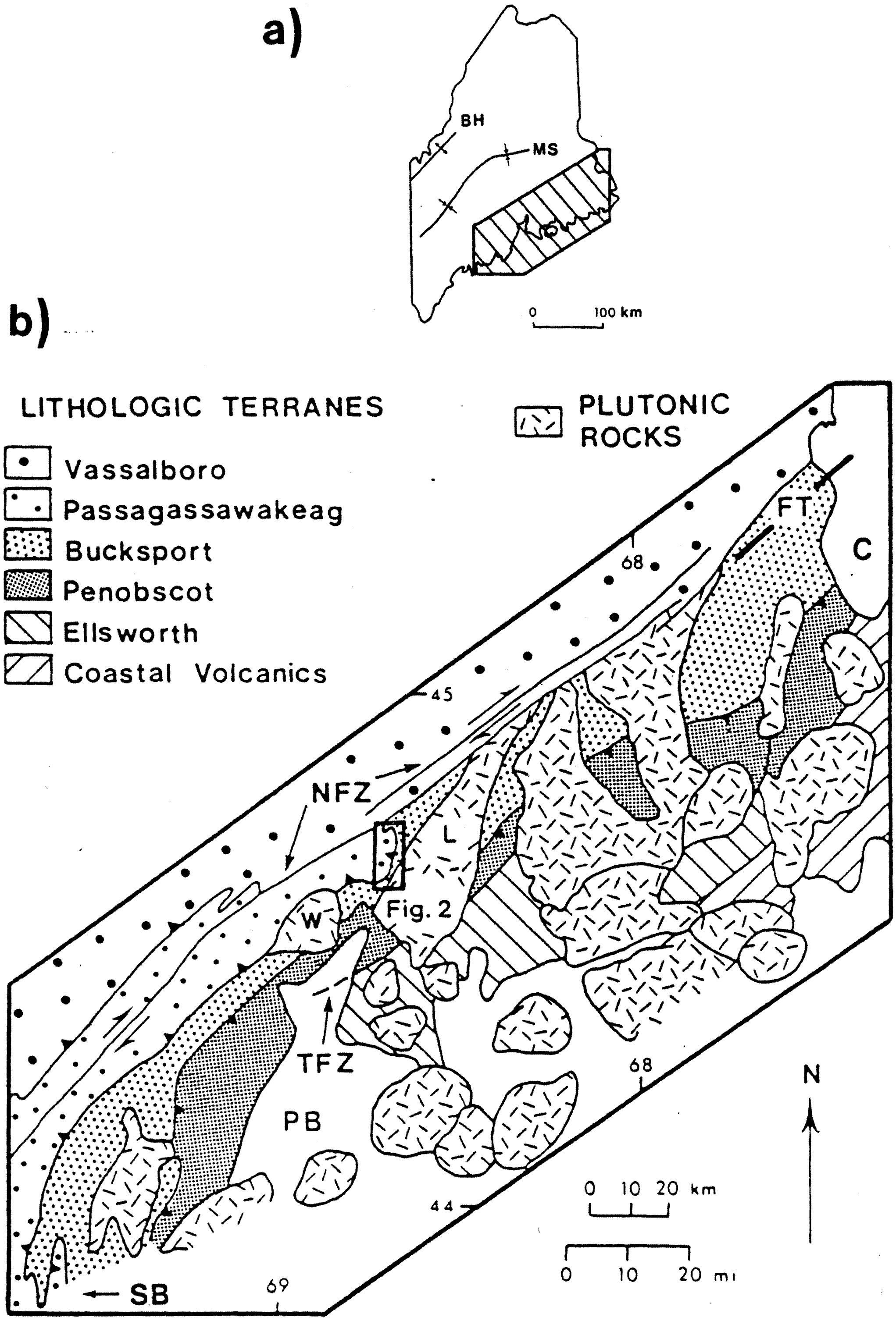
a)
BH
MS
0
100 km
b)
LITHOLOGIC TERRANES
Vassalboro
Passagassawakeag
Bucksport
Penobscot
Ellsworth
Coastal Volcanics
PLUTONIC ROCKS
FT
C
68
45
NFZ
L
W
Fig. 2
TFZ
PB
68
44
69
SB
N
0 10 20 km
0 10 20 mi

Figure 2. Simplified geologic map of study area. See Figure 1 for location. $F_{1,2,4}$, attitude of axial surfaces of minor folds with bearing and plunge of associated fold hinges for deformational events 1, 2, and 4. S_0, attitude of bedding. S_1, attitude of foliation. S_3, attitude of mylonitic foliation. $L_{2,4}$, attitude of mineral elongation lineation, crenulation axis. Cross section highly schematic, vertical dimension not to scale. Θ = movement away, $\cdot$ = movement toward viewer. Ages of units shown in Table 1. Data for Lucerne pluton from Wones (1980).

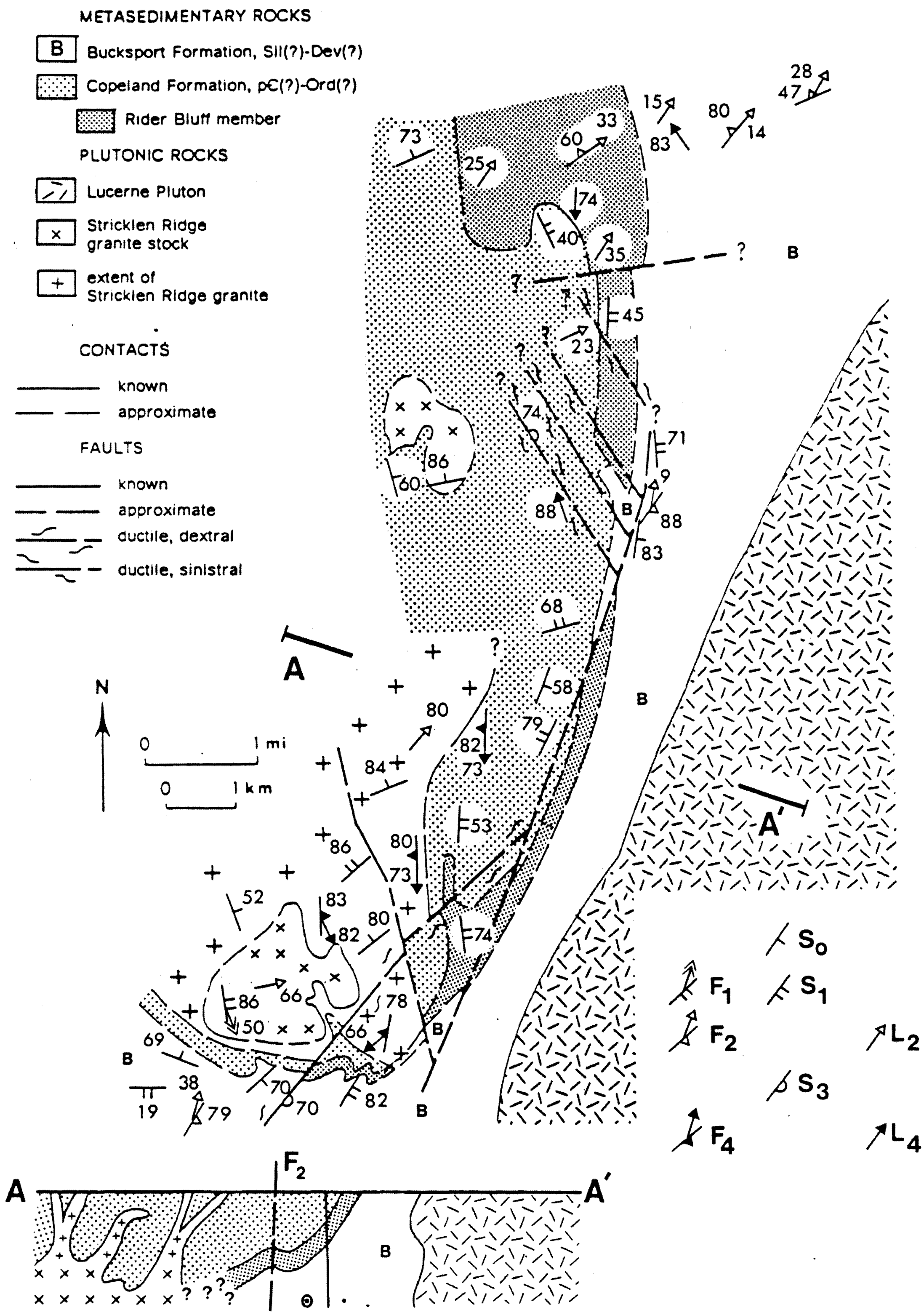
METASEDIMENTARY ROCKS
B Bucksport Formation, Sil(?)-Dev(?)
Copeland Formation, p€(?)-Ord(?)
Rider Bluff member
PLUTONIC ROCKS
Lucerne Pluton
Stricklen Ridge granite stock
extent of Stricklen Ridge granite
CONTACTS
known
approximate
FAULTS
known
approximate
ductile, dextral
ductile, sinistral
N
0 1 mi
0 1 km
A
A'
F2
S0
F1
S1
F2
L2
S3
F4
L4

structural and metamorphic analysis. The implications of these data on the nature of this terrane boundary and for the structural, metamorphic, and tectonic evolution of the study area and the coastal Maine region as a whole are then discussed.

GEOLOGY OF PENOBSCOT BAY AREA

Crystalline basement rocks of northwestern Maine and eastern Quebec, located to the north and west of the Bronson Hill Anticlinorium (Fig. 1a), have been interpreted as continental material analogous to the basement rocks of Vermont, western New Hampshire, Massachusetts, and Connecticut (Osberg, 1978). The northwestern Maine basement rocks may represent part of the North American craton or a small crustal fragment which was welded onto the North American craton during the Ordovician (Taconic Orogeny) (Osberg, 1978). To the southeast of the basement tract lies the Merrimack synclinorium (Fig. 1a) which contains large thicknesses of metavolcanic and clastic metasedimentary rocks (Osberg and others, 1968; Moench and Zartman, 1976) thought to be part of Cambrian to Ordovician volcanic arc, Silurian shelf, and Silurian and Devonian turbidite sequences (Osberg, 1978).

The Penobscot Bay area of coastal Maine contains several different tectonic terranes (Stewart and Wones, 1974; Zen, 1983; Gates and others, 1984; Osberg and others, 1985) (Fig. 1b). 'Terrane' as used in this paper is defined by Coney and others (1980) as a rock package characterized by internal homogeneity and continuity of stratigraphy, tectonic style, and history. Boundaries between terranes are discontinuities not explained by facies changes or unconformities.

Vassalboro Terrane

The Silurian Vassalboro Formation (Perkins and Smith, 1925; Osberg, 1968, 1979; Pankiwskyj and others, 1976) constitutes the Vassalboro terrane in the Penobscot Bay area (Fig. 1b) and has been correlated with the metasediments of the Merrimack synclinorium (Stewart and Wones, 1974). The Vassalboro Formation is a slightly calcareous wacke which contains thin, interbedded quartz-mica sulfide-bearing phyllite/schist (Osberg, 1968; Stewart and Wones, 1974). A single graptolite locality within the Vassalboro Formation suggests a Llandoverian to Ludlovian age (Pankiwskyj and others, 1976) (Table 1). The Vassalboro Formation was interpreted as part of a turbidite sequence (Osberg, 1968, 1979) now metamorphosed to greenschist facies (Stewart and Wones, 1974).

Passagassawakeag Terrane

Southeast of the Vassalboro terrane lie the complexly folded and metamorphosed rocks of the Passagassawakeag (PGW) terrane (Fig. 1b). In the Penobscot Bay area, this terrane is composed of the PGW Formation, the Mixer Pond Member of the PGW Formation, the Copeland Formation, the Rider Bluff member of the Copeland Formation, and the Stricklen Ridge granite, but only the latter three units crop out in the study area (Fig. 2). The PGW Formation (Bickel, 1976) is a quartz-feldspar-biotite gneiss that is recognized for ~ 50 km from near the northeastern margin of the PGW terrane to west of the Mount Waldo pluton (Fig. 1b) (Stewart and Wones, 1974; Bickel, 1976). It contains sillimanite-bearing metamorphic assemblages and is intercalated with layers and boudins of biotite schist (Stewart and Wones, 1974; Bickel, 1976; Guidotti, 1985). Numerous granitic and pegmatitic dikes and sills intrude these gneisses. The age of the gneisses is poorly constrained but is thought to be Precambrian (Table 1) based

Table 1. Ages and correlation of units in terranes of coastal Maine. References are for age determinations, not lithologic descriptions. 1. Hussey, 1968. 2. Brookins and Hussey, 1978. 3. Brookins, 1976. 4. Bickel, 1976. 5. Stewart and Wones, 1974. 6. Zartman and Gallego, 1979. 7. Wones, 1974, 1976. 8. Pankiwskyj and others, 1976. 9. Boucot and others, 1972. 10. Wingard, 1958. 11. Osberg and others, 1985. 12. Ruitenberg, 1967. 13. Ruitenberg and Ludman, 1978. Bickel (1976) described the Passagassawakeag terrane west of the Mount Waldo pluton, Stewart and Wones (1974) described it north and east of the pluton (Fig. 1b).

STRUCTURAL BLOCK / PERIOD	SHEEPSCOT BAY AREA	PASSAGASSAWAKEAG TERRANE [4]	PASSAGASSAWAKEAG TERRANE [5]	VASSALBORO TERRANE	BUCKSPORT TERRANE	PENOBSCOT TERRANE	ELLSWORTH TERRANE	FREDERICTON TROUGH AREA
DEVONIAN							Castine Volcanics [10]	
SILURIAN			Stricklen Ridge granites [6]	Vassalboro Fm. [8]	Bucksport Fm. [7]			Flume Ridge Fm. [12,13]
ORDOVICIAN		Appleton Ridge Fm. [3] =(?) Hogback Schist [4]				Penobscot Fm. [3,9]		Cookson Fm. [12,13]
CAMBRIAN	Casco Bay Group [1,2]		Copeland Fm. [7]				Ellsworth Fm. [3,11]	
PRECAMBRIAN	?—?	?—? Passagassawakeag Fm. [5]	?—? ?—? Passagassawakeag Fm. [5]					

on: 1, intrusion by pegmatites related to the Silurian to Devonian Stricklen Ridge granites; and 2, lithologic similarity to other Precambrian rocks in New England (Stewart and Wones, 1974). Bickel (1976) interpreted the gneisses as metamorphosed feldspathic sedimentary and volcanic rocks on the basis of lithology.

The Mixer Pond member of the PGW Formation (Bickel, 1976) is a light-colored, feldspathic quartz-oligoclase-microcline gneiss interlayed with the PGW Formation. It also crops out within fault-bound slices within the Norumbega Fault Zone (NFZ). The Mixer Pond member is indistinctly layered on a scale of a few meters, and has been interpreted on the basis of lithology as a feldspathic metavolcanic unit (Bickel, 1976). It has been assigned a 468 ± 36 Ma metamorphic age from Rb/Sr whole-rock data (Gaudette, 1986, personal communication).

The Copeland Formation (Trefethen, 1950; Wing, 1957) (Fig. 2) is composed of interlayered, bluish-gray pelitic schist and quartzite (Fig. 3a). It crops out in the study area (Fig. 2) near the eastern margin of the PGW terrane and extends ~10 km to the southwest within fault-bound slices of the NFZ. Compositional grading of layers in this unit from quartzite to pelite on individual outcrops (Fig. 3a), and from west to east across the study area, is interpreted to represent bedding (plotted in Fig. 4). The Copeland Formation has been correlated on the basis of similar lithologies (Wones, 1976; Loiselle and Wones, 1983) with the Hogback Schist (Perkins and Smith, 1925; Bickel, 1976) and the Ordovician Appleton Ridge Formation (Bickel, 1976; Brookins, 1976) (both located 10-20 km west of the Mount Waldo pluton, Fig. 1b), and the Late Precambrian to Ordovician Cape Elizabeth Formation of the Sheepscot Bay area (Hussey, 1968, 1985; Brookins and Hussey, 1978) (Fig. 1b; Table 1). The contact between the Copeland and PGW Formations is not exposed in the study area. It is not known whether this contact is lithologic or tectonic, and the relative structural position between the two units is also unknown.

Figure 3. Field relationships in study area. a. compositional grading of S_0 from quartzite (Q) to pelite (P) in a horizontal pavement of Copeland Formation. Swiss Army knife 8.5 cm long. b. view to northeast of subvertical outcrop face of Bucksport Formation. F_1 fold deforms S_0. S_1 is axial planar to F_1. Quartz-filled fractures crosscut S_0, S_1, and F_1. Coin 2.4 cm diameter. c. horizontal pavement in Copeland Formation. F_1 fold deforms S_0 and is cut by pegmatite of Stricklen Ridge granite (G). Coin 2.4 cm diameter. d. horizontal pavement of Copeland Formation. F_1 isocline (arrowhead), S_1 axial plane foliation, and S_0 (Q, quartzite; P, pelite) deformed by open F_4 fold. Hammer 32 cm long.

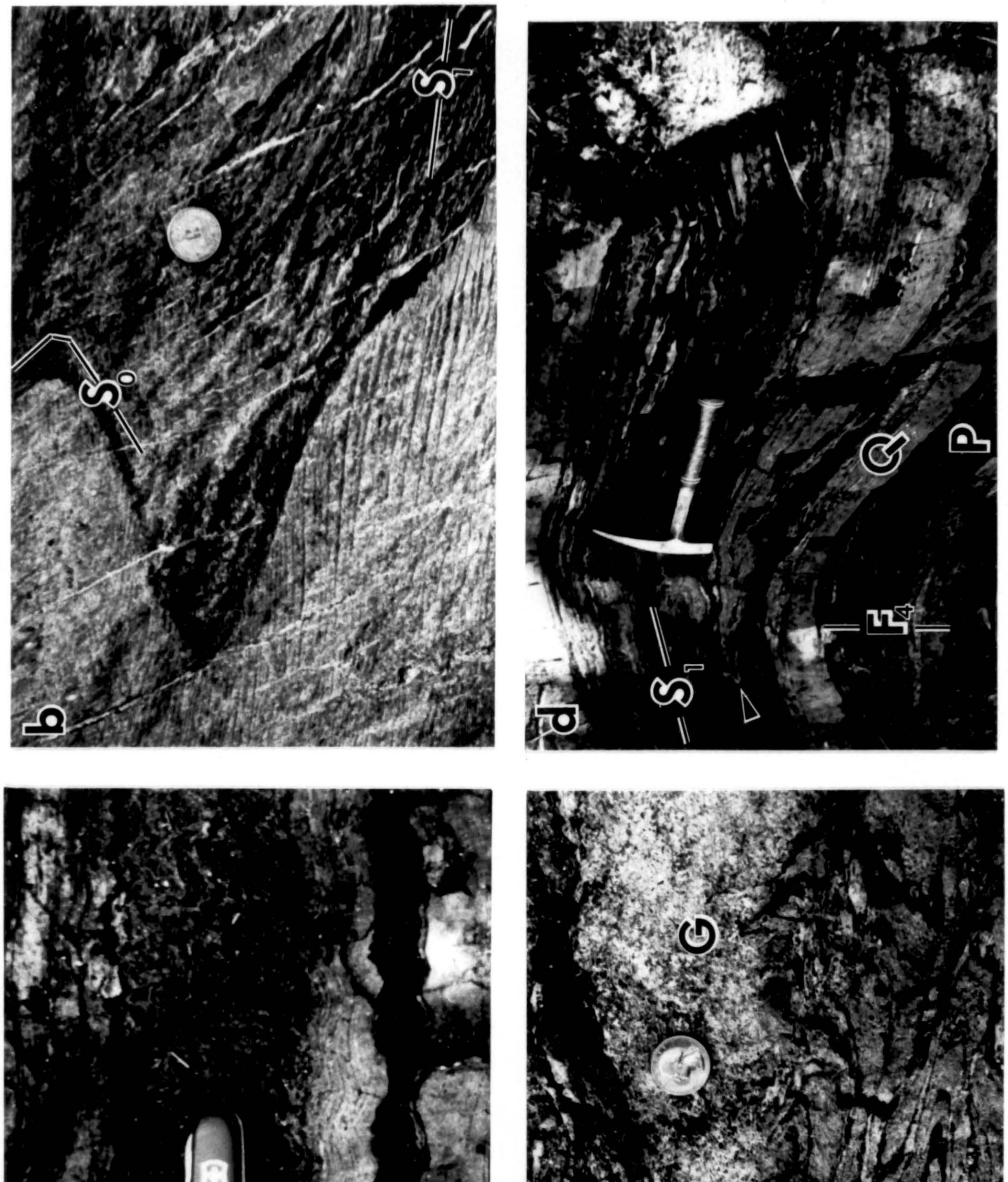
a
P
G
b
S0
S1
c
G
S0
d
S1
G
P
F4

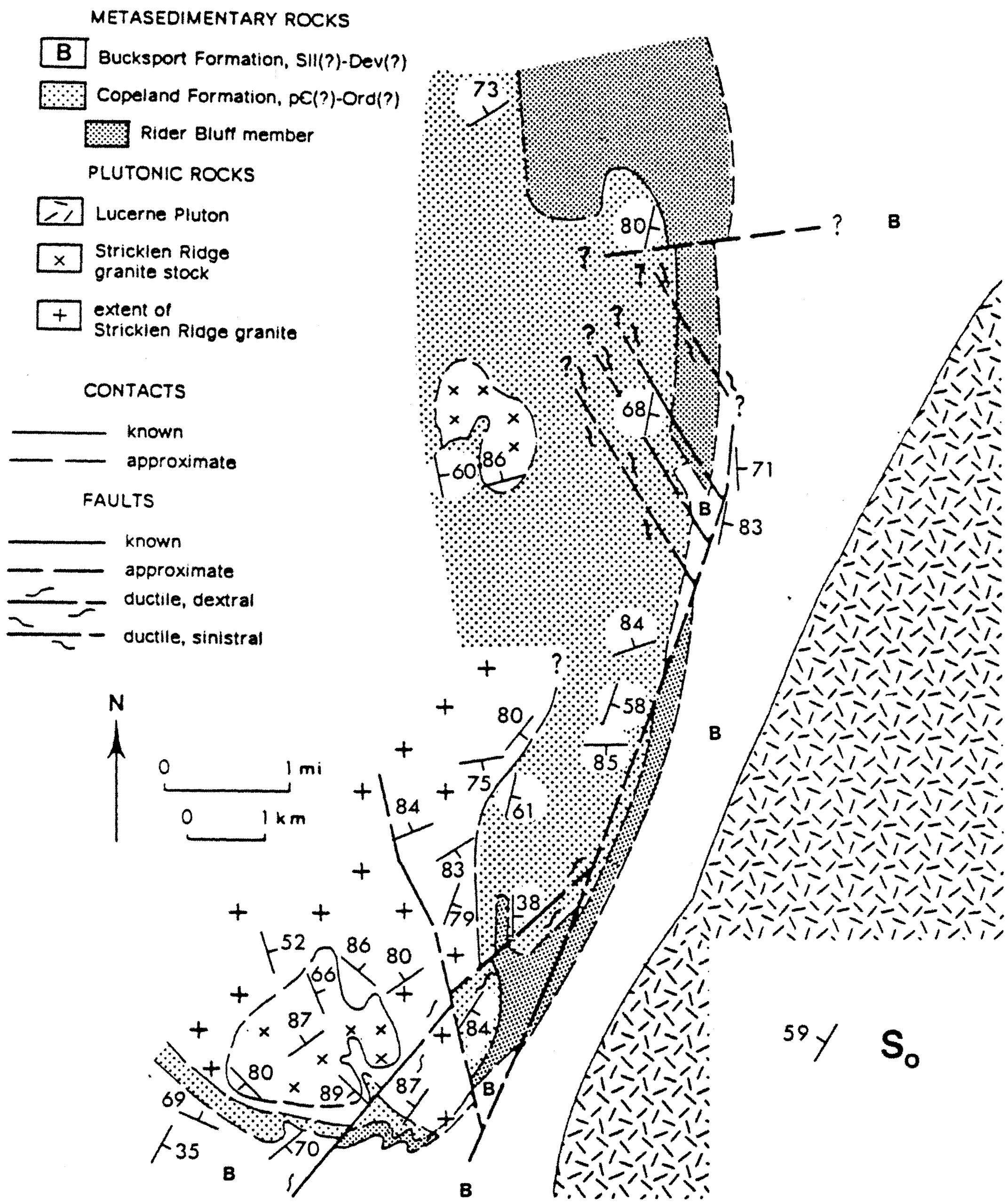

Figure 4. Simplified geologic map of study area showing attitude of bedding (S_0). Data for Lucerne pluton from Wones (1980).

The Rider Bluff member (informally used by Stewart and Wones, 1974; Wones, 1976) (Fig. 2) of the Copeland Formation is a green, finely-laminated pelitic siltstone. It only occurs in the study area where it crops out as a ≤ 2 km wide, discontinuous belt along the eastern margin of the Copeland Formation (Fig. 2). Local magnetite- or garnet-rich layers may represent bedding. It has been assigned to the Copeland Formation on the basis of lithological similarities (Wones, unpublished data). Kaszuba and Wones (1985) interpreted the Rider Bluff member as ductilely deformed Copeland Formation. Subsequent work revealed that the two units are lithologically distinct where undeformed, but that ductilely deformed Rider Bluff member is almost indistinguishable from deformed Copeland Formation. No fossils have been found in the Rider Bluff member, and no radiometric dating has been attempted. The contact between the Rider Bluff member and the Copeland Formation is not exposed.

The area on Fig. 2 showing the extent of Stricklen Ridge granite (informally used by Stewart and Wones, 1974; Wones, 1974, 1976) outlines the occurrence of a two-mica, garnet-bearing leucogranite that intruded the Copeland Formation and Rider Bluff member as dikes, sills, and very small stocks. Granitic dikes that intrude the PGW Formation crop out for a few km's to the southwest of the study area and are thought to be Stricklen Ridge granite (Wones, unpublished data). The regional stratigraphy is traceable through the granite terrane. Overall the granite comprises less than one-eighth of the total map area outlined as Stricklen Ridge granite except where two stocks of granite crop out (Fig. 2). Within these two stocks, the granite comprises from 50% to 90% of the map area. The Stricklen Ridge granite is a compositionally restricted (Pitcher, 1979) monzogranite (IUGS classification scheme, Streckeisen, 1973), but includes variations in kinds and abundance of accessory minerals, texture, and enclaves (see Appendix). Dikes of Stricklen Ridge granite have been assigned a 412 ± 14 Ma age based on concordant U-Pb data from zircons (Zartman and Gallego, 1979) (Table 1).

The Vassalboro and PGW terranes are separated by the NFZ in the northeastern Penobscot Bay area (Wones and Stewart, 1976) and by a thrust fault farther to the southwest (Fig. 1b). The NFZ is a steeply-dipping, northeast-trending zone of ductile and brittle deformation (Devonian or younger) which consists of five distinct fault traces (Johnson and Wones, 1984). These fault traces bound slices of the units through which the fault zone extends. At least 13 km of right-lateral strike-slip motion is suggested by displacement of a Devonian syenite body north of the Lucerne pluton (Osberg and others, 1985). Johnson and Wones (1984) suggested ca. 35 km of right-lateral offset along the fault zone and a component of south-side-up dip-slip movement based on best-fit considerations of units across it. Loiselle and Ayuso (1980) first suggested that the NFZ is a major crustal fracture at depth, separating two different source regions for plutonic rocks exposed on either side of the fault zone. Late Paleozoic and Mesozoic fault reactivation of the NFZ was postulated because Triassic and Jurassic sedimentary basins were interpreted as forming during NFZ movements (Wones, 1978).

Bucksport Terrane

The Bucksport terrane (Fig. 1b) is composed of the Bucksport Formation (Trefethen, 1950; Wing, 1957), a greenschist facies calcareous siltstone that is finely-laminated and sometimes interlayered with sulfide-bearing pelite beds. This unit is recognized from southwest of Sheepscot Bay to the Lucerne pluton (Fig. 1b). In the study area, it crops out between the PGW terrane and the Lucerne pluton (Fig. 2). The Bucksport Formation is lithologically similar to the Silurian Vassalboro Formation and has been correlated with it (Stewart and Wones, 1974; Wones, 1976, 1980; Osberg, 1980; Loiselle and Wones, 1983; Gates and others, 1984; Hussey, 1984) (Table 1). However, no fossils are found within the Bucksport Formation and it cannot be traced directly into the Vassalboro Formation. Correlations are based strictly on lithologic similarities between units that occur on either side of the NFZ. The Late Silurian to Early Devonian Flume Ridge Formation (Ruitenberg, 1967; Ruitenberg and Ludman, 1978), part of the Fredericton Trough (Fig. 1b), has also been correlated with the Bucksport Formation based on lithologic similarities (Wones, 1980; Ludman, 1981; Gates and others, 1984) (Table 1).

The boundary between the PGW and Bucksport terranes in the Penobscot Bay area has previously been interpreted as a normal or reverse fault (Stewart and Wones, 1974), an unconformity (Wones, 1976), and a thrust fault (Kaszuba and Wones, 1985; Osberg and others, 1985). To the southwest in the Sheepscot Bay area (Fig. 1b), the PGW terrane has been interpreted to structurally overlie the Bucksport terrane along a pre-metamorphic thrust fault (Hussey, 1985). The boundary is not exposed in the study area and no observed strain gradient or structural or metamorphic discontinuity coincides with it. Two-dimensional modeling of gravity data collected over this boundary just northeast of the Mount Waldo pluton (Kane and Bromery, 1966; Sweeney, 1974, 1976) (Fig. 1b) suggests it dips 45°-55°N. The boundary between the Vassalboro and Bucksport terranes is the NFZ (Fig. 1b) (Stewart and Wones, 1974).

Penobscot Terrane

To the south of the Bucksport terrane the Penobscot terrane (Fig. 1b) contains the Penobscot Formation (Smith and others, 1907), a graphitic, sulfidic, greenschist facies schist composed of interlayered siltstone and pelite (Stewart and Wones, 1974). Primary sedimentary structures are still recognizable (Stewart and Wones, 1974). The Penobscot Formation in the northern portion of Penobscot Bay (Fig. 1b) has been assigned a 440 ± 10 Ma age from Rb/Sr whole-rock isochron data (Brookins, 1976), while in the southwest portion of Penobscot Bay it has been assigned a 460 ± 10 Ma age and has produced Caradocian brachiopods (Boucot and others, 1972) (Table 1). The Penobscot

Formation has been correlated on lithological grounds by Wones (1980) with the Cookson Formation (Ruitenberg, 1967) (Table 1) of New Brunswick, Canada and eastern Maine (southeast of Fredericton Trough, Fig. 1b). However, the Cookson Formation contains Tremadocian graptolites (Ruitenberg and Ludman, 1978). The contact between the Bucksport and Penobscot terranes has been interpreted as both a thrust fault (Loiselle and Wones, 1983; Gates and others, 1984; Osberg and others, 1985) and an unconformity (Wones, 1976). Near the Canadian border this contact has been interpreted as a high-angle reverse fault (Ludman, 1978).

Ellsworth Terrane

Southeast of the Penobscot terrane lies the Ellsworth terrane (Fig. 1b). This terrane contains the polydeformed Ellsworth Formation (Smith and others, 1907), which is feldspathic and chlorite-rich (Stewart and Wones, 1974). It has been assigned a 510 ± 15 Ma age from Rb/Sr whole-rock isochron data (Brookins, 1976) (Table 1). The Castine Volcanics of Smith and others (1907) unconformably overlie the Ellsworth Formation (Wingard, 1958) and comprise a variety of igneous and sedimentary rocks (Stewart and Wones, 1974) that have been assigned a 390 ± 5 Ma age from Rb/Sr whole-rock isochron data (Brookins and others, 1973) (Table 1). The Ellsworth terrane is separated from the Penobscot terrane by the Turtle Head Fault Zone (Fig. 1b). Stewart and Wones (1974) interpreted the Turtle Head Fault Zone as a right-lateral strike-slip fault zone with a minor component of dip-slip motion. Osberg (1978) on the other hand suggested that it may be a thrust or high angle reverse fault. The Turtle Head Fault Zone was intruded by the Middle Devonian Lucerne Pluton (Fig. 1b) (Stewart and Wones, 1974).

The boundary between the PGW and Bucksport terranes (Fig. 1b) separates a Precambrian (?) to Lower Paleozoic basement terrane to the west from its Middle

Paleozoic cover to the east. This basement/cover relationship constrains regional tectonic models for coastal Maine. The structure of the rocks that comprise the boundary zone is discussed below.

STRUCTURAL GEOLOGY OF PASSAGASSAWAKEAG AND BUCKSPORT TERRANE BOUNDARY ZONE

Polyphase deformation and metamorphism are characteristic of most of the Northern Appalachians (e.g. Moench and Zartman, 1976) and are ubiquitous to the study area. The structural history outlined below is based on detailed work in a small area (Fig. 2). Temporal relationships among different small-scale structures were established in outcrop using overprinting relationships. Sets of structures were correlated on the basis of orientation, style, and position within temporal sequences. Microstructural characteristics of the various fabrics and relationship of these fabrics to metamorphic mineral growth were determined in thin section. Using these methods, four major groups of structures (D_1, D_2, D_3, and D_4) (Table 2) have been distinguished in the study area (Fig. 2). D_1 produced folds and axial plane foliations whereas D_2 produced folds and hinge-parallel mineral elongation lineations. D_3 strike-slip ductile shear zones and D_4 folds followed. A separate event of granitic plutonism and thermal metamorphism (M_{1-2}) is recognized and interpreted to have occurred between D_1 and D_2 (Table 2). Late brittle joints and faults crosscut all ductile structures.

Table 2. Characteristics of deformational and metamorphic events. NFZ, Norumbega Fault Zone; $L_{2,4}$ crenulation, hinge line of $F_{2,4}$ microfolds.

Feature \ Event	D_1	M_{1-2}	D_2	D_3	D_4	Brittle
Structures	-F_1 folds -S_1 axial plane foliation -rare L_1 mineral lineation	-porphyroblasts overgrow S_1	-F_2 folds -L_2 mineral lineation and crenulation -weak S_2 axial plane foliation	-ductile shear zones -L_3 stretching lineation -S_3 mylonitic foliation and compositional layering	-F_4 folds -weak L_4 mineral lineation and crenulation -weak S_4 axial plane foliation	-brittle joints and faults -slickensides -veins filled with quartz ± hematite
Metamorphic Conditions	greenschist (?)	amphibolite	upper greenschist to lower amphibolite	upper greenschist to lower amphibolite	greenschist	sub-greenschist
Relative Timing	pre-Stricklen Ridge granite intrusion	between D_1 & D_2, syn-granite (?) intrusion	post-granite intrusion	post-L_2	post-mylonite	after all ductile deformation
Orogeny	pre-412 ± 14 Ma, early Acadian (?), possibly Taconic (?)	Acadian (?), ~412 ± 14 Ma	Acadian	post-Lucerne (380 ± 4 Ma), syn-NFZ, Alleghanian	post-D_3 shear zones syn-NFZ, Alleghanian	

First Deformation Phase

Macroscopic

The earliest recognizable deformation phase (D_1) (Table 2) produced F_1 folds (Table 3) and a strong axial plane foliation (S_1) (Figs. 2, 3b, 5) defined by a uniform compositional layering. F_1 folds (Table 3) occur in all three metasedimentary units but are prevalent in the Copeland Formation in the southern part of the study area (Fig. 5). They deform bedding (S_0) (Fig. 3b) and are cut by dikes of Stricklen Ridge granite in the Copeland Formation (Fig. 3c). Style and geometry of folds vary among the three metasedimentary units in the area (Table 3). F_1 folds in the Copeland Formation (Table 3) are steeply-reclined to vertical (classification of Fleuty, 1964) and tight to isoclinal (Figs. 3c, 3d). Their axial planes strike predominantly east-west (Fig. 6a) and fold hinges plunge steeply to the east (Fig. 6b). F_1 folds in the Rider Bluff member (Table 3) are recumbent to gently reclined isoclines that deform quartz veins. In the Bucksport Formation, F_1 folds are tight and inclined (Fig. 3b; Table 3) with hinges that plunge moderately to the northeast. Preliminary work by Kaszuba and Wones (1985) did not recognize F_1 folds in the Bucksport Formation.

Foliations measured in outcrops where fold closures are not observed strike predominantly north-northeast and dip steeply to the west (Fig. 6c) in contrast to the F_1 axial plane data measured within fold noses (Fig. 6a). These foliations may either be a bedding-parallel foliation which is common to the area or the S_1 axial plane foliation. The data plotted in Fig. 6c probably represents a combination of both.

Table 3. Characteristics of fold generations. Fold classification of Fleuty (1964).

	F_1			F_2			F_4		
	Copeland Formation	Rider Bluff member	Bucksport Formation	Copeland Formation	Rider Bluff member	Bucksport Formation	Copeland Formation	Rider Bluff member	Bucksport Formation
Style	steeply reclined to vertical; tight to isoclinal	recumbent to gently reclined isoclines	inclined; tight	upright to inclined; open to tight			steeply reclined to vertical; open to tight		
wave-length	rarely > 0.5m	rarely > 10cm	—	6cm to 6m			6cm to 1.5m		
amplitude: wavelength	4:1 to 8:1	4:1 to 8:1	—	1:1 to 2:1			1:9 to 1:2		
relative abundance	abundant	rare	rare	common			abundant	rare	common
structures it deforms	S_0	quartz veins	S_0	S_1	S_1, L_1	S_0, S_1	S_0, S_1, F_1, S_3	S_1	S_1, F_2

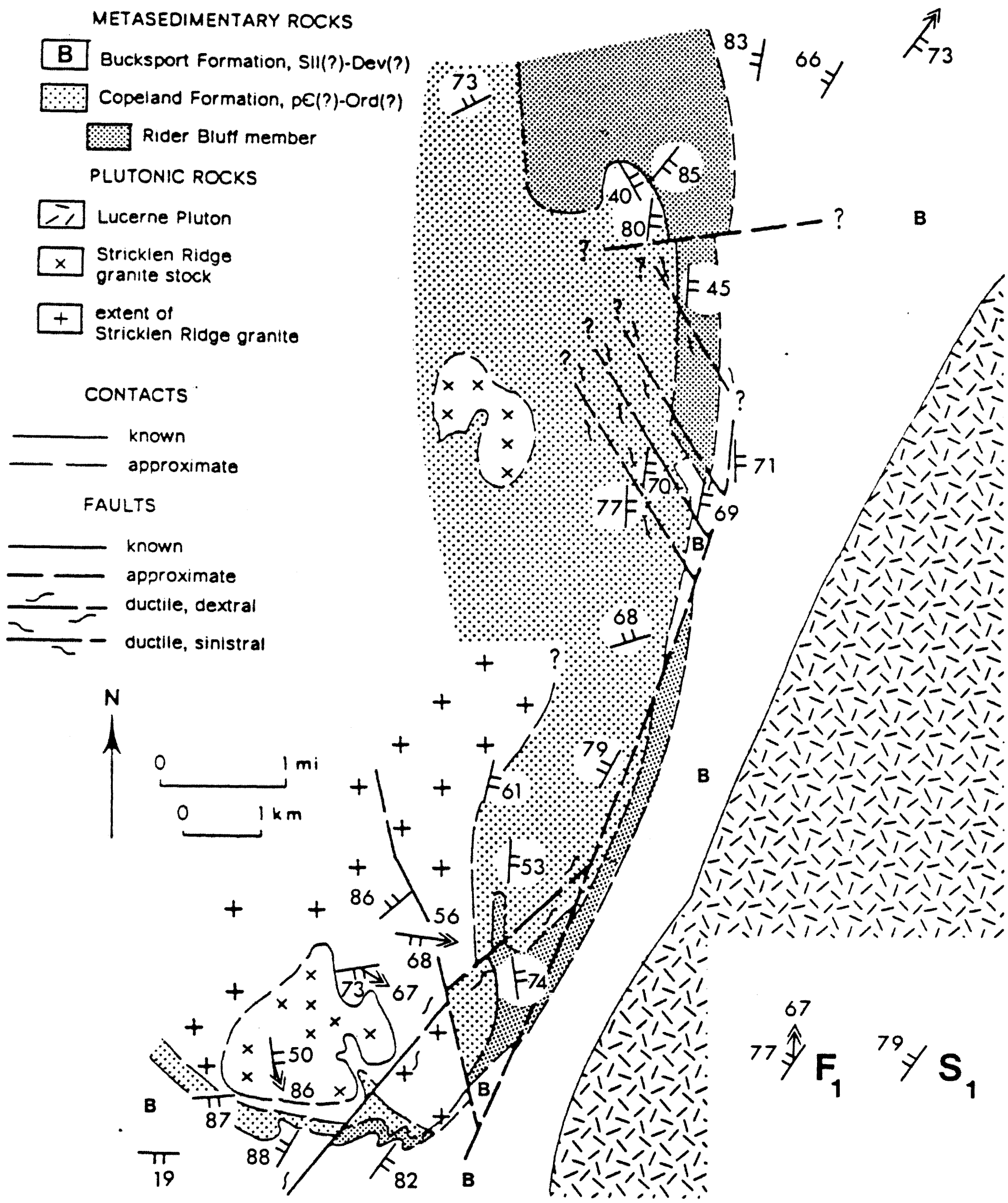

Figure 5. Simplified geologic map of study area showing D_1 structures. F_1, attitude of axial surface of minor fold with bearing and plunge of associated fold hinge. S_1, attitude of foliation. Data for Lucerne pluton from Wones (1980).

Figure 6. Lower hemisphere, equal area stereographic projections of D_1 field data. For all projections, original orientation data is plotted on left and contoured on right. Solid triangle, Copeland Formation; solid circle, Rider Bluff member; open diamond, Bucksport Formation. For all contoured projections, highest density contour interval is shaded, second highest is stippled. a. Poles to axial surfaces of F_1 folds. Data measured where fold closures occur. b. F_1 fold hinges. c. Poles to S_0 and S_1 foliations. Data measured where fold closures not observed.

a) F$_1$ AXIAL SURFACES

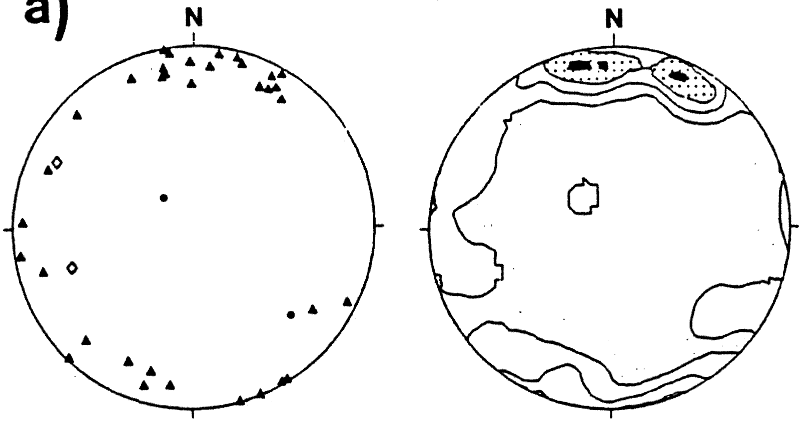

n = 39,
contours at
1, 3, 5, and 7
points per 2.6%
of circle's area

b) F$_1$ HINGES

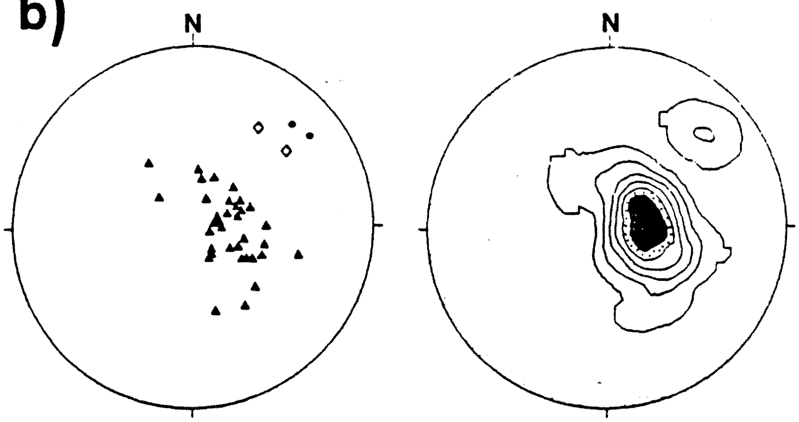

n = 39,
contours at
1, 3, 5, 7,
9, and 11
points per 2.6%
of circle's area

c) S$_0$ /S$_1$ FOLIATIONS

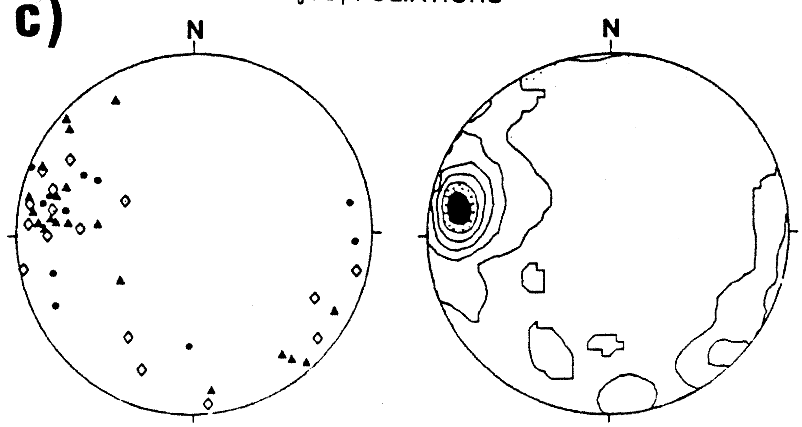

n = 47,
contours at
1, 3, 5, 7,
9, and 11
points per 2.1%
of circle's area

Microscopic

S_1 compositional layering in the Copeland Formation is defined by alternating quartz- and mica-rich layers up to 5 mm thick. Biotite and muscovite folia are folded and recrystallized by both D_2 and D_4 (Table 4). In mica-rich layers, elongate 0.1-0.5 mm diameter plagioclase (An_{21-28}) and quartz grains are pinned by adjacent micas and are oriented subparallel to S_1. Undulatory extinction is developed in plagioclase, and larger grains contain subgrains along their margins. Albite growth twins are bent where plagioclase grains occur near microfolds. In quartz-rich layers, quartz grains are anhedral and up to several mm's in diameter, but most are < 1 mm in diameter (Fig. 7a). Many of these are recrystallized to 20-40 μm diameter grains (Fig. 7a). Quartz in both mica- and quartz-rich layers contains undulatory extinction, elongate subgrains and re-crystallized new grains (Fig. 7a), deformation bands, and core and mantle structures (White, 1973, 1976). Undulatory extinction and subgrains are more extensively developed in quartz than in plagioclase, and quartz microstructures are more thoroughly developed in quartz- than in mica-rich layers. Quartz grain-shape preferred orientations (elongate subgrains and recrystallized new grains) and deformation bands in quartz in quartz-rich layers are parallel to axial planes of F_2 and F_4 microfolds (Fig. 7a, Table 4), a texture also developed in the Rider Bluff member and calcareous Bucksport Formation. S_1 is enclosed in porphyroblasts interpreted to have grown between D_1 and D_2 (event labeled M_{1-2}, see Table 2). Elongate, 10-100 μm long quartz, biotite, plagioclase, magnetite, and/or ilmenite often define this internal foliation.

S_1 compositional layering in the Rider Bluff member is defined by millimeter-scale quartz- (90% quartz) and chlorite-rich (50% quartz, 50% chlorite) laminae. Magnetite-rich laminae, 0.1-0.3 mm diameter elongate quartz and plagioclase grains, and fibers of chlorite and white mica are preferentially oriented parallel to S_1. Plagioclase

Table 4. Foliation development.

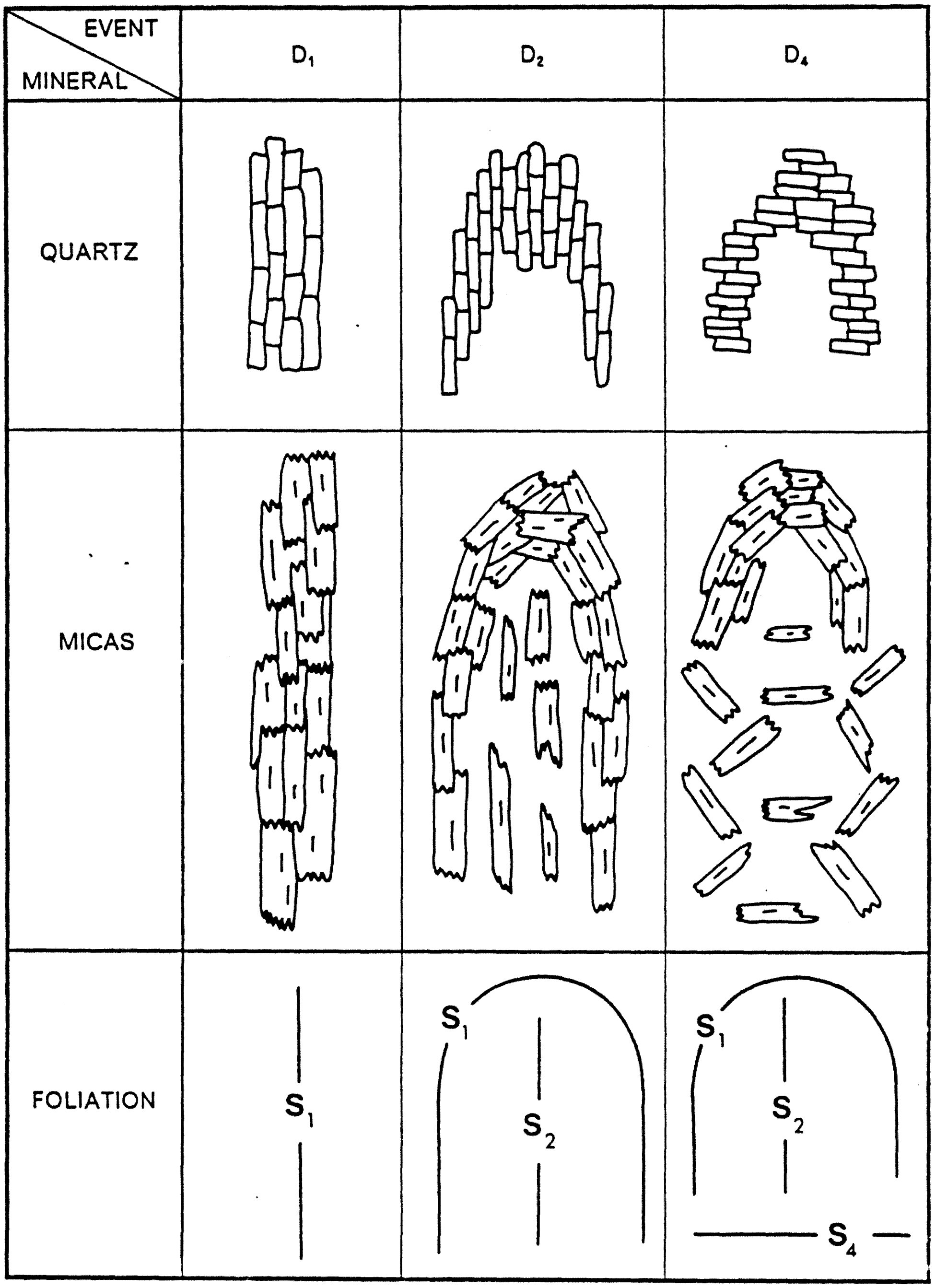

Figure 7. Microstructural characteristics of deformational features. a. elongate garnet (Gt) in Copeland Formation. Garnet is restricted to pelitic compositional layer. Elongate quartz subgrains and recrystallized new grains parallel axial surface of F_2. Crossed nikols. Scale bar = 200 µm. b. non-calcareous siltstone of Bucksport Formation. Elongate quartz grains (Q) and fibrous beards within the pressure shadows of these grains (arrowhead) define S_1 . Quartz grains and fibrous beards that paralleled S_1 now parallel and are truncated by S_2 . Bt, biotite. Plane-polarized light. Scale bar = 100 µm. c. calcareous Bucksport Formation. S_1 compositional layering contains quartz veins (Q) and M_{1-2} amphibole porphyroblasts (arrowhead). F_1 microfold preserved by quartz vein. F_2 deforms S_1. Plane-polarized light. Scale bar = 500 µm. d and e. mylonitic Stricklen Ridge granite. Quartz ribbon (Q), mica fish (muscovite, Mu), and S_3 mylonitic foliation are folded by F_4. Elongate quartz subgrains and recrystallized new grains in quartz ribbon parallel F_4 axial surface. Crossed nikols. Scale bar = 100 µm.

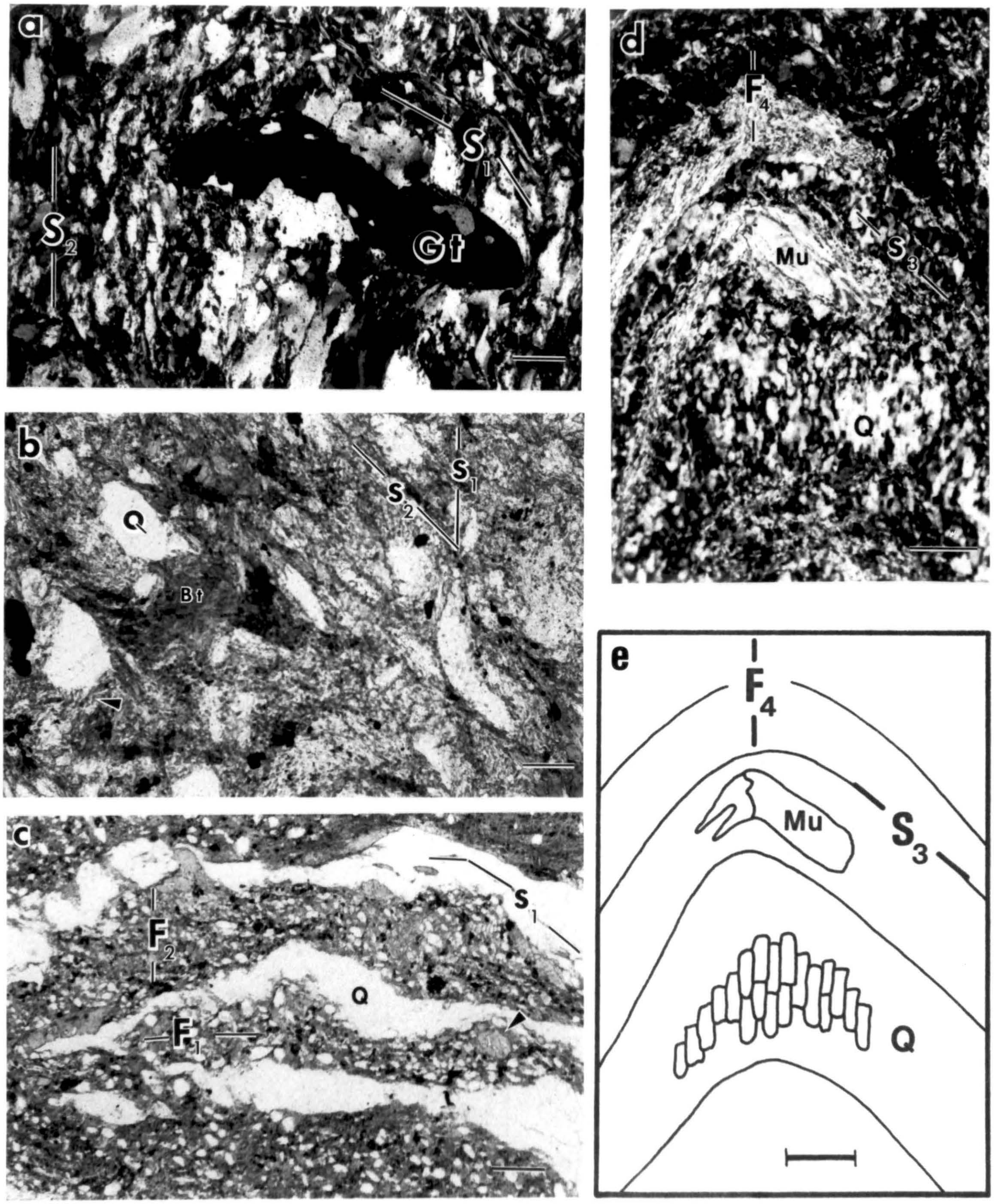
a
S1
S2
Gt
b
Q
Bt
S2
S1
c
F2
F1
Q
S1
d
F4
Mu
S3
Q
e
F4
Mu
S3
Q

and quartz grains display undulatory extinction, but it is more extensively developed in quartz. Larger quartz grains (up to 1 mm in diameter) also contain elongate subgrains and recrystallized new grains, deformation bands, and core and mantle structures. Quartz veins in both the Rider Bluff member and the Copeland Formation are sometimes flattened within S_1 and extended parallel to quartz rods that define an L_1 mineral lineation.

The character of S_1 in the Bucksport Formation varies with the different lithologies and grain sizes of that unit. In siltstone containing little to no carbonate, S_1 is a continuous to disjunctive cleavage (classification of Powell, 1979) (Fig. 7b). A continuous, slaty cleavage occurs in very fine-grained siltstone whereas coarser-grained siltstone displays a 0.1 mm-scale disjunctive cleavage that ranges from smooth to rough to anastomosing. A mm-scale compositional layering is defined by alternating quartz- and phyllosilicate-rich layers, elongate quartz grains, fibrous beards occurring in the pressure shadows of these grains, and fibrous white mica and chlorite that are oriented parallel to S_1 (Fig. 7b). Quartz grains are up to 0.5 mm in diameter (Fig. 7b), but the majority of grains are <0.15 mm in diameter. Quartz grains display undulatory extinction, and larger grains also contain ~ 20 μm diameter equant subgrains and recrystallized new grains. Adjacent quartz grains may also be sutured together and/or indent each other. Beards in quartz pressure shadows contain fibrous quartz, white mica, and chlorite (Fig. 7b). Cleavage zones contain chlorite and sometimes pyrite, and may truncate quartz grains (Fig. 7b). S_1 in carbonate-rich Bucksport Formation is a compositional layering (Fig. 7c) up to 1 cm thick that is defined by a range in modal composition of phyllosilicates, calcite, quartz, and plagioclase. Quartz in quartz-rich compositional layers or veins occurs as elongate subgrains and recrystallized new grains. S_1 is refracted across bedding planes between carbonate-rich and carbonate-poor lithologies probably because of the competency contrasts between them (Hobbs and others, 1976, p. 215-216).

F_1 microfolds in all three metasedimentary units occur in quartz-rich veins and layers and S_1 compositional layers (Fig. 7c). F_1 fold noses are attenuated relative to fold limbs and adjacent S_1 compositional layers (Fig. 7c), suggesting that these folds have been deformed.

Second Deformation Phase

Macroscopic

The second deformation phase (D_2) (Table 2) produced F_2 folds (Figs. 2, 8; Table 3) that deform S_1 (Fig. 9) in all three metasedimentary units and fold dikes of Stricklen Ridge granite in the Copeland Formation. F_2 folds (Table 3) are open to tight, upright to inclined folds (Fig. 9). Axial plane and hinge line orientations are grouped into two geographic domains. In the northern half of the study area, axial planes are subvertical and strike northeast (Figs. 8, 10a). Hinge lines plunge gently northeast (Figs. 8, 10b). In the southern half of the study area, axial planes strike north-south and range in dip (Figs. 8, 10c). Hinge lines plunge at moderate angles to the north-northeast and south-southwest (Figs. 8, 10d).

A strong mineral lineation (L_2) occurs parallel to F_2 fold hinges throughout the study area (compare Figs. 10b and 10e) but is best developed in the north. The L_2 mineral lineation is defined by a strong grain-shape preferred orientation of elongate quartz grains in quartz veins and quartz-rich layers, and by elongate micas, feldspar, and garnet in pelitic layers. In Stricklen Ridge granite, L_2 is defined by quartz rods and by stretched and reoriented feldspars and micas. In outcrop, F_2 microfolds often appear as a crenulation of S_1. Their fold hinges were measured as L_2 and are included in the data plotted in Fig. 10e.

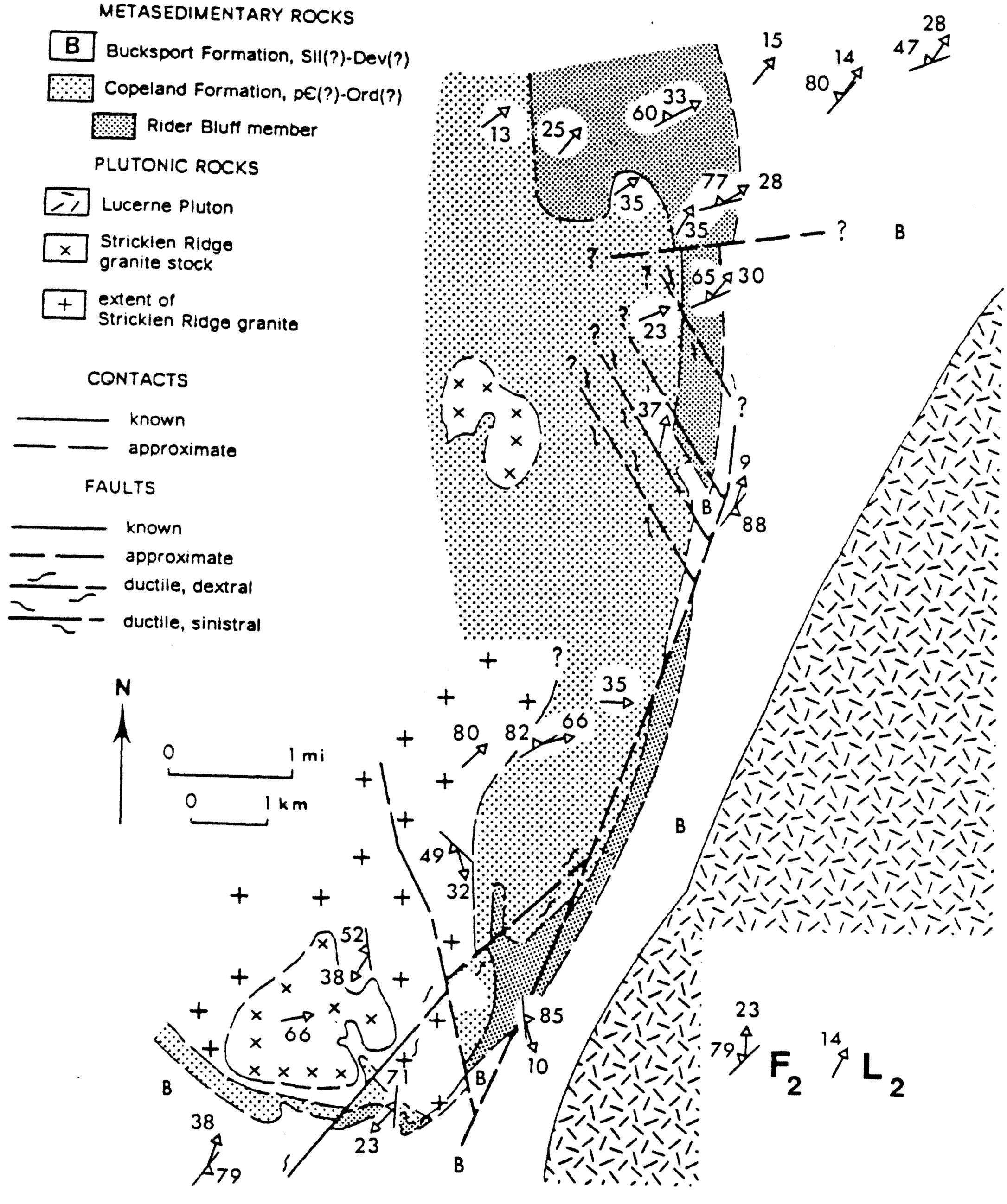

Figure 8. Simplified geologic map of study area showing D_2 structures. F_2, attitude of axial surface of minor fold with bearing and plunge of associated fold hinge. L_2 , bearing and plunge of mineral lineation, crenulation axis (Tables 2, 3). Data for Lucerne pluton from Wones (1980).

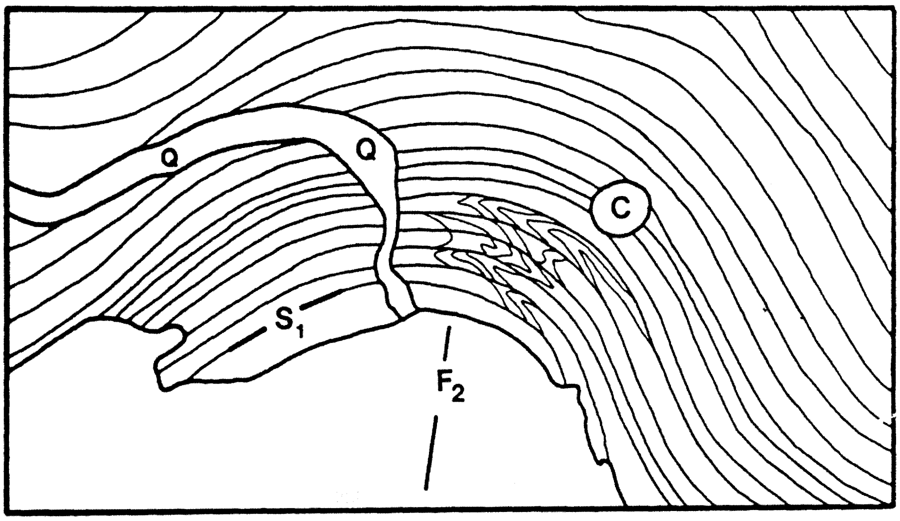

Figure 9. Sketch of view to northeast of subvertical face of Bucksport Formation. Open F_2 fold deforms S_1 axial plane foliation. Relict S_0 and F_1 fold nose visible between S_1 planes in detailed portion of sketch. Quartz vein (Q) crosscuts S_0, S_1, and F_2. Coin (C) 2.4 cm diameter.

Figure 10. Lower hemisphere, equal area stereographic projections of D_2 field data. For all paired projections, original orientation data is plotted on left and contoured on right. Solid triangle, Copeland Formation; solid circle, Rider Bluff member; open diamond, Bucksport Formation. For all contoured projections, highest density contour interval is shaded, second highest is stippled. a. Poles to axial surfaces of F_2 folds in all metasedimentary units in the northern half of the study area. b. F_2 fold hinges in all metasedimentary units in the northern half of the study area. c. Poles to axial surfaces of F_2 folds in all units in the southern half of the study area. d. F_2 fold hinges in all units in the southern half of the study area. e. L_2 mineral elongation lineations (open circle) and crenulation axes (solid star) in all metasedimentary units in the northern half of the study area.

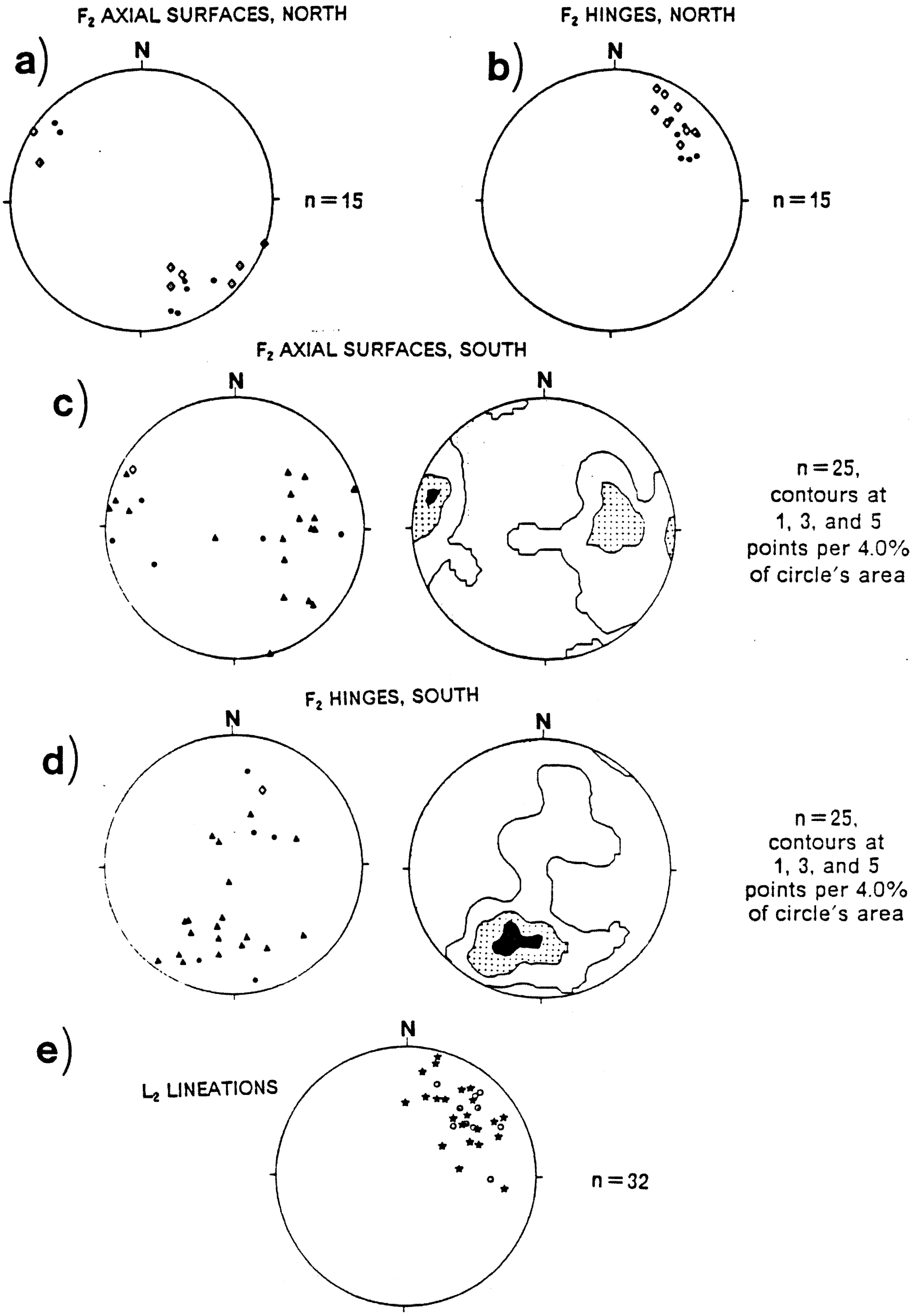
F2 AXIAL SURFACES, NORTH
a)
N
n=15
F2 HINGES, NORTH
b)
N
n=15
F2 AXIAL SURFACES, SOUTH
c)
N
N
n=25,
contours at
1, 3, and 5
points per 4.0%
of circle's area
F2 HINGES, SOUTH
d)
N
N
n=25,
contours at
1, 3, and 5
points per 4.0%
of circle's area
e)
L2 LINEATIONS
N
n=32

Microscopic

Asymmetric F_2 microfolds deform S_1 in the Copeland Formation. Quartz displays undulatory extinction and core and mantle structures, but these textures are more extensively developed in quartz-rich layers and veins. Deformation bands, elongate subgrains, and recrystallized new grains in quartz in quartz-rich layers display grain-shape preferred orientations parallel to F_2 axial planes (Fig. 7a; Table 4), and quartz rods parallel L_2. These quartz textures are also developed in the Rider Bluff member and Bucksport Formation. Biotite and muscovite are recrystallized into an S_2 foliation which is axial planar to F_2 microfolds and into polygonal grains in F_2 microfold noses (Table 4). Micas are also locally folded and kinked with kink band boundaries oriented subparallel to F_2 axial planes, and elongate micas are also preferentially oriented parallel to L_2. Elongate M_{1-2} porphyroblasts of garnet and tourmaline are brittlely fractured around F_2 microfold hinges and extended along L_2. Micas wrap around these rigid grains and biotite, chlorite, and quartz crystallized within their pressure shadows and fractures. Fibrous white mica pseudomorphs of M_{1-2} porphyroblasts are flattened parallel to S_2 and elongate parallel to L_2, and micas and quartz in S_1 compositional layers that are recrystallized parallel to S_2 grow across them. S_2 is not as pronounced as S_1 because the mica foliation is not as pervasive and no new compositional layering is developed.

In the Rider Bluff member, a variable, mm-scale zonal crenulation cleavage (classification of Powell, 1979) (S_2) deforms S_1 . White mica and chlorite in cleavage zones (< 1 mm thick) are recrystallized parallel to S_2. Equant and euhedral 0.5-2.0 mm diameter garnet and albite M_{1-2} porphyroblasts are wrapped by micas and have pressure shadows in which chlorite $\pm$ quartz crystallized. Albite porphyroblasts display undulatory extinction, Pericline twins, and < 1 mm diameter recrystallized grains. Some albite porphyroblasts are myrmekitic, but it is uncertain whether these are primary myrmekites that crystallized during M_{1-2} or secondary ones related to exsolution during post-M_{1-2} deformation (e.g. Simpson, 1985). M_{1-2} biotite porphyroblasts are kinked by S_2, retrograded to chlorite; have pressure shadows in which muscovite, chlorite, and quartz crystallized, and are elongate parallel to L_2. All of the above M_{1-2} porphyroblasts contain an internal foliation which sometimes parallels S_1 but often occurs at a range of angles to it.

D_2 structures in the Bucksport Formation vary with lithology. Siltstone develops a discrete (Fig. 7b) to zonal crenulation cleavage (classification of Powell, 1979) (S_2) which deforms S_1. Discrete, elongate quartz grains, fibrous beards of quartz, biotite, chlorite, white mica, and calcite in the pressure shadows of these grains, and matrix biotite, chlorite, and white mica that had defined S_1 are now parallel to S_2 (Fig. 7b). Quartz grains and calcite veins are truncated and displaced along S_2 cleavage zones, and biotite fibers and pyrite commonly occur in these zones. M_{1-2} biotite porphyroblasts are recrystallized parallel to S_2 and are commonly truncated by S_2 cleavage zones. S_2 in carbonate-rich lithologies is a zonal crenulation cleavage (classification of Powell, 1979) (S_2) that deforms S_1 compositional layering and is subparallel to the axial planes of F_2 microfolds. Matrix biotite is recrystallized parallel to S_2. Quartz in veins occurs as ribbons (type 2B of Boullier and Bouchez, 1978) parallel to S_1 that are recrystallized to S_2-parallel 50-100 μm diameter elongate subgrains and recrystallized new grains (aspect ratio of 2:1). F_2 microfolds associated with quartz veins have thick hinges and attenuated, locally boudinaged limbs. M_{1-2} porphyroblasts of albite and titanite are brittlely fractured and broken. Albite also displays undulatory extinction and development of Pericline twins, and titanite is locally polysynthetically twinned. M_{1-2} porphyroblasts of euhedral, calcic amphibole are oriented parallel to S_2 and distributed around F_2 microfold noses. Amphibole porphyroblasts in both orientations are brittlely fractured and extended. Most fractures exploit the amphibole cleavage planes, but some fractures crosscut them. Amphibole porphyroblasts also locally display undulatory extinction and subgrain development. Amphiboles displaying these ductile microstructures occur in both quartz-rich and quartz-poor layers.

Shear Zones

Macroscopic

The Norumbega Fault Zone (NFZ) is a major strike-slip fault which strikes ~060° and crops out just northwest of the study area (Figs. 1b, 11). Ductile shear zones are ubiquitous to the study area (Fig. 11). They occur at both outcrop- and map-scales and offset contacts and juxtapose units within their boundaries. The shear zones deform Stricklen Ridge granites and L_2 and are deformed by later folds (F_4, see below), therefore they are labeled D_3 (Table 2). The majority of shear zones are subparallel to the NFZ and display right-lateral movements as determined by shear banding in metasediments (Platt and Vissers, 1980) and S (schistosité) and C (cisaillement, shear) foliations in granites (Berthé and others, 1979; Simpson and Schmid, 1983; Simpson, 1984). One major dextral shear zone (A on Fig. 11) is nearly parallel to the NFZ trend. Another major shear zone (B on Fig. 11) is orthogonal to the NFZ and displays left-lateral movements.

Microscopic

In ductile shear zones developed in Stricklen Ridge granites, quartz shows ribbon structure (type 2B of Boullier and Bouchez, 1978) and 20-50 μm diameter elongate subgrains and dynamically recrystallized new grains. Grain-shape preferred orientations of these grains are either oblique to the macroscopic foliation (e.g. Simpson and Schmid,

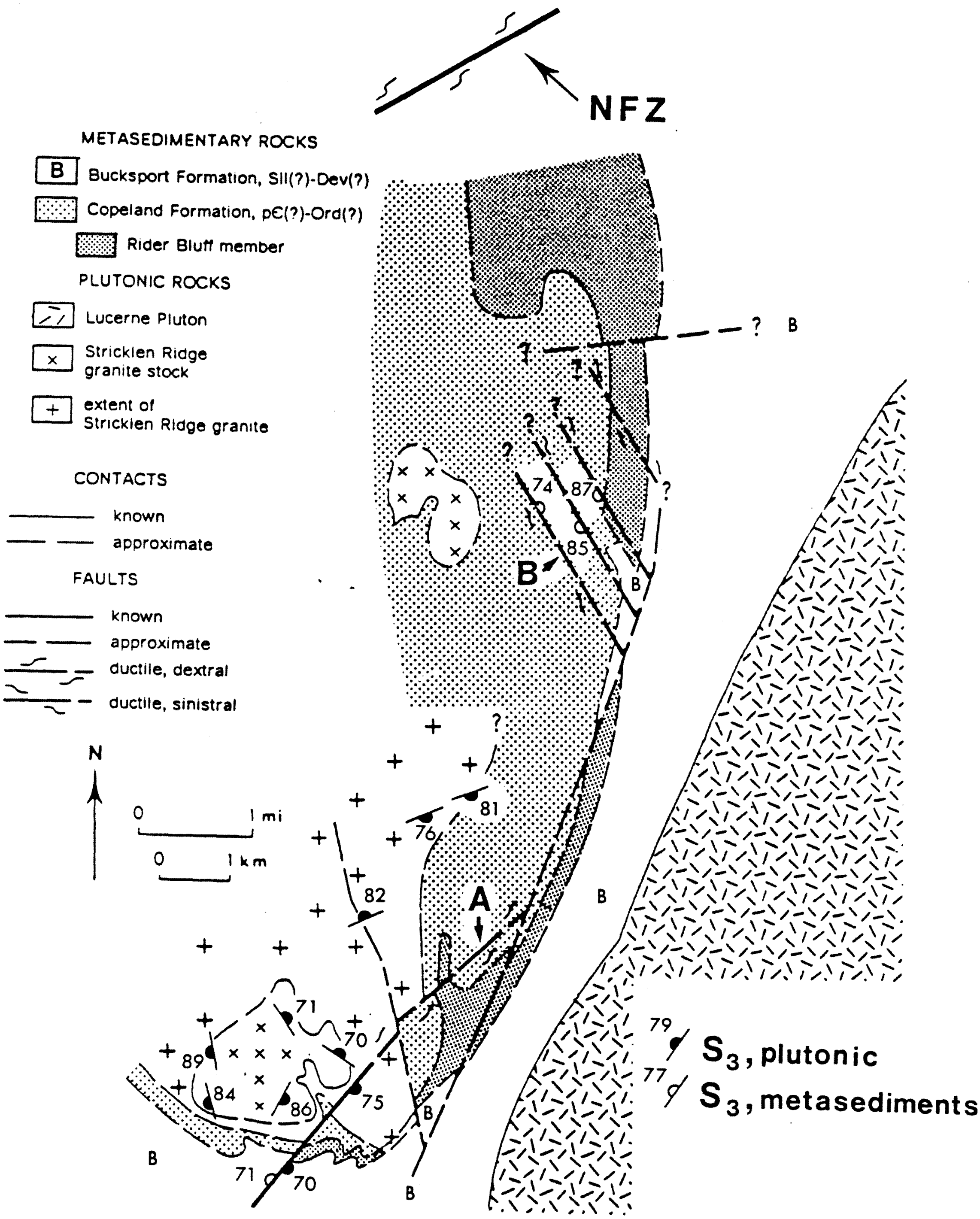

Figure 11. Simplified geologic map of study area showing D_3 shear zones. S_3, attitude of mylonitic foliation in plutonic and metasedimentary rocks. A and B: large-scale strike-slip ductile shear zones. Data for Lucerne pluton and trace of Norumbega Fault Zone (NFZ) from Wones (1980).

1983, p. 1285) or, when present, parallel to the axial planes of F_4 microfolds (Fig. 7d). Mylonitic Copeland Formation displays the same quartz textures. Fine-grained, recrystallized tails of mica fish (asymmetric mica porphyroclasts, e.g. Lister and Snoke, 1984) and wrapping of micas around rigid porphyroclasts indicate ductile deformation of micas. Large porphyroclasts ($\sim$ 1.0-2.0 mm in diameter, although $\sim$ 1 cm diameter and larger porphyroclasts occur in deformed pegmatites) of plagioclase (An_{10-15}), microcline, and orthoclase display brittle fractures, undulatory extinction, and dynamically recrystallized tails. Elongate, 10-20 μm diameter subgrains and recrystallized new grains occur within the tails, along intragranular fractures, and along grain margins of these porphyroclasts. Smaller feldspar porphyroclasts ($\leq$ 0.5 mm) also contain core and mantle structures; the subgrains and new grains occur within the 50-70 μm thick mantles. Crystal plastic microstructures are more extensively developed in K-feldspar than in plagioclase porphyroclasts. K-feldspar also displays sigmoidal perthite lamellae, deformation twins, and myrmekite development along recrystallized grain boundaries (e.g. Simpson, 1985). Garnet, tourmaline, and apatite are brittlely fractured and extended into the subhorizontal stretching direction (L_3) and contain recrystallized phyllosilicates ± quartz within their pressure shadows and fractures.

Ductile shear zones in the Copeland Formation display a mm- to μm-scale compositional layering defined by alternating quartz- and mica-rich (usually muscovite) layers and quartz ribbons (types 2A and 2B of Boullier and Bouchez, 1978). Discontinuous lenses composed of 50-200 μm diameter plagioclase or 40-70 μm diameter tourmaline are interspersed with the quartz and mica compositional layers. Plagioclase and tourmaline in these layers are brittlely fractured and broken and display no fabric. Asymmetric porphyroclasts of 0.1-2.0 mm diameter garnet, muscovite (i.e. mica fish), oligoclase, and tourmaline are dispersed throughout the matrix.

Ductile shear zones in the Rider Bluff member and the Bucksport Formation contain abundant M_{1-2} porphyroblasts (now asymmetric porphyroclasts) distributed in a foliated matrix of ≤ 50 μm diameter phyllosilicates and quartz. M_{1-2} albite porphyroblasts of the Rider Bluff member occur as 0.2-1.3 mm diameter, angular to rounded porphyroclasts. Most display undulatory extinction and are recrystallized along their grain margins. M_{1-2} albite porphyroblasts of calcareous Bucksport Formation occur as ≤ 0.5mm diameter, brittlely fractured and broken grains. Smaller grains (≤ 0.2mm diameter) display core and mantle structures and tails containing elongate, ~10 μm diameter subgrains and recrystallized new grains. M_{1-2} amphibole porphyroblasts of calcareous Bucksport Formation occur as 50-300 μm diameter angular fragments and subhedral porphyroclasts that display undulatory extinction, subgrain development, and polysynthetic twinning. Albite and amphibole porphyroclasts are often concentrated in mm-scale discontinuous lenses that parallel the matrix foliation. Within these lenses, these minerals display primarily brittle behavior in contrast to the ductile behavior of the surrounding matrix.

Rocks from all three metasedimentary units and Stricklen Ridge granites are juxtaposed within the shear zones on the outcrop scale, and minerals characteristic of each unit are interlayered on the thin section scale. For example, M_{1-2} albite porphyroblasts of calcareous Bucksport Formation or Rider Bluff member occur in mm-scale discontinuous lenses within Stricklen Ridge granite mylonites; and M_{1-2} amphibole porphyroblasts of calcareous Bucksport Formation are interspersed with M_{1-2} albite porphyroblasts of the Rider Bluff member.

Shear bands are developed in the metasedimentary units outside the main shear zone boundaries. They range in thickness (~40 μm to 0.5 mm) and spacing (< 1 mm to ~5 mm and larger), and contain recrystallized phyllosilicates and quartz and concentrations of magnetite, ilmenite, and pyrite. Pre-existing foliations are asymptotically deflected into the shear bands, and rigid mineral grains (e.g. albite porphyroclasts) are locally offset across them.

Microstructural criteria for movement direction in the shear zones are internally consistent and support the field observations. These criteria include asymmetric feldspar, tourmaline, and garnet porphyroclasts; mica fish (Lister and Snoke, 1984); antithetic and synthetic offset along microfractures in tourmaline and garnet and along microfractures and cleavages in feldspars (Simpson and Schmid, 1983); asymmetric microfolds; elongate, dynamically recrystallized quartz grains (Simpson and Schmid, 1983); S and C foliations in granites (Berthé and others, 1979; Simpson and Schmid, 1983; Simpson, 1984); and shear bands in metasediments (Platt and Vissers, 1980).

Fourth Deformation Phase

Macroscopic

The youngest observed deformation phase (D_4) (Table 2) produced F_4 folds (Figs. 2, 12; Table 3) that occur in all three metasedimentary units but are prevalent in the Copeland Formation in the southern portion of the study area. They deform S_0, D_1 (Fig. 3d), D_2, and D_3 structures. F_4 folds (Table 3) are open to tight, steeply-reclined to vertical folds (classification of Fleuty, 1964) (Fig. 3d). Axial planes strike predominantly north-south (Fig. 13a) and hinge lines are steeply plunging (Fig. 13b). F_4 microfold hinges were measured in outcrop as a lineation (L_4). An L_4 mineral lineation defined by elongate micas and quartz rods occurs parallel to these fold hinges, but it is not as pervasive as the L_2 mineral lineation.

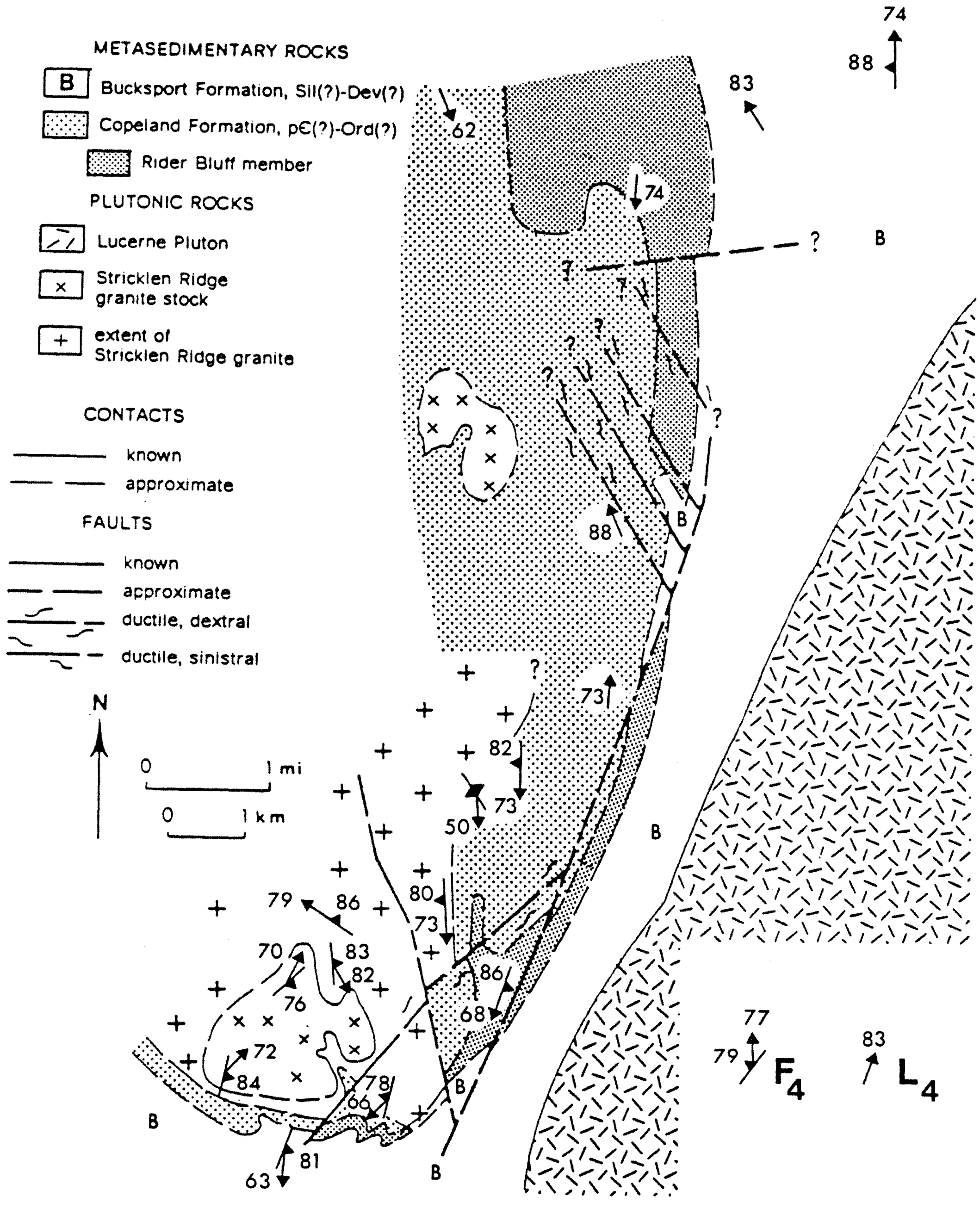

Figure 12. Simplified geologic map of study area showing D_4 structures. F_4, attitude of axial surface of minor fold with bearing and plunge of associated fold hinge. L_4 , bearing and plunge of mineral lineation, crenulation axis (Tables 2, 3). Data for Lucerne pluton from Wones (1980).

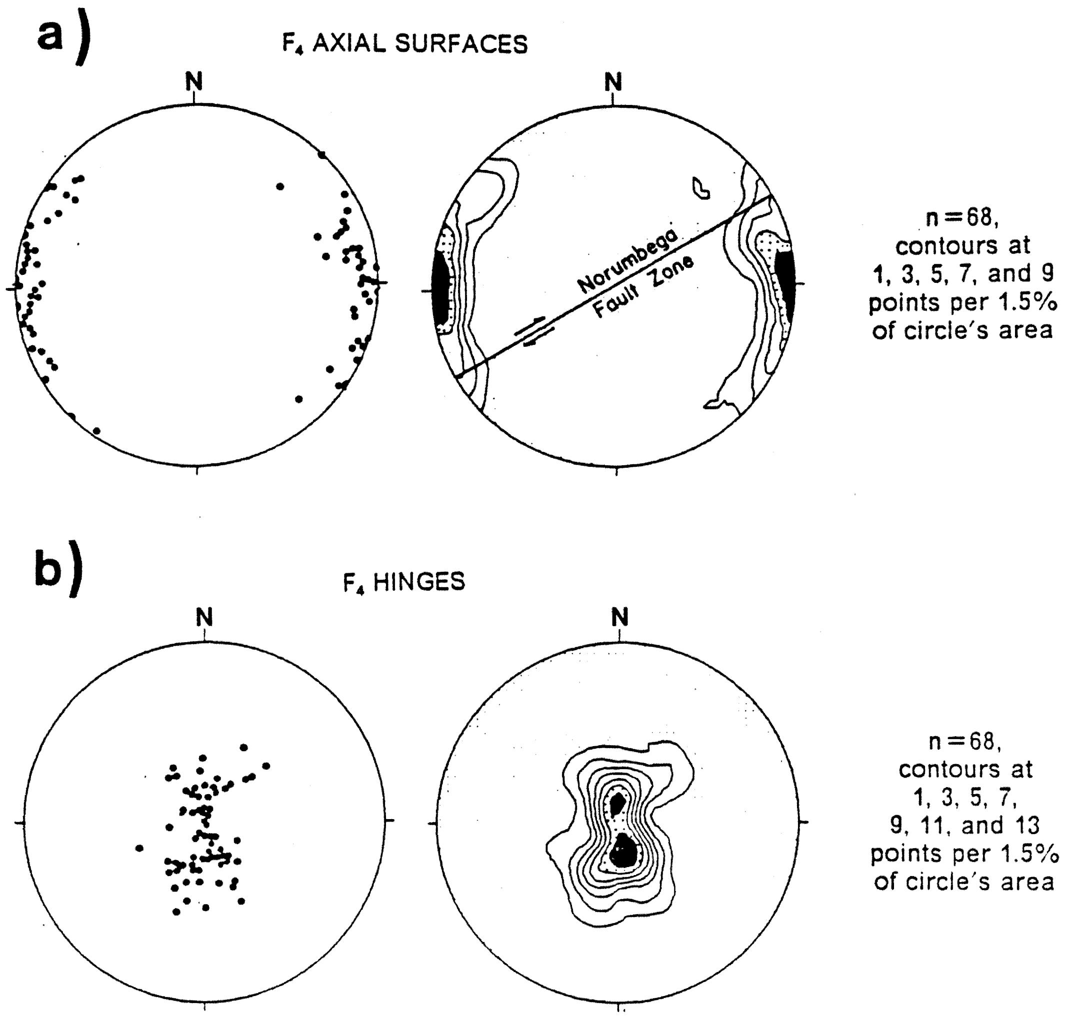

Figure 13. Lower hemisphere, equal area stereographic projections of D_4 field data in all units throughout the study area. For all projections, original orientation data is plotted on left and contoured on right. For all contoured projections, highest density contour interval is shaded, second highest is stippled.
a. Poles to axial surfaces of F_4 folds. Data measured where fold closures occur. Trace and sense of movement of the Norumbega Fault Zone also plotted. b. F_4 fold hinges

Microscopic

F_4 microfolds in mylonitic and non-mylonitic Copeland Formation occur as crenulations of S_1 compositional layers and F_2 fold limbs, especially in pelitic layers. Micas and mica fish are recrystallized along grain boundaries and kink band boundaries and into polygonal grains in F_4 microfold noses (Table 4), and are folded by F_4 microfolds (Fig. 7d). An S_4 foliation, defined by a preferred orientation of recrystallized micas and kink band boundaries, occurs parallel to F_4 axial planes (Table 4), but it is not well-developed and is not as penetrative as S_1 or S_2. Quartz displays undulatory extinction, core and mantle structures, and in quartz-rich layers elongate ≤ 0.12 mm diameter subgrains and recrystallized new grains and deformation bands display grain-shape preferred orientations parallel to F_4 axial planes (Fig. 7d; Table 4). These quartz textures are also developed in the Rider Bluff member and Bucksport Formation.

In Bucksport Formation siltstones, symmetrical microfolding of S_1 produces a zonal crenulation cleavage (classification of Powell, 1979) (S_4). Cleavage zones and microlithons are evenly-spaced (~ 0.5 mm) and have diffuse boundaries. Phyllosilicates and pressure shadows of quartz grains originally parallel to S_1 now parallel S_4 .

Brittle Deformation

Brittle faults and joints (Table 2) are ubiquitous to the study area. They crosscut all ductile fabrics (D_1, D_2, D_3 , and D_4) and are often filled with quartz (Figs. 3b, 9) and/or hematite. In thin section, quartz which fills the fractures occurs as polygonal grains that display no crystallographic or grain-shape preferred orientation.

Orientations of brittle structures and their movement sense are plotted in Fig. 14 according to the method of De Paor (personal communication, 1986). Movement sense was determined by fibrous mineral growth (slickensides) on and offset across fault

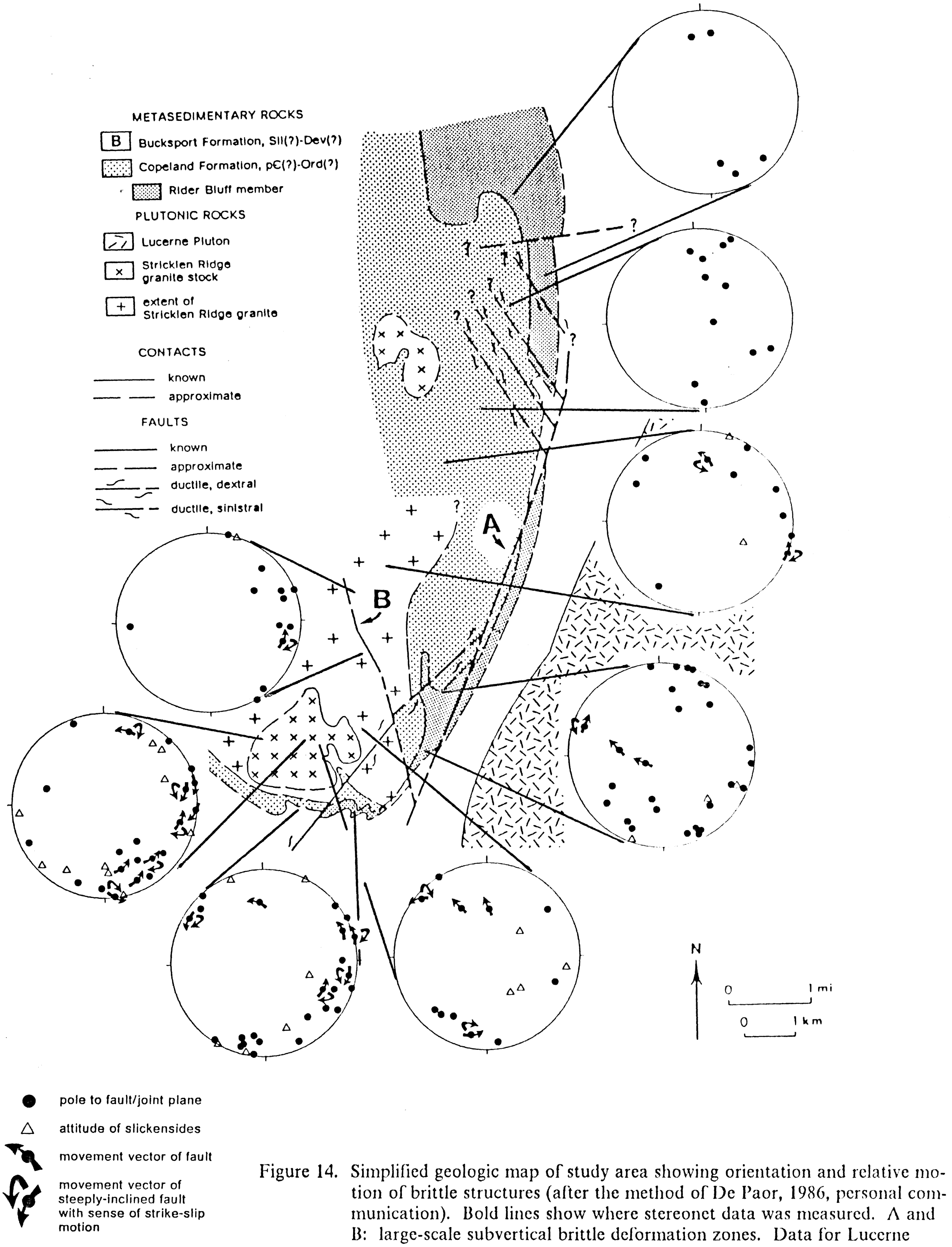

Figure 14. Simplified geologic map of study area showing orientation and relative motion of brittle structures (after the method of De Paor, 1986, personal communication). Bold lines show where stereonet data was measured. A and B: large-scale subvertical brittle deformation zones. Data for Lucerne pluton from Wones (1980).

planes, although slickensides were only observed in Stricklen Ridge granites. Joint and minor brittle fault orientations parallel the major brittle faults with which they are associated (Fig. 14). Relative movement along these fractures is the same as the D_3 shear zones which they exploit (Fig. 14). Minor brittle structures which do not occur near major brittle faults display the same orientations and movement directions as the major brittle faults (Fig. 14).

INTERDEFORMATIONAL METAMORPHISM

Textural Relationships

The porphyroblasts listed in Table 5 occur in all three metasedimentary units in the study area and share the following textural relationships: except for fibrolitic sillimanite, they are euhedral to subhedral and large (up to several millimeters in diameter) in contrast to other minerals in thin section which crystallized or recrystallized during D_1, D_2, D_3 , or D_4 (Fig. 15a); they overgrow S_1 and often contain an internal foliation (S_i) oriented subparallel to and often continuous with S_1 (Fig. 15a); porphyroblasts containing S_i lack synmetamorphic rotational textures (e.g. Spry, 1969, p. 253); grain-shape preferred orientations of porphyroblasts parallel D_2, D_3 , or D_4 structures. These textural relationships suggest that the porphyroblasts crystallized between D_1 and D_2, therefore they are labeled M_{1-2}.

Garnet porphyroblasts in the Rider Bluff member and in enclaves of Copeland Formation in Stricklen Ridge granites are euhedral and equant whereas those in the Copeland Formation are euhedral/subhedral and equant or anhedral and elongate (Figs. 7a, 15b, 15c). All garnets in the Rider Bluff member contain an S_i, but not all in the Copeland Formation do (compare Fig. 7a with Figs. 15b and 15c). Elongate garnets display the same chemical zoning profile as euhedral garnets (discussed below). Garnets

Table 5. Inferred stable mineral assemblages in metasediments. $M_{1\text{-}2}$ assemblages are listed in order of decreasing metamorphic grade. All $M_{1\text{-}2}$ assemblages in the Copeland Formation include muscovite + quartz. Abbreviations: musc, muscovite; bt, biotite; qtz, quartz; olig, oligoclase ($An_{21\text{-}28}$), plagioclase; mag, magnetite; ilm, ilmenite; chl, chlorite; plag, plagioclase; pyr, pyrite; Cc, calcite; sill, sillimanite; gt, garnet; tour, tourmaline; and, andalusite; staur, staurolite; ab, albite; Ca-amph, calcic amphibole; ti, titanite; ep, epidote.

UNIT \ EVENT	D_1	$M_{1\text{-}2}$	D_2	D_4
COPELAND FORMATION	-musc + bt + qtz ± olig ± mag ± ilm	-sill + bt ± gt ± tour -and + bt ± gt -staur -bt + gt ± tour	-bt + musc + qtz	-bt + musc + qtz ± chl ± ilm ± hem
RIDER BLUFF MEMBER	-qtz + chl + white mica + plag + mag ± pyr	-bt + gt + ab	-qtz + white mica + chl + bt	-chl + qtz
BUCKSPORT FORMATION	-qtz + white mica + chl + Cc + plag ± mag ± ilm ± pyr	-Ca-amph + ab + ti -bt + chl + ti + ep -bt + chl ± tour	-bt + Cc + qtz -qtz + white mica + chl + bt + Cc ± ilm ± mag ± pyr	-chl + white mica + qtz -bt + Cc + qtz

Figure 15. $M_{1\text{-}2}$ porphyroblasts and their textures. a. andalusite porphyroblast (A) in Copeland Formation has overgrown S_1 foliation. Andalusite mantled by intergrown fibrous white mica and fibrolitic sillimanite (arrowhead). Crossed nikols. Scale bar = 400 µm. b. elongate, anhedral garnet (Gt) in Copeland Formation. S_i in garnet (arrowheads) defined by elongate ilmenite parallels external S_1 foliation. Bt, biotite; Q, quartz. Plane-polarized light.. Scale bar = 100 µm. c. equant, subhedral garnet (Gt) in Copeland Formation. Same thin section as Fig. 15b. S_i in garnet (arrowheads) defined by elongate ilmenite and quartz parallels external S_1 foliation. Bt, biotite; Q, quartz. Plane-polarized light. Scale bar = 100 µm.

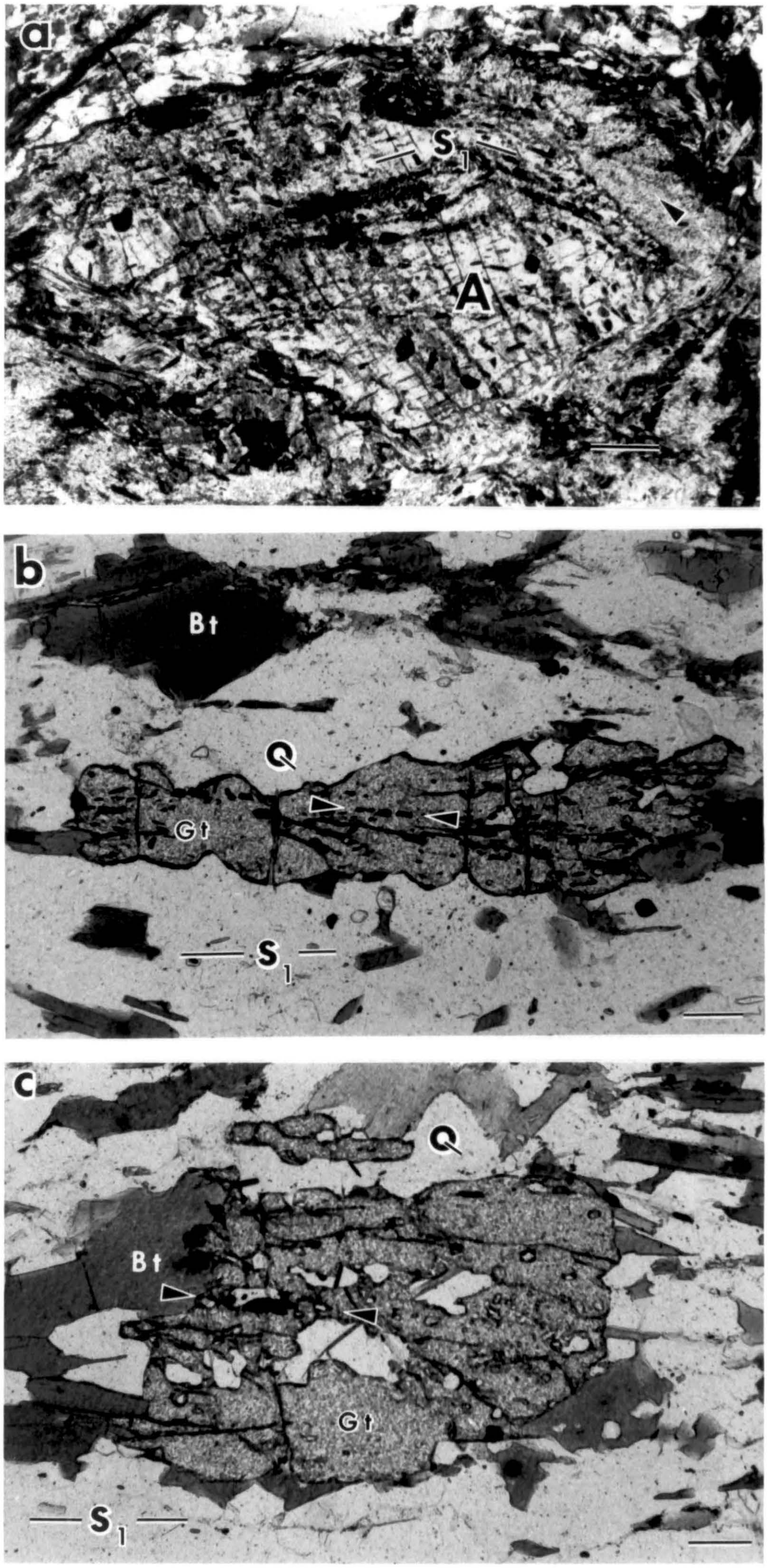
a
S1
A
b
Bt
Q
Gt
S1
c
Q
Bt
Gt
S1

are not offset along any foliation planes (Figs. 15b, 15c), indicating that shearing did not produce the elongate shapes. Comparison of garnet morphology to homogeneity of host rock reveals that equant garnets occur in rocks with an homogeneous compositional layering (Rider Bluff member, enclaves of Copeland Formation) whereas elongate garnets occur in rocks with a strong, inhomogeneous compositional layering (Copeland Formation). Elongate garnets are restricted to pelitic compositional layers and are composed of several tiny, euhedral, equant garnets which have coalesced into a linear shape (Figs. 7a, 15b, 15c). Coalescing garnet centers are a well-documented texture (Tracy, 1982). The degree of elongation ranges within a single thin section and is a function of thickness and spacing of compositional layers; elongate and euhedral garnets often occur in the same thin section (Figs. 15b, 15c). These elongate garnets are therefore interpreted to have grown in a hydrostatic stress environment at the same time as the euhedral, equant garnets. The two garnet textures are not thought to represent two distinct events. Elongate shapes are augmented by later deformation, including brittle extension into the L_2 mineral lineation and the shear zone stretching lineation (L_3). Elongate garnet morphologies are discussed by Blackburn and Dennen (1968) and Toteu and Macaudiere (1984), who interpreted elongate garnets as primary textures. They are not necessarily the result of synkinematic growth during flattening, nor are they the result of the effects of the force of crystallization (Blackburn and Dennen, 1968; Toteu and Macaudiere, 1984).

Staurolite occurs as embayed, anhedral grains mantled by optically continuous andalusite, and blebs of staurolite scattered throughout the andalusite are in optical continuity. Andalusite and staurolite are mantled by massive, felty intergrowths of very fine-grained white mica and fibrolitic sillimanite (Fig. 15a). Scattered through these fibrous intergrowths are coarse-grained, polygonal muscovite and very fine-grained zircon surrounded by yellow pleochroic halos. Staurolite is also partially pseudomorphed by ~0.5 mm diameter, polygonal muscovite. Guidotti (1968), Kwak

(1974), and Triboulet and Audren (1985) discussed similar muscovite pseudomorphs of staurolite and suggested these textures resulted from prograde metamorphism.

Mineral Chemistry

Representative garnet compositions are listed in Table 6 and plotted in almandine-pyrope-spessartine and almandine-pyrope-grossular ternary diagrams (Figs. 16, 17). In garnet in the Rider Bluff member, Mn, Ca, and Mg/Fe decrease from core to rim (Figs. 16, 17). The Mn and Ca patterns are typical for prograde growth zoning in rocks metamorphosed to a maximum of kyanite-staurolite grade, but the Mg/Fe pattern is not (Loomis and Nimick, 1982; Tracy, 1982). Garnet in the Copeland Formation displays a slightly different zoning pattern: Mn increases, Ca remains relatively constant, and Mg/Fe decreases from core to rim (Figs. 16, 17). Garnet in enclaves of Copeland Formation in Stricklen Ridge granite and in Stricklen Ridge granite displays a zoning pattern similar to Copeland Formation garnet, except that the Mn and Mg/Fe decrease (from core to rim) is smaller (Figs. 16, 17). These zoning patterns have been observed in other lower amphibolite facies garnets and were explained as the result of diffusion (Anderson and Olimpio, 1977) and retrogression (Tracy, 1982). Garnet rim compositions in all rock types trend to the same garnet composition (Figs. 16, 17), suggesting that garnet rims re-equilibrated to an homogeneous composition after initial M_{1-2} growth. Three post-M_{1-2} events (D_2, D_3, and D_4) occurred, and metamorphism associated with one or more of them is probably responsible for homogenization of garnet compositions.

Representative biotite compositions are listed in Table 7. Biotite in the metasediments plots in a small field in the ideal biotite plane at $Al^{VI} = 0.80\text{-}1.45$ and $Mg/Mg + Fe_{Total} = 0.35\text{-}0.50$ (Fig. 18). Biotite occurring in Stricklen Ridge granite and in enclaves of Copeland Formation in Stricklen Ridge granite plots in a small field at

Table 6. Representative garnet compositions. Alm, almandine; Pyr, pyrope; Spe, spessartine; Gro, grossular. Sample locations plotted in Fig. 21.

	1	2	3	4	5	6	7	8
SiO_2	38.27	38.70	37.13	39.03	37.73	38.48	37.10	37.00
TiO_2	0.11	0.12	0.13	0.13	0.21	0.10	0.22	0.14
Al_2O_3	20.58	19.90	20.54	20.91	20.07	20.18	18.92	18.96
FeO	30.85	29.72	25.79	23.14	26.50	24.58	13.77	23.54
MnO	8.70	10.37	14.51	17.04	13.44	16.04	21.59	13.18
MgO	2.04	1.35	1.88	1.26	2.14	1.53	0.50	1.07
CaO	1.02	0.96	0.68	1.08	1.19	0.75	4.07	2.45
BaO	0.07	0.03	0.06	0.08	0.10	0.10	0.03	0.11
Na_2O	0.04	0.02	0.02	0.00	0.05	0.04	0.05	0.02
K_2O	0.03	0.08	0.03	0.07	0.03	0.03	0.03	0.02
F	0.09	0.04	0.14	0.07	0.00	0.00	0.03	0.02
Sum	101.64	101.22	100.71	102.66	101.36	101.73	96.25	96.38
number of cations on the basis of 12 anions								
Si	3.049	3.105	3.002	3.077	3.032	3.077	3.113	3.108
Ti	0.007	0.007	0.008	0.008	0.013	0.006	0.014	0.009
Al	1.932	1.881	1.957	1.943	1.900	1.901	1.871	1.877
Fe	2.056	1.994	1.744	1.525	1.781	1.644	0.966	1.653
Mg	0.242	0.161	0.227	0.148	0.256	0.182	0.063	0.134
Mn	0.587	0.705	0.994	1.138	0.915	1.086	1.534	0.938
Ca	0.087	0.083	0.059	0.091	0.102	0.064	0.366	0.220
Na	0.006	0.003	0.003	0.000	0.008	0.006	0.008	0.003
K	0.003	0.008	0.003	0.007	0.003	0.003	0.003	0.002
Alm	69.16	67.76	57.69	52.56	58.30	55.22	32.99	56.13
Pyr	8.15	5.49	7.49	5.10	8.39	6.13	2.13	4.55
Spe	19.75	23.95	32.87	39.20	29.95	36.50	52.39	31.83
Gro	2.93	2.80	1.95	3.14	3.35	2.16	12.49	7.49

1. Copeland Formation, core, #SR-17A.
2. Copeland Formation, rim, #SR-17A.
3. Enclave of Copeland Formation in Stricklen Ridge granite, core, #SR-9B.
4. Enclave of Copeland Formation in Stricklen Ridge granite, rim, #SR-9B.
5. Stricklen Ridge granite, core, #SR-9D.
6. Stricklen Ridge granite, rim, #SR-9D.
7. Rider Bluff member, core, #SR-35.
8. Rider Bluff member, rim, #SR-35.

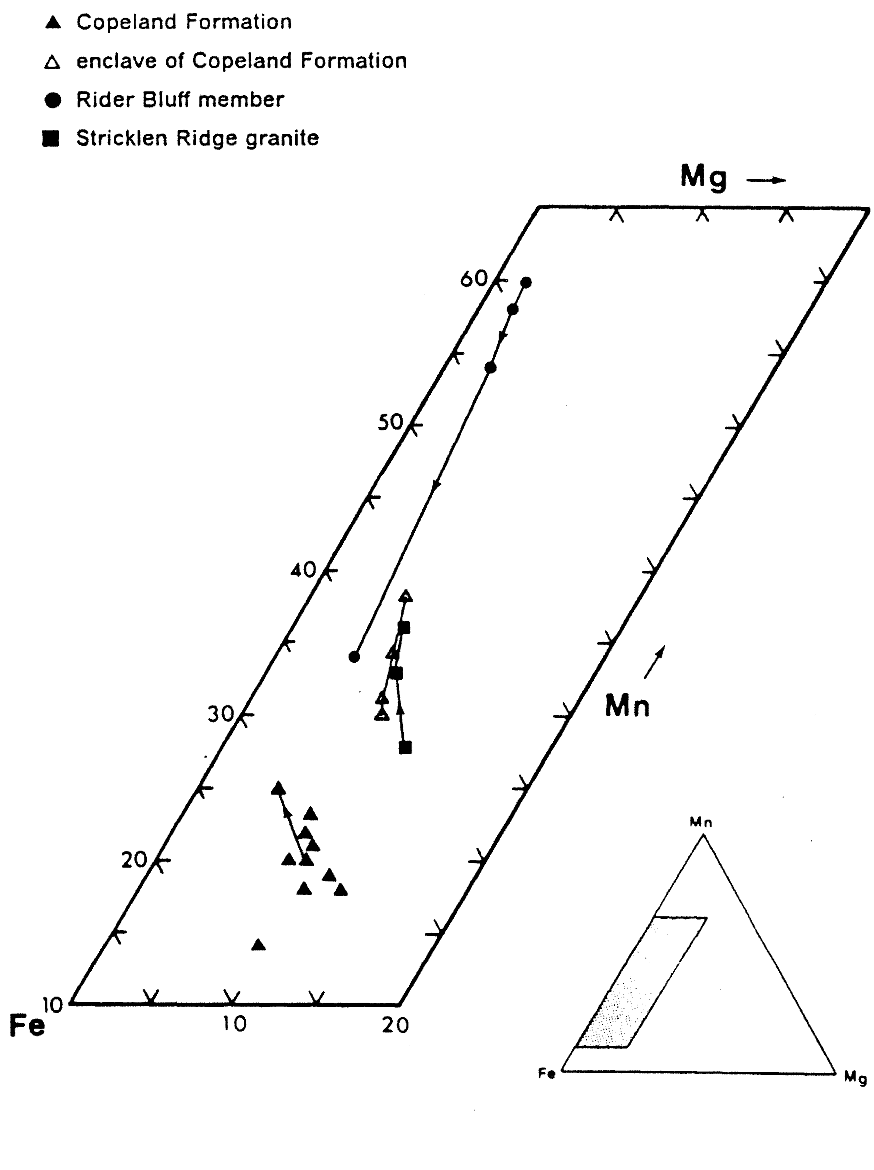

Figure 16. Fe-Mg-Mn ternary atomic percent plot of representative garnet compositions. Arrowheads point from core to rim.

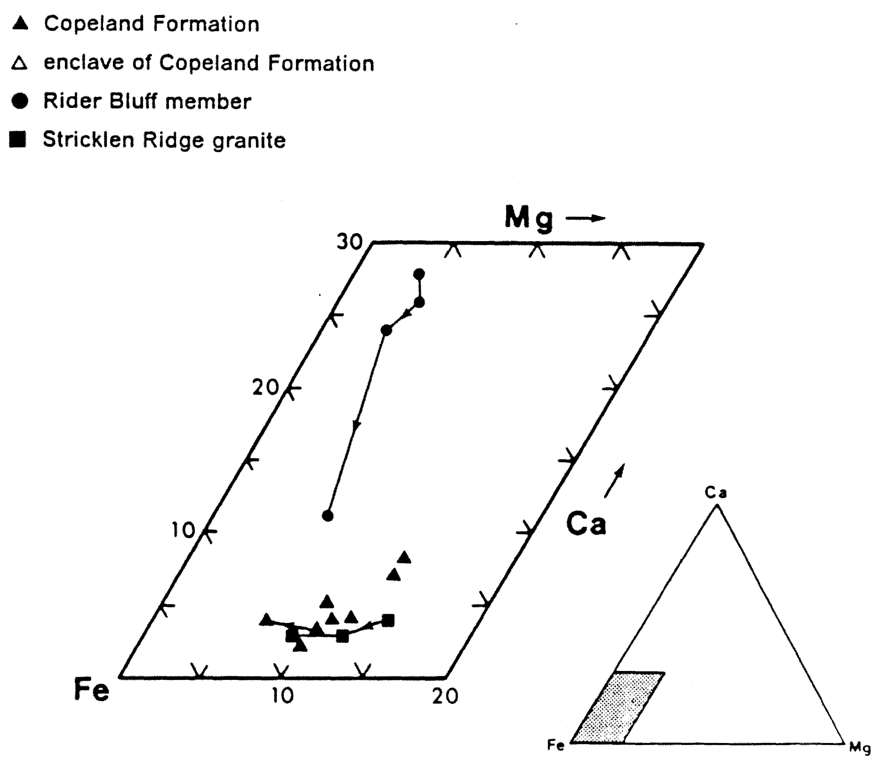

Figure 17. Fe-Mg-Ca ternary atomic percent plot of representative garnet compositions. Arrowheads point from core to rim.

Table 7. Representative biotite compositions. H_2O was not analyzed but is added into total oxides based on the calculated mineral formula. Sample locations plotted in Fig. 21.

	1	2	3	4	5	6	7
SiO_2	35.80	36.48	36.06	34.82	35.65	36.50	36.83
TiO_2	2.09	1.69	1.60	1.66	3.05	1.75	1.77
Al_2O_3	19.14	21.97	19.94	19.53	17.83	18.21	18.59
FeO	21.41	18.25	22.21	22.51	22.56	18.57	18.57
MnO	0.18	0.16	0.38	0.63	0.65	0.44	0.38
MgO	7.95	8.04	7.69	7.52	6.97	9.89	9.84
CaO	0.07	0.07	0.12	0.04	0.08	0.03	0.25
BaO	0.19	0.07	0.03	0.14	0.02	0.12	0.06
Na_2O	0.08	0.05	0.05	0.03	0.07	0.13	0.64
K_2O	8.86	8.37	8.96	9.46	8.79	9.13	7.78
F	0.22	0.36	0.46	0.54	3.56	0.79	0.48
H_2O	3.83	3.84	3.86	3.69	3.64	3.56	3.74
Sum	99.82	99.35	101.15	100.49	99.85	99.12	98.93
number of cations on the basis of 12 anions							
Si	2.728	2.726	2.716	2.671	2.743	2.779	2.783
Al^{IV}	1.272	1.274	1.284	1.329	1.257	1.221	1.217
Al^{VI}	0.446	0.660	0.486	0.436	0.359	0.412	0.438
Ti	0.120	0.095	0.091	0.096	0.176	0.100	0.101
Fe	1.364	1.140	1.399	1.444	1.451	1.182	1.173
Mn	0.012	0.010	0.024	0.041	0.042	0.028	0.024
Mg	0.903	0.895	0.863	0.860	0.799	1.122	1.108
Ca	0.006	0.006	0.010	0.003	0.007	0.002	0.020
Na	0.012	0.007	0.007	0.004	0.010	0.019	0.094
K	0.861	0.798	0.861	0.926	0.863	0.887	0.750
Ba	0.006	0.002	0.001	0.004	0.001	0.004	0.002
F	0.053	0.085	0.060	0.112	0.131	0.190	0.115
H	1.947	1.914	1.939	1.888	1.868	1.808	1.885

1. Copeland Formation, recrystallized S_1 biotite. #SR-17A.
2. Copeland Formation, undeformed S_4 biotite, overgrows S_3 mylonitic foliation, #SR-27B.
3. Copeland Formation, biotite inclusion in garnet, #SR-15.
4. Enclave of Copeland Formation in Stricklen Ridge granite, #SR-9C.
5. Stricklen Ridge granite, #SR-9D.
6. Rider Bluff member, undeformed biotite, #SR-1A.
7. Rider Bluff member, kinked biotite, #SR-1A.

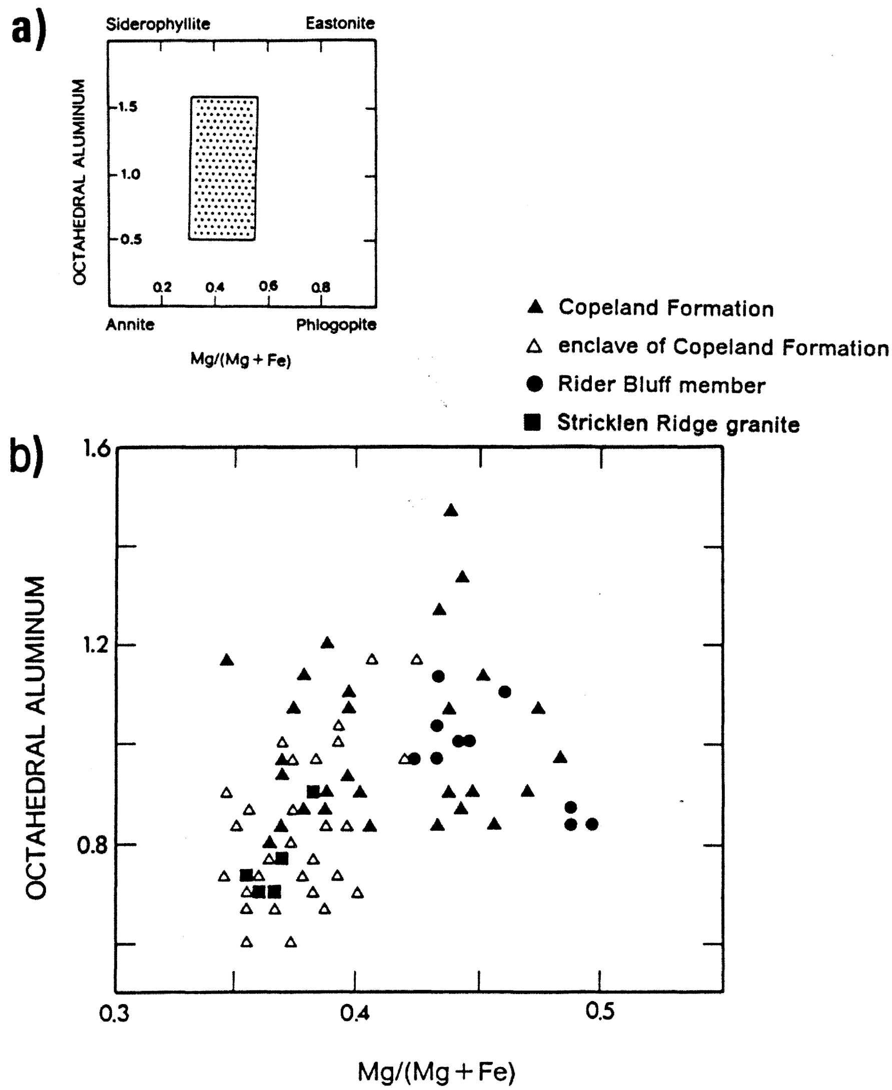

Figure 18. Composition of biotite. a. Biotite quadrilateral. Stipled area enlarged in b. b. Enlarged portion of biotite quadrilateral showing composition of biotite.

Al^{VI} = 0.60-1.15 and Mg/Mg + Fe_{Total} = 0.35-0.43 (Fig. 18). These Al^{VI} and Mg/Mg + Fe_{Total} values are slightly lower than values for biotite from the metasediments (Fig. 18). Both groups are 'typical' biotite compositions from muscovite-bearing assemblages in pelitic rocks metamorphosed up to amphibolite facies (Guidotti, 1984). Included in Fig. 18 is biotite from different units (Copeland Formation and Rider Bluff member) interpreted to have grown during each of the different events (D_1, D_2, D_3 , and D_4) discussed in the text (e.g. inclusions in M_{1-2} porphyroblasts, undeformed and kinked + recrystallized M_{1-2} porphyroblasts, and folia defining post-M_{1-2} fabrics).

Muscovite is uniform in composition across the study area (representative compositions, see Table 8). In the Copeland Formation and Rider Bluff member it is 85-93% muscovite and 15-7% paragonite. In the Stricklen Ridge granite and enclaves of Copeland Formation in the granite it is 90-94% muscovite and 6-10% paragonite. Negligible amounts of margarite component occur in analyzed muscovite, and phengite component in muscovite from all rock types is also uniform (Table 8).

Conditions of Metamorphism

Sillimanite-bearing assemblages (Table 5) occur in the Copeland Formation within ~0.6 km of Stricklen Ridge granite stocks, and lower grade assemblages are stable with increasing distance from these stocks, suggesting that M_{1-2} metamorphism is related to the intrusion of Stricklen Ridge granite. Occurrence of staurolite as embayed grains mantled by optically continuous andalusite in the Copeland Formation suggests the reaction: (1) staurolite + muscovite + quartz = biotite + aluminum silicate + garnet + H_2O. Muscovite, quartz, and sillimanite are abundant in the Copeland Formation near the Stricklen Ridge granites, but K-feldspar is absent, suggesting that the reaction: (2) muscovite + quartz = K-feldspar + aluminum silicate + H_2O has not occurred. Andalusite/sillimanite textures (Fig. 15a) and the absence of kyanite suggest that

Table 8. Representative muscovite compositions. H_2O was not analyzed but is added into total oxides based on the calculated mineral formula. Musc, muscovite; Parg, paragonite; Marg, margarite. Sample locations plotted in Fig. 21.

	1	2	3	4	5
SiO_2	45.63	46.27	46.66	45.85	46.26
TiO_2	0.48	0.37	0.58	0.65	0.12
Al_2O_3	34.21	34.94	34.15	33.08	33.67
FeO	1.41	1.53	1.04	2.69	2.54
MnO	0.0	0.0	0.01	0.05	0.03
MgO	0.63	0.47	0.52	0.71	0.68
CaO	0.02	0.0	0.0	0.04	0.12
BaO	0.31	0.28	0.26	0.02	0.06
Na_2O	0.96	1.08	0.80	0.64	0.39
K_2O	9.39	9.30	9.69	10.05	10.21
F	0.04	0.03	0.04	0.04	0.08
H_2O	4.38	4.45	4.43	4.38	4.39
Sum	97.46	98.72	98.18	98.20	98.55
number of cations on the basis of 12 anions					
Si	3.105	3.105	3.143	3.121	3.133
Al^{IV}	0.895	0.895	0.857	0.879	0.867
Al^{VI}	1.849	1.867	1.854	1.775	1.819
Ti	0.025	0.019	0.029	0.033	0.006
Fe	0.080	0.086	0.059	0.153	0.144
Mn	0.0	0.0	0.001	0.003	0.002
Mg	0.064	0.047	0.052	0.072	0.069
Ca	0.001	0.0	0.0	0.003	0.009
Na	0.127	0.141	0.104	0.084	0.051
K	0.815	0.796	0.833	0.873	0.882
Ba	0.008	0.007	0.007	0.001	0.002
F	0.009	0.006	0.009	0.009	0.017
H	1.988	1.992	1.991	1.989	1.983
Musc	86.25	85.00	88.85	90.90	93.64
Parg	13.60	15.00	11.15	8.80	5.44
Marg	0.15	0.0	0.0	0.30	0.92

1. Copeland Formation, fresh S_1 muscovite, #SR-17A.
2. Copeland Formation, mica fish in mylonite, #SR-27B.
3. Copeland Formation, folded S_1 muscovite, #SR-15.
4. Enclave of Copeland Formation in Stricklen Ridge granite, #SR-9B.
5. Stricklen Ridge granite, #SR-9D.

sillimanite crystallized by the reaction: (3) andalusite = sillimanite. Metamorphic reactions (1), (2), and (3) bracket the pressure-temperature space where peak metamorphic conditions occurred (Fig. 19), assuming that $P_{H_2O} = P_{Total}$ and that the assemblages represent peak metamorphic conditions as suggested by the mineral textures.

Pressure-temperature brackets depend on the choice of aluminum silicate triple point data. Richardson and others' (1969) and Holdaway's (1971) triple point data are the two generally accepted data sets. Holdaway's (1971) data is argued to be: 1, the only set consistent with all of the experimental data (Anderson and others, 1977; Hegelson and others, 1978, p. 117-118; Grambling, 1981, 1984; and Hodges and Spear, 1982), and 2, preferred by field petrologists who have tested aluminum silicate occurrences against other geothermobarometers (Essene, 1982). Holdaway's (1971) data is therefore preferred and plotted in Fig. 19. However, Richardson and others' (1969) data place the triple point (and therefore the first appearance of sillimanite) close to the upper stability of staurolite + quartz and are therefore consistent with the petrographic evidence of many studies (e.g. Turner, 1981; Bickle and Archibald, 1984). Furthermore, the lower pressure-temperature triple point of Holdaway (1971) implies the first appearance of sillimanite within the chloritoid stability field, and sillimanite + chloritoid occurrences are rare compared with kyanite and andalusite + staurolite occurrences (Holdaway, 1978; Bickle and Archibald, 1984). Because of these conflicting arguments, Richardson and others' (1969) data are plotted for comparison (Fig. 19). Holdaway's (1971) data bracket peak M_{1-2} metamorphic conditions at 1-2.5 kb and 490°-615°C (Fig. 19). For comparison, Richardson and others' (1969) data bracket pressure-temperature conditions at 1-5 kb and 490°-680°C (Fig. 19). Both pressure-temperature brackets suggest amphibolite facies metamorphic conditions (Winkler, 1979, p. 65). In Ca-poor rocks, paragonite in solid solution with muscovite lowers the temperature at which muscovite + quartz (reaction 2; Fig. 19) is stable (Chatterjee and Froese, 1975). Muscovite in the Copeland Formation contains 10-15% paragonite and negligible margarite (Table 8).

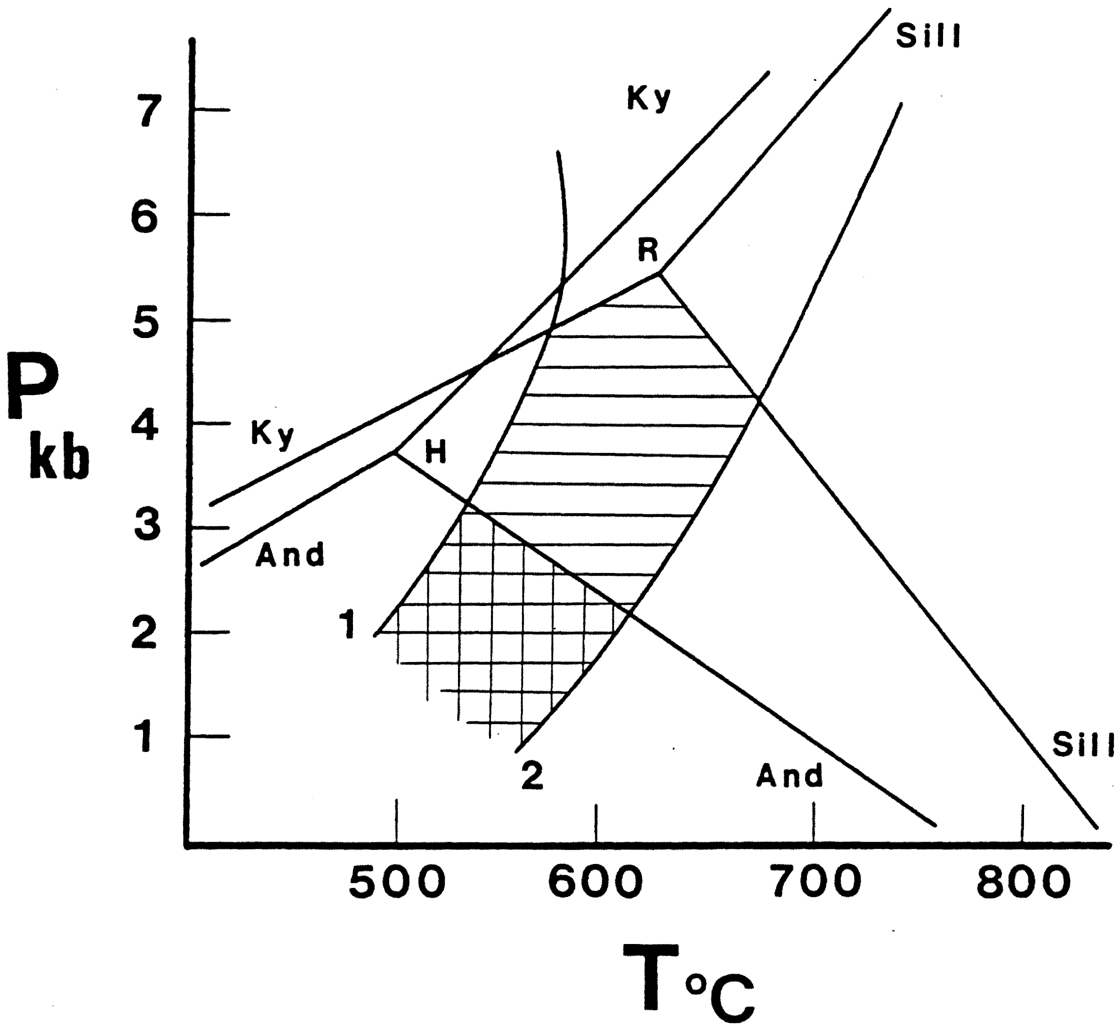

Figure 19. Selected reactions bracketing pressure-temperature conditions of M_{1-2} porphyroblasts. Aluminum silicate data: R, Richardson and others, 1969; H, Holdaway, 1971. Reaction 1, staurolite + muscovite + quartz = biotite + garnet + aluminum silicate + H_2O (Carmichael, 1978; Archibald and others, 1983). Reaction 2, muscovite + quartz = aluminum silicate + K-feldspar + H_2O (Chatterjee and Johannes, 1974). H_2O on high-temperature side of all reactions. Pressure-temperature space bracketing peak conditions: horizontal ruling, assumes Richardson and others's (1969) data; vertical ruling, assumes Holdaway's (1971) data.

This muscovite composition lowers the equilibrium temperature of reaction (2) ~30°-50°C (Chatterjee and Froese, 1975). The temperature bracket is therefore reduced to 490°-575°C, temperatures still consistent with amphibolite facies.

Minimum pressure of crystallization of granitic magmas may be estimated by comparison of rock composition to experimental work in the quartz-orthoclase-albite-anorthite-H_2O system. This approach assumes the granitic magma was H_2O -saturated and a minimum melt. The abundance of aplites, tourmaline-bearing pegmatites, and miarolitic cavaties in Stricklen Ridge granite suggests H_2O saturation (see Appendix). Normative compositions of two samples of Stricklen Ridge granite are plotted in the quartz-albite-orthoclase ternary diagram in Fig. 20. Normative data from Carl and others (1984) is plotted because their modal data compare well with the data of this study (see Appendix). The normative composition of a typical granite sample in this study was calculated from modal and mineral chemical data. Also plotted in Fig. 20 are compositions of minimum granite liquids as a function of Ab/An ratio and pressure. This data was compiled by Anderson and Cullers (1978) from the experimental data of Winkler and Von Platen (1957, 1958, 1960, 1961), Von Platen (1965), Von Platen and Höller (1966), James and Hamilton (1969), and Brown and Fyfe (1970). Normative compositions of Stricklen Ridge granite plot near minimum compositions for granitic liquids at < 1 kb (Fig. 20), suggesting that Stricklen Ridge granite represents a minimum melt that crystallized at or near this pressure. This pressure is consistent with that independently derived for crystallization of M_{1-2} porphyroblasts (1-2.5 kb), suggesting that both events occurred at approximately the same depth.

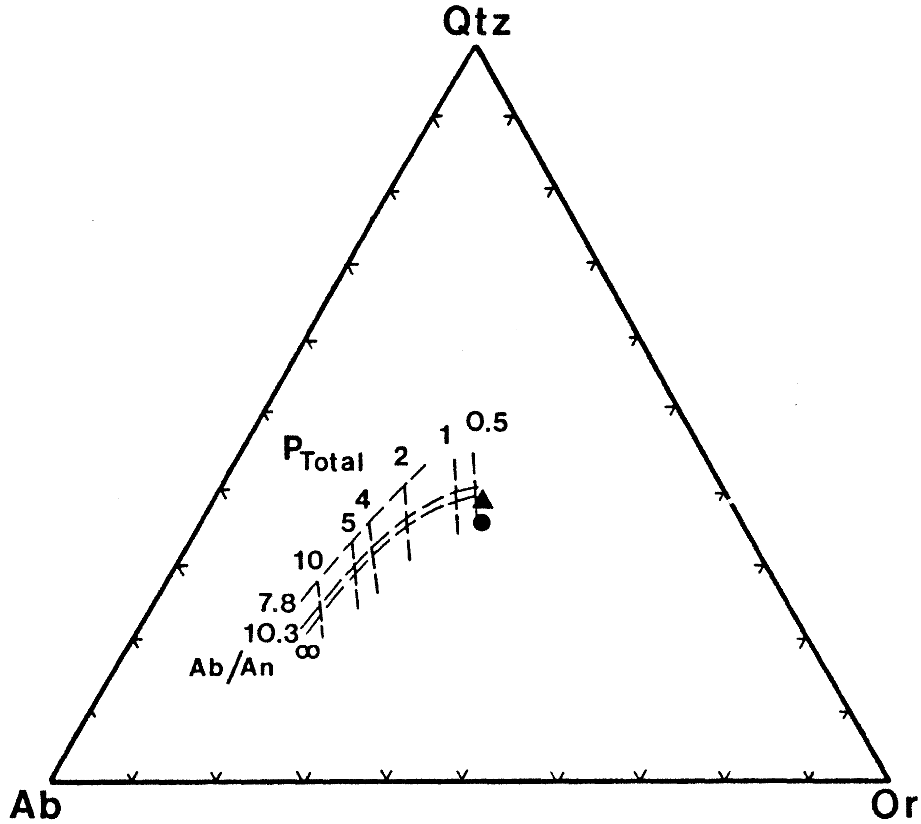

Figure 20. Normative compositions of Stricklen Ridge granite in terms of quartz (Qtz), albite (Ab), and orthoclase (Or) and comparison to experimental work in the granite system. Minimum melt compositions plotted as a function of Ab/An ratio and pressure. Solid circle, calculated normative composition of representative granite sample from this study; solid triangle, normative data of Carl and others (1984). Minimum melt experimental grid compiled by Anderson and Cullers (1978) from the experimental data of Winkler and Von Platen (1957, 1958, 1960, 1961), Von Platen (1965), Von Platen and Höller (1966), James and Hamilton (1969), and Brown and Fyfe (1970).

Geothermobarometry

The presence of garnet-biotite assemblages in the metasediments provides a means to quantitatively evaluate peak metamorphic conditions. The results of two calibrations of the garnet-biotite geothermometer are listed with the data in Table 9. The Thompson (1976) calibration was chosen because it is empirically derived by comparison of natural assemblages with experimental phase equilibria, and the Ferry and Spear (1978) experimental calibration was chosen because it accounts for pressure. The occurrence of peak metamorphic conditions near reaction (3) and the absence of kyanite suggest a maximum pressure of the aluminum silicate triple point: 3.76 kb (Holdaway, 1971). This triple point pressure is used as the upper pressure limit in the Ferry and Spear (1978) calibrations. However, an increase of ~2.5 kb increases temperatures no more than 9°C, therefore pressure does not significantly effect the results.

Although neither calibration used in this study accounts for compositional effects outside of the Fe-Mg binary, and garnet in these rocks is spessartine-rich (Table 6), the results of these calibrations yield reasonable results that are consistent with the pressure-temperature conditions bracketed in Fig. 19. The data suggest temperatures increase with closer proximity to Stricklen Ridge granite stocks (Table 9; Fig. 21).

RELATIONSHIP BETWEEN STRUCTURE AND METAMORPHISM

Mesoscopic and Macroscopic

Folds defined by contacts between metasedimentary units display a closed geometry and refolded pattern characteristic of F_1 (Figs. 2, 5). S_1 parallels the axial trace of these folds (Figs. 2, 5), and geometric relationships between S_0 and S_1 and the closures

Table 9. Compositional parameters of co-existing biotite and garnet and temperatures (in °C) calculated from the Fe-Mg exchange equilibrium between biotite and garnet. Calibrations: T_1, Thompson, 1976; T_2, Ferry and Spear, 1978. Pound sign = number of analyses or temperatures averaged. Average deviation enclosed in parentheses. #SR-9B is an enclave of Copeland Formation in Stricklen Ridge granite. #SR-9D is Stricklen Ridge granite. #SR-27B is mylonitic Copeland Formation. Sample locations plotted in Fig. 21.

	Garnet			Biotite			Temperature		
Sample	#	Fe	Mg	#	Fe	Mg	#	T_1	T_2
SR-1A	2	(.004)	(.001)	2	(0.0)	(.003)	4	(10)	(12)
core		1.322	0.118		1.174	1.114		422	393
SR-1A	2	(.012)	(.002)	2	(0.0)	(.003)	4	(8)	(12)
rim		1.374	0.118		1.714	1.114		410	386
SR-35	3	(.119)	(.024)	2	(.029)	(.024)	6	(12)	(49)
core		1.073	0.074		1.291	0.989		453	392
SR-35	3	(.124)	(.024)	2	(.029)	(.024)	6	(20)	(35)
rim		1.651	0.139		1.291	0.989		457	436
SR-9B	3	(.028)	(.014)	3	(.115)	(.050)	3	(11)	(22)
core		1.722	0.241		1.464	0.875		630	664
SR-9B	6	(.172)	(.054)	3	(.115)	(.050)	6	(42)	(65)
rim		1.697	0.202		1.464	0.875		595	617
SR-9D	7	(.073)	(.027)	3	(.090)	(.013)	7	(36)	(69)
core		1.779	0.268		1.397	0.812		664	729
SR-9D	14	(.080)	(.043)	3	(.090)	(.013)	14	(63)	(62)
rim		1.724	0.225		1.397	0.812		622	659
SR-2H	2	(.012)	(.012)	3	(.047)	(.030)	3	(3)	(7)
pairs		1.982	0.316		1.230	0.982		594	617
SR-5	1			3	(.031)	(.066)	3	(18)	(44)
		2.238	0.275		1.317	0.781		607	629
SR-15	3	(.016)	(.004)	3	(.017)	(.039)	3	(4)	(23)
		2.060	0.236		1.396	0.849		574	594
SR-17A	4	(.034)	(.012)	8	(.085)	(.078)	4	(2)	(13)
core		2.086	0.247		1.413	0.877		582	599
SR-17A	6	(.039)	(.024)	8	(.085)	(.078)	6	(25)	(28)
rim		2.093	0.244		1.413	0.877		574	593
SR-27B	2	(.077)	(.002)	6	(.133)	(.145)	12	(21)	(50)
		2.036	0.296		1.171	0.944		570	580

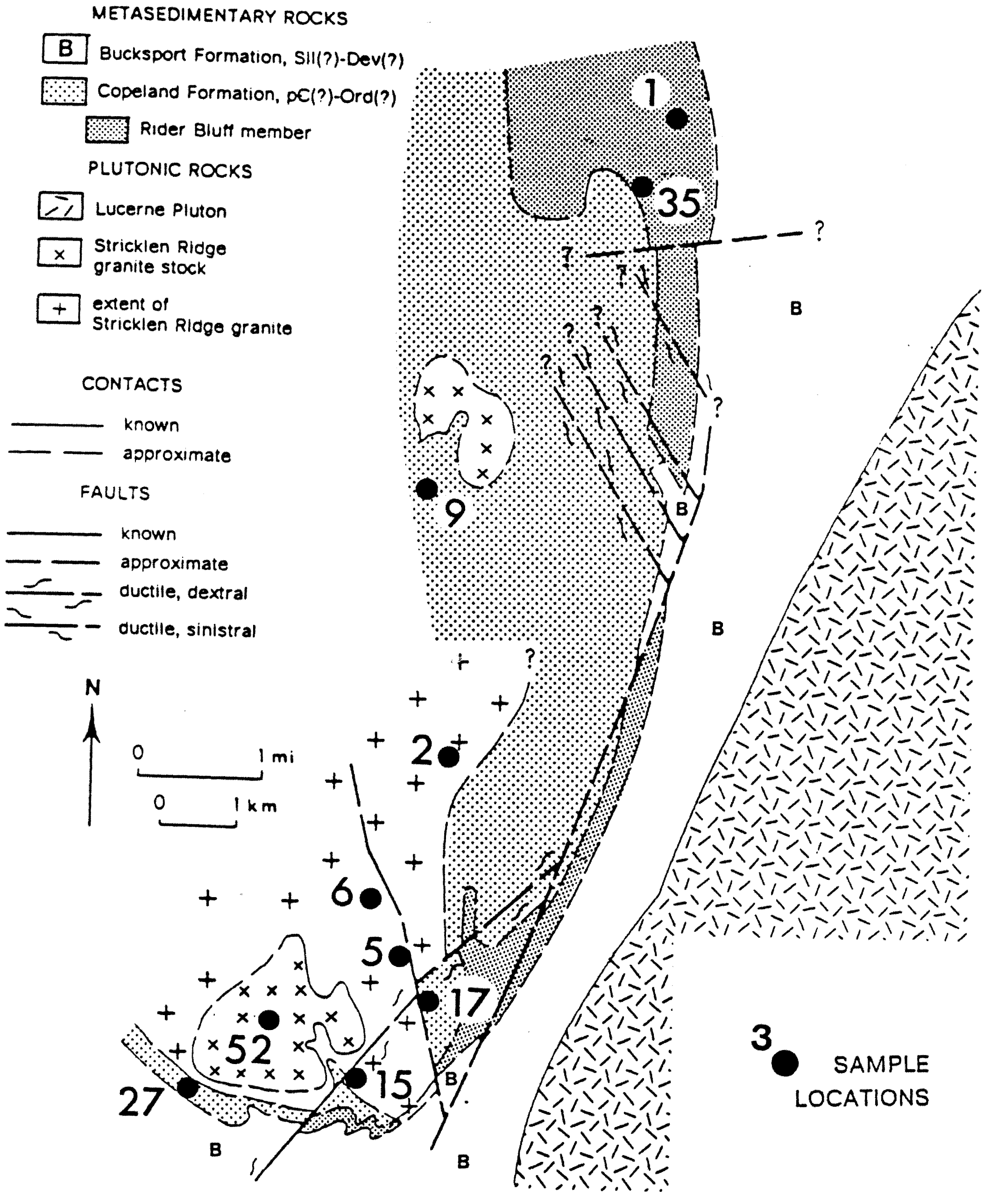

Figure 21. Location of representative samples. Within tables that refer to this Figure, letters following sample numbers refer to one of several samples collected from one location (e.g. #SR-9B and #SR-9D in Table 9 were collected from #SR-9 plotted above). Data for Lucerne pluton from Wones (1980).

of these folds (i.e. cleavage/bedding relationship, Ramsay, 1967, p. 410-411) are consistent with F_1 folding. These contacts are therefore interpreted as being deformed by F_1. S_0 and S_1 compositional layering are distinguished from each other in F_1 fold noses where S_0 is transposed into S_1. F_1 and F_4 fold hinges are subparallel (Figs. 3d, 6b, 13b), suggesting that the range of F_1 axial plane orientations (Fig. 6a) may be partly the result of refolding about the F_4 fold axis.

The domainal distribution of F_2 fold orientations may be controlled by the superposition of F_2 on F_1 or by refolding of F_2 by F_4. However, the change in strike of F_2 axial planes from north-south (Fig. 10c) to northeast-southwest (Fig. 10a) and in F_2 fold hinge orientations from moderate north-northeast and south-southwest plunges (Fig. 10d) to gentle northeast plunges (Fig. 10b) occurs with closer proximity to the NFZ, suggesting that right-lateral strike-slip movement on the NFZ reoriented F_2 structures in the northern portion of the study area.

The NFZ is a major strike-slip fault zone near the study area with a long history of Paleozoic ductile and Late Paleozoic and Mesozoic brittle deformation (Wones and Stewart, 1976; Wones, 1978; Loiselle and Wones, 1983; Johnson and Wones, 1984). The majority of D_3 shear zones are subparallel to and display the same movement sense as the NFZ (e.g. A on Fig. 11), suggesting they are related to the same deformation event. The orientation and sense of motion of deformation zones oblique to the NFZ trend (e.g. B on Figs. 11 and 14) suggest they may be second-order shears similar to those discussed by Chinnery (1966a, 1966b). Conjugate sets of vertical northeast-trending dextral and north- to northwest-trending sinistral ductile shear zones and brittle faults and fractures occur along the entire extent of the NFZ (Wones, 1978; Loiselle and Wones, 1983; Johnson and Wones, 1984).

The northeast-trending shear zone (A on Fig. 11) and nearby brittle structures that parallel it (A on Fig. 14) coincide with the Penobscot Lineament of O'Leary and others (1978), a 0.8 km wide zone that trends ~025° from eastern Penobscot Bay for at least

64 km to north of the Lucerne pluton. It is represented topographically by aligned streams and elongate lakes and hills, and geologically by right-lateral ductile shear zones and brittle faults (O'Leary and others, 1978).

Microscopic

Index minerals that uniquely define a metamorphic facies are absent from tectonic fabrics formed during each ductile deformation event. Metamorphic conditions for each ductile event are bracketed based on the mineral assemblages that are present to define each fabric, microstructures displayed by these minerals, and textural relationships among minerals of different tectonic fabrics.

The mineral assemblages interpreted to be stable in S_1 and in the S_i of M_{1-2} porphyroblasts are listed in Table 5. The presence of quartz pressure shadows containing fibrous minerals, the truncation of quartz grains along S_1 cleavage zones, and the concentration of phyllosilicates and sulfide minerals within these zones in Bucksport Formation siltstones suggest that pressure solution (Rutter, 1976) was an important deformation mechanism in this lithology during D_1. Deformation mechanism maps (Ashby, 1972) suggest that dislocation flow and diffusional mass transfer mechansims may both occur at greenschist facies metamorphic conditions, and that diffusive mass transfer may predominate at smaller grain-sizes (Rutter, 1976; White, 1976). Therefore, fine-grained siltstones of the Bucksport Formation probably deformed predominantly by pressure solution. However, evaluation of deformation mechanisms operative at a specific temperature and grain-size is imprecise because these mechansims are also functions of mineralogy, strain rate, fluid pressure, fluid composition, and confining pressure.

In the Copeland Formation, Rider Bluff member, and calcareous Bucksport Formation, the occurrence of undulatory extinction, elongate subgrains and recrystallized new grains, deformation bands, and core and mantle structures in quartz within S_1 suggests it has deformed by dislocation creep (Nicolas and Poirier, 1976; White, 1976). Internal strain of the quartz lattice was relieved by dynamic recovery and dynamic recrystallization (Nicolas and Poirier, 1976; White, 1976, 1977). The similarity of plagioclase microstructures to those observed in quartz suggests they may have the same origin (Olsen and Kohlstedt, 1985). However, the parallel relationship between quartz grain-shape preferred orientations and axial planes of F_2 and F_4 microfolds (Fig. 7d; Table 4) suggests that dynamic recrystallization which produced these quartz fabrics is related to post-D_1 deformation (D_2 and D_4). Intracrystalline strain observed in quartz and plagioclase in the Copeland and Bucksport Formations and the Rider Bluff member is therefore the result of dislocation creep during D_2 and D_4.

M_{1-2} mineral assemblages (Table 5) and textures suggest M_{1-2} metamorphism occurred at 490°-575°C and 1-2.5 kb (Fig. 19) (amphibolite facies conditions). M_{1-2} porphyroblasts overgrow S_1 (Fig. 15a) and are deformed by D_2 , D_3, and D_4 structures, suggesting that M_{1-2} occurred between D_1 and D_2. However, M_{1-2} may have been part of a continuum of events at the end of D_1 or the beginning of D_2 . Stricklen Ridge granite intrusion occurred between D_1 and D_2 at a minimum pressure of crystallization of < 1.0 kb (3.8 km) (Fig. 20). Sillimanite-bearing M_{1-2} mineral assemblages occur in Copeland Formation pelites next to and within Stricklen Ridge granite stocks, and progressively lower-grade M_{1-2} assemblages occur with increasing distance from these stocks. Temperatures calculated from garnet-biotite geothermometry (Table 9) display a pattern of increased temperature with closer proximity to the stocks. These relationships suggest that M_{1-2} metamorphism may have occurred in a contact aureole in association with the intrusion of Stricklen Ridge granite.

The mineral assemblages interpreted to be stable in S_2 and L_2 are listed in Table 5. These assemblages commonly occur as retrograde products of M_{1-2} porphyroblasts and suggest D_2 deformation occurred under greenschist facies metamorphic conditions.

Albite may begin to deform ductilely under upper greenschist to lower amphibolite facies metamorphic conditions (Lorimer and others, 1974; Wilson, 1980), but amphibole generally does not deform ductilely until lower amphibolite facies (Brodie and Rutter, 1985). The stable presence of phyllosilicates in S_2 and L_2 and the retrogression of calcic amphibole to biotite + calcite suggests that at least some water was present during D_2. Experimental studies indicate that the transition from brittle to ductile behavior in feldspars is lowered ~200°C in the presence of trace amounts of water (Tullis and Yund, 1980), and the strength and ductility of quartz and olivine are similarly sensitive to the concentration of structurally-bound water and/or the presence of intergranular water (e.g. Hobbs, 1981; Kekulawala and others, 1981; Mackwell and others, 1985). Similar behavior is therefore also expected for amphibole. Ductile microstructures in albite and calcic amphibole are therefore interpreted as having formed under upper greenschist to lower amphibolite facies metamorphic conditions. The presence of quartz pressure shadows containing fibrous minerals and the truncation of quartz grains along and the concentration of sulfide minerals within S_2 cleavage zones in siltstones of the Bucksport Formation suggest that pressure solution (Rutter, 1976) was an important S_2-forming mechanism in that lithology.

In general, plagioclase (oligoclase and andesine) and K-feldspar deformed under upper amphibolite to granulite facies metamorphic conditions deform ductilely whereas they are relatively strong and resistant to ductile deformation under greenschist to lower amphibolite facies metamorphic conditions (Marshall and Mclaren, 1977; Tullis, 1983; Tullis and Yund, 1985). However, development of subgrains, recrystallized new grains, and core and mantle structures have been reported for feldspars deformed under lower amphibolite facies metamorphic conditions (e.g. White, 1975; Hanmer, 1982; Simpson, 1985). Phyllosilicates are stable in the mylonitic foliation (S_3), suggesting the presence of water and consequently the reduction of the metamorphic conditions under which feldspar begins to deform ductilely (Tullis and Yund, 1980). The lack of upper amphibolite to granulite facies mineral assemblages and the presence of water during deformation suggest that feldspar porphyroclast textures formed under upper greenschist to lower amphibolite facies metamorphic conditions in D_3 shear zones. Ductile microstructures in feldspar, quartz, and micas reported for shear zones in the NFZ (Johnson and Wones, 1985) are similar to those in D_3 shear zones, suggesting that both structures formed under similar deformation conditions, probably during the same deformation event. However, metamorphic condition estimates based on feldspar microstructures are probably imprecise because the ductile response of feldspar is controlled by strain rate, fluid pressure and composition, and confining pressure as well as temperature and the presence of water.

The mineral assemblages interpreted to be stable in S_4 (Table 5) suggest D_4 deformation occurred under greenschist facies metamorphic conditions. The prevalence of mineral assemblages consistent with greenschist facies metamorphism in all three fold events (Table 5) seems a bit fortuitous. Greenschist facies assemblages clearly define L_2, S_2 , and S_4 and are probably representative of the conditions prevalent during D_2 and D_4. However, it is possible that D_1 contained different metamorphic assemblages which have not survived M_{1-2} metamorphism or subsequent deformation. Greenschist facies conditions for D_1 are therefore only best estimates.

TECTONIC SIGNIFICANCE

There has been some debate as to whether the boundary between the Passagassawakeag (PGW) and Bucksport terranes is tectonic or lithologic in nature (Stewart and Wones, 1974; Wones, 1976; Osberg, 1980; Gates and others, 1984; Kaszuba and Wones, 1985; Osberg and others, 1985; Hussey, 1968, 1985). Although the present study does not conclusively resolve the conflict, several observations are relevant. D_1 is characterized by tight to isoclinal folding and the formation of a strong S_1 axial plane.

The Stricklen Ridge granite cuts D_1 structures and has been assigned a 412 ± 14 Ma age (Zartman and Gallego, 1979), therefore D_1 must be pre-Late Silurian to Early Devonian in age. Since F_1 folds occur within, and deform contacts between, all three metasedimentary units, these units and therefore the PGW and Bucksport terranes must have been in contact and have shared a common structural and metamorphic history by the time of D_1 at the latest. Emplacement of the PGW terrane as a thrust sheet over the Bucksport terrane could not have taken place between 390 and 410 my as suggested by the preliminary work of Kaszuba and Wones (1985). These interpretations are consistent with Ludman's (1981, 1985) suggestion that the terranes of coastal Maine were not exotic to each other by Early Devonian at the latest. Ludman (1981, 1985) based his interpretation on the lack of stratigraphic and metamorphic discontinuities between, and the structural and radiometric age continuity across, the terranes of northeast Maine (i.e. Fredericton Trough area, Fig. 1b).

Several authors have grouped the Bucksport, Vassalboro, and Flume Ridge Formations into one terrane (the Silurian-Early Devonian central Maine turbidite belt) based on lithologic and age similarities (Hussey, 1978; Osberg, 1980; Gates and others, 1984). If this correlation of the Bucksport Formation with the Silurian- to Devonian-aged Vassalboro and Flume Ridge Formations is valid, then D_1 must be no older than Silurian. Precambrian (?) to Early Ordovician (?) units of the PGW terrane are interpreted to structurally overlie units of the central Maine turbidite belt along a pre-metamorphic thrust fault because of the apparent age disparity between these units (Osberg, 1980; Gates and others, 1984; Hussey, 1985). The occurrence of a pre-metamorphic thrust fault between the PGW and Bucksport terranes (Copeland and Bucksport Formations) is neither proven nor disproven by this study. However, any pre-metamorphic thrust fault separating the PGW and Bucksport terranes could be no older than the Silurian. D_1 and pre-metamorphic thrusting would therefore be Acadian events. If the correlation of Vassalboro and Bucksport Formations is not correct, however, and the Bucksport Formation is pre-Silurian in age, then D_1, and pre-metamorphic thrusting if present, could be Taconic events. Pre-Acadian (Taconic ?) isoclinal folding has been recognized in northeast Maine both north and east of the Fredericton Trough (Ludman, 1981, 1985) (Fig. 1b). Most other first-recognized folds in coastal Maine are recumbent isoclines assigned to the Acadian orogeny (Bickel, 1976; Ludman, 1981; Hussey, 1985), and structural features of undoubted Taconic age are exposed only in western Maine (Osberg, 1978).

Correlation of the Bucksport Formation with the Vassalboro and Flume Ridge Formations and separation of the PGW and Bucksport terranes by an Acadian pre-metamorphic thrust fault are based on extensive mapping and stratigraphic analysis (Hussey, 1978, 1985; Osberg, 1980; Gates and others, 1984; Osberg and others, 1985). No existing evidence contradicts these interpretations, and D_1 is therefore interpreted as an Acadian event. Quartz veins are abundant in the Copeland Formation and Rider Bluff member near the PGW/Bucksport terrane boundary and are deformed by the entire structural sequence. Extensive quartz veining may reflect the presence of large amounts of fluid associated with faulting (e.g. Etheridge and others, 1983) and may mark the trace of the pre-metamorphic thrust fault.

The M_{1-2} event is a static metamorphism which occurred under amphibolite facies conditions between two ductile deformation events (D_1 and D_2). M_{1-2} metamorphism may have been a discrete event or part of a continuum of events at the end of D_1 or at the beginning of D_2. Intrusion of Stricklen Ridge granite and growth of M_{1-2} porphyroblasts at similar pressure-temperature conditions between D_1 and D_2, and prevalence of sillimanite-bearing M_{1-2} mineral assemblages and increased garnet-biotite temperatures with closer proximity to Stricklen Ridge granite stocks suggest that M_{1-2} metamorphism may have occurred in a contact aureole in association with the intrusion of Stricklen Ridge granite. Narrow, sillimanite-bearing thermal aureoles around granitic intrusions have also been reported from a number of other localities in New England

(Naylor, 1971). $M_{1\text{-}2}$ metamorphism is probably not related to intrusion of the nearby Lucerne pluton (Figs. 1b, 2). The Lucerne pluton is probably younger than deformation that affects $M_{1\text{-}2}$ porphyroblasts, and its contact aureole is only ~1 km wide (Novak, 1979). Sillimanite-bearing mineral assemblages and pervasive granitic intrusions occur throughout the PGW Formation to the west of the study area (Stewart and Wones, 1974; Guidotti, 1985), and their presence may be the result of regional, high-grade metamorphism. Granitic plutons may have been convectors of heat that produced local hotspots where they intruded.

D_2 is characterized by open, upright folding and the formation of a strong, hinge-parallel mineral lineation under upper greenschist to lower amphibolite facies metamorphic conditions. D_2 structures deform the 412 ± 14 Ma Stricklen Ridge granite but reportedly do not effect the 380 ± 4 Ma Lucerne pluton (Kaszuba and Wones, 1985). D_2 is therefore assumed to have occurred during the Acadian orogeny when upright folding occurred throughout New England (Osberg, 1978: Ludman, 1981; Hussey, 1985).

The Norumbega Fault Zone (NFZ) is a major structure near the study area. The orientation, sense of motion, and inferred deformation conditions (upper greenschist to lower amphibolite) for D_3 shear zones in the study area suggest they are related to the same deformation event. The coincidence of the Penobscot Lineament with D_3 shear zones and brittle structures suggests it is a second-order shear of the NFZ and not a major, continuous zone of faulting and shearing as suggested by O'Leary and others (1978). D_4 is characterized by open, reclined folding under greenschist facies metamorphic conditions. The relationship between the orientation of F_4 folds and the NFZ (Fig. 13) suggests that the stress field which produced right-lateral strike-slip movement on the NFZ could also have caused F_4 folding. Eusden and others (1986) suggest a similar relationship between folding and strike-slip faulting in southwestern Maine along a continuation of the NFZ. D_4 may therefore represent a later, lower temperature episode of the same stress event which produced the NFZ. Alternatively,

D_4 could represent a discrete ductile event unrelated to the one that produced the NFZ, but no such event is recognized elsewhere in coastal Maine (Hussey and Newburg, 1978; Hussey, 1985). D_3 shear zones and D_4 folds do not represent deformation associated with intrusion of Stricklen Ridge granite or the Lucerne pluton. D_3 deforms Stricklen Ridge granite, and shear zones similar to D_3 shear zones occur within and deform the Lucerne pluton (Wones, 1980). Furthermore, D_3 shear zones are probably related to the same deformation event as the NFZ, and the NFZ truncates the Lucerne pluton (Fig. 1b).

Brittle fracturing and faulting is common along the entire NFZ (Hussey, 1978, 1985; Hussey and Newburg, 1978; Wones, 1978; Ludman, 1981; Johnson and Wones, 1984). Brittle joints and faults cut all ductile structures observed in the study area and may be related to the same stress field which initially produced the NFZ, or to a later brittle event which exploited the NFZ as a pre-existing zone of weakness.

CONCLUSIONS

In the Penobscot Bay area of coastal Maine, metasediments of the Copeland Formation and Rider Bluff member in the eastern margin of the Passagassawakeag (PGW) terrane and of the Bucksport Formation in the adjacent area of the Bucksport terrane experienced four phases of ductile deformation (D_1, D_2, D_3 , and D_4) and an interdeformational event ($M_{1\text{-}2}$) of metamorphism and granitic plutonism. The earliest recognizeable deformation phase (D_1) produced F_1 folds and a strong axial plane foliation (S_1) defined by a uniform compositional layering. Since D_1 structures occur within and deform contacts between all metasedimentary units, these units and therefore the PGW and Bucksport terranes must have been in contact and shared a common history by the time of D_1 (early Acadian ?) at the latest. To the southwest of the study area, these terranes are bound by a pre-metamorphic thrust fault. No structural or metamorphic discontinuity coincides with the boundary between these two terranes in the study area, and the occurrence of a pre-metamorphic thrust fault is neither proven nor disproven by this study. A static thermal event (M_{1-2}) of shallow-level (~3.8 km) granitic plutonism (412 ± 14 Ma Stricklen Ridge granite) and porphyroblast growth at 490°-575°C and 1-2.5 kb (amphibolite facies metamorphism) occurred between D_1 and D_2. It may have been a discrete event or a part of a continuum at the end of D_1 or the beginning of D_2. The occurrence of sillimanite-bearing M_{1-2} mineral assemblages and higher temperatures calculated from garnet-biotite geothermometry with closer proximity to stocks of Stricklen Ridge granite suggest that this metamorphism may have occurred in a contact aureole in association with the intrusion of Stricklen Ridge granite. The second ductile deformation event (D_2, Acadian) produced open, upright folds and a strong, hinge-parallel mineral elongation lineation under upper greenschist to lower amphibolite facies metamorphic conditions. The orientation, sense of motion, and inferred deformation conditions (upper greenschist to lower amphibolite) for D_3 shear zones suggest they are related to the same stress system that produced right-lateral strike-slip movement on the Norumbega Fault Zone (Alleghanian). The orientation of open, reclined F_4 folds that formed under greenschist facies conditions suggests D_4 may represent a later, lower-temperature episode related to the same stress system. Brittle structures truncate all ductile structures, and their orientation and sense of movement suggests they are either related to the same stress field which initially produced D_3 and D_4 ductile structures, or to a later brittle event which exploited D_3 shear zones and the Norumbega Fault Zone as pre-existing zones of weakness.

REFERENCES

Anderson, D.E., and Buckley, G.R., Zoning in garnets--diffusion models: Contributions to Mineralogy and Petrology, v. 40, p. 87-104.

Anderson, J.L., and Cullers, R.L., 1978, Geochemistry and evolution of the Wolf River Batholith, a Late Precambrian rapakivi massif in North Wisconsin, U.S.A.: Precambrian Research, v. 7, p. 287-324.

Anderson, P.A.M., Newton, R.C., and Kleppa, O.J., 1977, The enthalpy change of the andalusite-sillimanite reaction and the Al_2SiO_5 diagram: American Journal of Science, v. 277, p. 585-593.

Archibald, D.A., Glover, J.K., Price, R.A., Farrar, E., and Carmichael, D.M., 1983, Geochronology and tectonic implications of magmatism and metamorphism, southern Kootenay Arc and neighboring regions, southeastern British Columbia; Part I: Jurassic to mid-Cretaceous: Canadian Journal of Earth Sciences, v. 20, p. 1891-1913.

Ashby, M.F., 1972, A first report on deformation mechanism maps: Acta. Metall., v. 20, p. 887-897.

Berthé, D., Choukroune, P., and Jegouzo, P., 1979, Orthogneiss, mylonite, and non-coxial deformation of granites: the example of the South Amorican Shear-Zone: Journal of Structural Geology, v. 1, p. 31-42.

Bickel, C.E., 1976, Stratigraphy of the Belfast quadrangle, Maine: Geological Society of America Memoir, no. 148, p. 97-128.

Bickle, M.J., and Archibald, N.J., 1984, Chloritoid and staurolite stability: implications for metamorphism in the Yilgarn Block, Western Australia: Journal of Metamorphic Geology, v. 2, p. 179-203.

Blackburn, W.H., and Dennen, W.H., 1968, Flattened garnets in strongly foliated gneisses from the Grenville series of the Ganonoque area, Ontario: American Mineralogist, v. 53, p. 1386-1393.

Boucot, A.J., Brookins, D.G., Forbes, W., and Guidotti, C.V., 1972, Staurolite zone Caradoc (Middle-Late Ordovician) age, Old World Province Brachiopods from Penobscot Bay, Maine: Geological Society of America Bulletin, v. 83, p. 1953-1960.

Boullier, A.M., and Bouchez, J.L., 1978, Le quartz en rubans dans les mylonites: Buletin de la Société Géologique de France, v. 20, p. 253-262.

Brodie, K.H., and Rutter, E.H., 1985, On the relationship between deformation and metamorphism, with special reference to the behavior of basic rocks; in Thompson, A.B., and Rubie, D.C., eds., Metamorphc Reactions: Kinetics, Textures, and Deformation: Springer-Verlag, New York, p. 138-179.

Brookins, D.G., 1976, Geochronologic contributions to stratigraphic interpretation and correlation in the Penobscot Bay area, eastern Maine: Geological Society of America Memoir, no. 148, p. 129-145.

Brookins, D.G., Berdan, J.M., and Stewart, D.B., 1973, Isotopic and paleontologic evidence for correlating three volcanic sequences in the Maine coastal volcanic belt: Geological Society of America Bulletin, v. 84, p. 1619-1628.

Brookins, D.G., and Hussey, A.M., II, 1978, Rb-Sr ages for the Casco Bay Group and other rocks from the Portland-Orrs Island area, Maine (abs.): Geological Society of America, Abstracts with Programs, v. 10, p. 34.

Brown, G.C., and Fyfe, W.S., 1970, The production of granitic melts during ultrametamorphism: Contributions to Mineralogy and Petrology, v. 28, p. 310-318.

Carl, J.D., Liptak, A.R., Savitz, S.L., Schmidt, D.T., Shay, S.G., Tom, V.J., and Wink, J.T., 1984, Geochemical characteristics of granitoid plutons in the Penobscot Bay area, Maine: Northeastern Geology, v. 6, p. 12-24.

Carmichael, D.M., 1978, Metamorphic bathozones and bathograds: A measure of the depth of post-metamorphic uplift and erosion on the regional scale: American Journal of Science, v. 278, p. 769-797.

Chatterjee, N.D., and Froese, E., 1975, A thermodynamic study of the pseudobinary join muscovite-paragonite in the system $KAlSi_3O_8$ -$NaAlSi_3O_8$- Al_2O_3 - Si_2-H_2): American Mineralogist, v. 60, p. 985-993.

Chatterjee, N.D., and Johannes, W., 1974, Thermal stability and standard thermodynamic properties of synthetic M_1-muscovite, $KAl_2[AlSi_3O_{10}(OH)_2]$: Contributions to Mineralogy and Petrology, v. 48, p. 89-114.

Chinnery, M.A., 1966a, Secondary faulting: I. Theoretical aspects: Canadian Journal of Earth Sciences, v. 3, p. 163-174.

Chinnery, M.A., 1966b, Secondary faulting: II. Geological aspects: Canadian Journal of Earth Sciences, v. 3, p. 175-190.

Coney, P.J., Jones, D.L., and Monger, J.W.H., 1980, Cordilleran suspect terranes: Nature, v. 288, p. 329-333.

Essene, E.J., 1982, Geologic thermometery and barometery, in Ferry, J.M., ed., Characterization of Metamorphism through Mineral Equilibria: Reviews in Mineralogy, v. 10, Mineralogical Society of America, p. 153-206.

Etheridge, M.A., Wall, V.J., and Vernon, R.H., 1983, The role of the fluid phase during regional metamorphism and deformation: Journal of Metamorphic Geology, v. 1, p. 205-226.

Eusden, J.D., Jr., Bothner, W.A., and Hussey, A.M., II, 1986, The Kearsage-Central Maine Synclinorium of southeastern New Hampshire and southwestern Maine: Structural relations of an inverted section (abs.): Geological Society of America, Abstracts with Programs, v. 18, p. 15.

Ferry, J.M., and Spear, F.S., 1978, Experimental calibration of Fe and Mg between biotite and garnet: Contributions to Mineralogy and Petrology, v. 66, p. 113-117.

Fleuty, M.J., 1964, The description of folds: Geol. Assoc. Proc., v. 75, p. 461-492.

Gates, O., Hussey, A.M., II, and Osberg, P.H., 1984, Acadian thrust plates in coastal Maine (abs.): Geological Society of America, Abstracts with Programs, v. 16, p. 17.

Grambling, J.A., 1981, Kyanite, andalusite, and sillimanite, and related mineral assemblages in the Truchas Peaks region, New Mexico: American Mineralogist, v. 66, p. 702-722.

Grambling, J.A., 1984, Coexisting paragonite and quartz in sillimanitic rocks from New Mexico: American Mineralogist, v. 69, p. 79-87.

Guidotti, C.V., 1968, Prograde muscovite pseudomorphs after staurolite in the Rangeley-Oquossoc area, Maine: American Mineralogist, v. 53, p. 1368-1376.

Guidotti, C.V., 1984, Micas in metamorphic rocks; in Bailey, S.W., ed., Micas: Reviews in Mineralogy, v. 13, Mineralogical Society of America, p. 357-467.

Guidotti, C.V., 1985, Generalized map of regional metamorphic zones; in Osberg, P.H., Hussey, A.M., II, and Boone, G.M., Bedrock geologic map of Maine: Maine Geological Survey, Augusta, Maine, scale 1:500,000.

Hanmer, S.K., 1982, Microstructure and geochemistry of plagioclase and microcline in naturally deformed granite: Journal of Structural Geology, v. 7, p. 197-213.

Helgeson, H.C., Delany, J.M., Nesbitt, H.W., and Bird, D.K., 1978, Summary and critique of the thermodynamic properties of rock forming minerals: American Journal of Science, v. 278-A, 229p.

Hobbs, B.E., 1981, The influence of metamorphic environment on the deformation of minerals: Tectonophysics, v. 78, p. 335-383.

Hobbs, B.E., Means, W.D., and Williams, P.F., 1976, An Outline of Structural Geology: New York, John Wiley & Sons, 571p.

Hodges, K.V., and Spear, F.S., 1982, Geothermometery, geobarometry and the Al_2SiO_5 triple point at Mt. Moosilauke, New Hampshire: American Mineralogist, v. 67, p. 1118-1134.

Holdaway, M.J., 1971, Stability of andalusite and the aluminum-silicate phase diagram: American Journal of Science, v. 271, p. 97-131.

Holdaway, M.J., 1978, Significance of chloritoid-bearing rocks in the Picuris Range, New Mexico: Geological Society of America Bulletin, v. 89, p. 1404-1414.

Hussey, A.M., II, 1968, Stratigraphy and structure of southwestern Maine; in Zen, E., White, W.S., Hadley, J.B., and Thompson, J.B., Jr., eds., Studies of Appalachian Geology: Northern and Maritime: New York, Wiley-Interscience, p. 291-301.

Hussey, A.M., II, 1978, Sequence of deformation events in southwestern Maine (abs.): Geological Society of America, Abstracts with Programs, v. 10, p. 48.

Hussey, A.M., II, 1984, Age and correlation of stratigraphic units of southwestern Maine: a reconsideration (abs.): Geological Society of America, Abstracts with Programs, v. 16, p. 26.

Hussey, A.M., II, 1985, The bedrock geology of the Bath and Portland 2°sheets, Maine: Maine Geological Survey, Augusta, Maine, Open File Report no. 85-87, 80p.

Hussey, A.M., II, and Newburg, D.W., 1978, Major faulting in the Merrimack Synclinorium between Hollis, New Hampshire and Biddeford, Maine (abs.): Geological Society of America, Abstracts with Programs, v. 10, p. 48.

Jahns, R.H., and Burnham, C.W., 1969, Experimental studies of pegmatite genesis: I. A model for the derivation and crystallization of granitic pegmatites: Economic Geology, v. 64, p. 843-864.

Jahns, R.H., and Tuttle, O.F., 1963, Layered pegmatite-aplite intrusives: Mineralogical Society of America, Special Paper 1, p. 78-92.

James, R.S., and Hamilton, D.L., 1969, Phase relations in the system $NaAlSi_3O_8$-$KAlSi_3O_8$-$CaAl_2Si_2O_8$ -SiO_2 at 1 kilobar water vapour pressure: Contributions to Mineralogy and Petrology, v. 21, p. 111-141.

Johnson, T.D., and Wones, D.R., 1984, Sense and mode of shearing along the Norumbega Fault Zone, eastern Maine (abs.): Geological Society of America, Abstracts with Programs, v. 16, p. 27.

Johnson, T.D., and Wones, D.R., 1985, Microstructures and sequence of deformation along the Norumbega Fault Zone (abs.): Journal of Structural Geology, v. 7, p. 493-494.

Kane, M.F., and Bromery, R.W., 1966, Simple Bouguer anomaly map of Maine: U.S. Geological Survey Geophysical Investigations Map GP-580, scale 1:500,000.

Kaszuba, J.P., and Wones, D.R., 1985, Early Devonian thrusting in the Penobscot Bay area, Maine (abs.): Geological Society of America, Abstracts with Programs, v. 17, p. 27.

Katz, F.J., 1917, Stratigraphy in southeastern New Hampshire and southwestern Maine: U.S. Geological Survey Professional Paper 108, p. 11-29.

Kekulawala, K.R.S.S., Paterson, M.S., and Boland, J.N., 1981, An experimental study of the role of water in quartz deformation; in Carter, N.L., Friedman, M., Logan, J.M., and Stearns, D.W., eds., Mechanical behavior of crustal rocks, The Handin Volume: American Geophysical Union, Geophysical Monograph 24, Washington, D.C., p. 49-60.

Krauskopf, K.B., 1979, End stages of magmatic crystallization; in Krauskopf, K.B., Introduction to Geochemistry: McGraw-Hill, New York, second edition, p. 346-367.

Kwak, T.A.P., 1974, Natural staurolite breakdown reactions at moderate to high pressures: Contributions to Mineralogy and Petrology, v. 44, p. 57-80.

Lister, G.S., and Snoke, A.W., 1984, S-C mylonites: Journal of Structural Geology, v. 6, p. 617-638.

Loiselle, M., and Ayuso, R.A., 1980, Geochemical and petrographic characteristics of granitoids across the Merrimack synclinorium, eastern and central Maine; in Wones, D.R., ed., The Caledonides in the USA: VPI & SU Memoir, no. 2, p. 117-121.

Loiselle, M., and Wones, D.R., 1983, Plutonism and post-Acadian faulting in east-central Maine; in Hussey, A.M., II, and Westerman, D.S., eds., Maine Geology, Field Trips of the Geological Society of Maine, 1978-1983: The Geological Society of Maine, Inc., Bulletin no. 3, p. 72-85.

Loomis, T.P., and Nimick, F.B., 1982, Equilibrium in Mn-Fe-Mg aluminous pelitic compositions and the equilibrium growth of garnet: Canadian Mineralogist, v. 20, p. 393-410.

Lorimer, G.W., Nissen, H.U., and Champness, P.E., 1974, High voltage electron microscopy of a deformed plagioclase from an Alpine gneiss: Schweizerische Mineralogische und Petrographische Mitteilungen, v. 54, p. 707-715.

Ludman, A., 1978, Stratigraphy, structure, and progressive metamorphism of lower Paleozoic rocks in the Calais area, southeastern Maine; in Ludman, A., ed., Guidebook for Fieldtrips in Southeastern Maine and Southwestern New Brunswick: Queens College Press, Flushing, New York, p. 78-101.

Ludman, A., 1981, Significance of transcurrent faulting in eastern Maine and location of the suture between Avalonia and North America: American Journal of Science, v. 281, p. 463-483.

Ludman, A., 1985, Pre-Silurian (Taconian?) deformation of the Cookson Formation (Cambro-Ordovician) in southeastern Maine (abs.): Geological Society of America, Abstracts with Programs, v. 17, p. 32.

Mackwell, S.J., Kohlstedt, D.L., and Paterson, M.S., 1985, The role of water in the deformation of olivine single crystals: Journal of Geophysical Research, v. 90, p. 11319-11333.

Marshall, D.B., and McLaren, A.C., 1977, The direct observation and analysis of dislocations in experimentally deformed plagioclase feldspars: Journal of Materials Sciences, v. 12, p. 893-903.

Moench, R.H., and Zartman, R.E., 1976, Chronology and styles of multiple deformation, plutonism, and polymetamorphism in the Merrimack Synclinorium of western Maine: Geological Society of America Memoir, no. 146, p. 203-238.

Naylor, R.S., 1971, Acadian orogeny: an abrupt and brief event: Science, v. 172, p. 558-560.

Nicolas, A., and Poirier, J.P., 1976, Crystalline Plasticity and Solid State Flow in Metamorphic Rocks: John Wiley & Sons, London, 444p.

Novak, S.W., 1979, Contact metamorphism of the Lucerne Pluton, Hancock County, Maine; unpublished M.S. thesis, Virginia Polytechnic Institute and State University, Blacksburg, Virginia, 109p.

O'Leary, D.W., Lee, F.T., and Barosh, P.T., 1978, Evidence for faulting along a lineament through Orland, Maine (abs.): Geological Society of America, Abstracts with Programs, v. 10, p. 79.

Olsen, T.S., and Kohlstedt, D.L., 1985, Natural deformation and recrystallization of some intermediate palgioclase feldspars: Tectonophysics, v. 111, p. 107-131.

Osberg, P.H., 1968, Stratigraphy, structural geology and metamorphism of the Waterville-Vassalboro area, Maine: Maine Geological Survey Bulletin, v. 20, 64p.

Osberg, P.H., 1978, Synthesis of the geology of the northeastern Appalachians, U.S.A.; in Caledonian-Appalachian Orogen of the North Atlantic Region: Project 27, International Geologic Correlations Project: Geological Survey of Canada Paper 78-13, p. 137-148.

Osberg, P.H., 1979, Geologic relationships in south-central Maine; in Skehan, J.W., S.J., and Osberg, P.H., eds., The Caledonides in the U.S.A., IGCP Project 27, Geological Excursions in the northeast Appalachians: Department of Geology and Geophysics, Boston College, p. 37-62.

Osberg, P.H., 1980, Stratigraphic and structural relations in the turbidite sequence of south central Maine; in Roy, D.C., and Naylor, R.S., eds., A guidebook to the geology of northeast Maine and neighboring New Brunswick: 72 N.E.I.G.C. Guidebook, Department of Geology and Geophysics, Boston College, p. 278-296.

Osberg, P.H., Hussey, A.M., II, and Boone, G.M., 1985, Bedrock geologic map of Maine: Maine Geological Survey, Augusta, Maine, scale 1:500,000.

Osberg, P.H., Moench, R.H., and Warner, J., 1968, Stratigraphy of the Merrimack synclinorium in west-central Maine, in Zen, E., White, W.S., Hadley, J.B., and Thompson, J.B., Jr., eds., Studies of Appalachian geology, northern and maritime: New York, Interscience Publishers, p. 241-253.

Pankiwskyj, K.A., Ludman, A., Griffin, J.R., and Berry, W.B.N., 1976, Stratigraphic relationships on the southeast limb of the Merrimack Synclinorium in central and west-central Maine: Geological Society of America Memoir, no. 146, p. 263-280.

Perkins, E.H., and Smith, E.S.C., 1925, Contributions to the geology of Maine, no. 1: A geological section from the Kennebec River to Penobscot Bay: American Journal of Science, v. 209, p. 204-228.

Pitcher, W.S., 1979, The nature, ascent, and emplacement of granitic magmas: Journal of the Geological Society of London, v. 136, p. 627-662.

Platt, J.P., and Vissers, R.L.M., 1980, Extensional structures in anisotropic rocks: Journal of Structural Geology, v. 2, p. 397-410.

Powell, C. McA., 1979, A morphological classification of rock cleavage: Tectonophysics, v. 58, p. 21-34.

Ramsay, J.G., 1967, Folding and fracturing of rocks: McGraw-Hill Book Company, New York, 568p.

Richardson, S.W., Gilbert, M.C., and Bell, P.M., 1969, Experimental determination of kyanite-andalusite and sillimanite-andalusite equilibrium: the aluminum silicate triple point: American Journal of Science, v. 267, p. 259-272.

Ruitenberg, A.A., 1967, Stratigraphy, structure, and metallization, Piskahegan-Rolling Dam area, New Brunswick: Leidse geologische mededelingen, v. 40, p. 79-120.

Ruitenberg, A.A., and Ludman, A., 1978, Stratigraphy and tectonic setting of early Paleozoic sedimentary rocks of the Wirral-Big Lake area, southwestern New Brunswick and southeastern Maine: Canadian Journal of Earth Sciences, v. 15, p. 22-32.

Rutter, E.H., 1976, The kinetics of rock deformation by pressure solution: Philosophical Transactions of the Royal Society of London, v. A283, p. 203-219.

Simpson, C., 1984, Borrego Springs-Santa Rosa mylonite zone: A Late Cretaceous west-directed thrust in southern California: Geology, v. 12, p. 8-11.

Simpson, C., 1985, Deformation of granitic rocks across the brittle-ductile transition: Journal of Structural Geology, v. 7, p. 503-511.

Simpson, C., and Schmid, S.M., 1983, An evaluation of criteria to deduce the sense of movement in sheared rocks: Geological Society of America Bulletin, v. 94, p. 1282-1288.

Smith, G.O., Bastin, E.S., and Brown, C.W., 1907, Description of the Penobscot Bay quadrangle: U.S. Geological Survey, Geologic Atlas of the United States Folio 149, 14p.

Spry, A., 1969, Metamorphic Textures: Pergamon Press, Oxford, 350p.

Stewart, D.B., Unger, J.D., Phillips, J.D., Goldsmith, R., Poole, W.H., Spencer, C.P., Green, A.G., Loiselle, M.C., and St-Julien, P., 1986, The Quebec-western Maine seismic reflection profile: Setting and first years results; in Reflection Seismology: The Continental Crust: AGU, Geodynamics Series, v. 14, p. 189-199.

Stewart, D.W., and Wones, D.R., 1974, Bedrock geology of northern Penobscot Bay area; in Osberg, P.H., ed., Geology of east-central and north-central Maine: 66th N.E.I.G.C. Guidebook, University of Maine, Orono, p. 223-240.

Streckeisen, A.L., 1973, Plutonic rocks: Geotimes, v. 18, p. 26-30.

Sweeney, J.F., 1974, Subsurface density distributions east and northeast of Penobscot Bay, south-central Maine; appendix in Wones, D.R., Igneous petrology of some plutons in the northern part of the Penobscot Bay area; in Osberg, P.H., ed., Geology of east-central and north-central Maine: 66th N.E.I.G.C. Guidebook, University of Maine, Orono, p. 115-122.

Sweeney, J.F., 1976, Subsurface distribution of granitic rocks, south-central Maine: Geological Society of America Bulletin, v. 87, p. 241-249.

Thompson, A.B., 1976, Mineral reactions in pelitic rocks: II. Calculations of some P-T-X(Fe-Mg) phase relations: American Journal of Science, v. 276, p. 425-454.

Tracy, R.J., 1982, Compositional zoning and inclusions in metamorphic minerals, in Ferry, J.M., ed., Characterization of Metamorphism through Mineral Equilibria: Reviews in Mineralogy, v. 10, Mineralogical Society of America, p. 355-397.

Trefethen, J.M., 1944, Mt. Waldo batholith and associated igneous rocks, Walso County, Maine: Geological Society of America Bulletin, v. 55, p. 895-904.

Trefethen, J.M., 1950, Bucksport-Orland map area: 42nd N.E.I.G.C. Guidebook, 5p.

Triboulet, C., and Audren, C., 1985, Continuous reactions between biotite, garnet, staurolite, kyanite-sillimanite-andalusite and P-T-time-deformation path in mica-schists from the estuary of the river Vilaine, South Brittany, France: Journal of Metramorphic Geology, v. 3, p. 91-105.

Toteu, S.F., and Macaudiere, J., 1984, Complex synkinematic and postkinematic garnet porphyroblast growth in polymetamorphic rocks: Journal of Structural Geology, v. 6, p. 669-677.

Tullis, J., 1983, Deformation of feldspars; in Ribbe, P.H., ed., Feldspar Mineralogy: Mineralogical Society of America, Reviews in Mineralogy, v. 2, 2nd edition, p. 297-341.

Tullis, J., and Yund, R.A., 1980, Hydrolitic weakening of experimentally deformed Westerly granite and Hale albite rock: Journal of Structural Geology, v. 2, p. 439-451.

Tullis, J., and Yund, R.A., 1985, Dynamic recrystallization of feldspar: a mechanism for ductile shear zone formation: Geology, v. 13, p. 238-241.

Turner, F.J., 1981, Metamorphic Petrology: Mineralogical, Field, and Tectonic Aspects: McGraw Hill, New York, 524p.

Von Platen, H., 1965, Kristallization granitischer Schmelzen: Beiträge zur Mineralogische und Petrographische, v. 11, p. 334-381.

Von Platen, H., and Höller, H., 1966, Experimentelle Anatexis des Stainzer Plattengneisses von der Koralpe, Steiermark, bei 2, 4, 7 und 10 Kb H_2O -Druck: Neues Jahrbuch für Mineralogie Abhandlungen, v. 106, p. 106-130.

White, A.J.R., and Chappell, B.W., 1977, Ultrametamorphism and granitoid genesis: Tectonophysics, v. 43, p. 7-22.

White, S., 1973, The dislocation structures responsible for the optical effects in some naturally deformed quartzites: Journal of Materials Science, v. 9, p. 490-499.

White, S., 1975, Tectonic deformation and recrystallization of oligoclase: Contributions to Mineralogy and Petrology, v. 50, p. 287-304.

White, S., 1976, The effects of strain on the microstructures, fabrics, and deformation mechanisms in quartzites: Philosophical Transactins of the Royal Society of London, v. A283, p. 69-86.

White, S., 1977, Geologic significance of recovery and recryatallization processes in quartz: Tectonophysics, v. 39, p. 143-170.

Wilson, C.J.L., 1980, Shear zones in a pegmatite: a study of albite-mica-quartz deformation: Journal of Structural Geology, v. 2, p. 203-209.

Wing, L.A., 1957, An aeromagnetic and geologic reconnaissance survey of portions of Hancock and Penobscot counties, Maine: Maine Geological Survey, Geophysical and Geological Survey no. 1, 10 sheets.

Wingard, P.S., 1958, Stratigraphic relations between the Ellsworth and Castine Formations, Castine, Maine: Kansas Academy of Science Transactions, v. 61, p. 330-333.

Winkler, H.G.F., 1979, Petrogenesis of Metamorphic Rocks: Springer-Verlag, New York, Fifth Edition, 348p.

Winkler, H.G.F., and Von Platen, H., 1957, Experimentelle Gesteinmetamorphose: Geochimica et Cosmochimica Acta, v. 13, p. 42-69.

Winkler, H.G.F., and Von Platen, H., 1958, Experimentelle Gesteinmetamorphose: Geochimica et Cosmochimica Acta, v. 15, p. 91-112.

Winkler, H.G.F., and Von Platen, H., 1960, Experimentelle Gesteinmetamorphose: Geochimica et Cosmochimica Acta, v. 18, p. 294-316.

Winkler, H.G.F., and Von Platen, H., 1961, Experimentelle Gesteinmetamorphose: Geochimica et Cosmochimica Acta, v. 24, p. 48-69, 250-259.

Wones, D.R., 1974, Igneous petrology of some plutons in the northern part of the Penobscot Bay area; in Osberg, P.H., ed., Geology of east-central and north-central Maine: 66th N.E.I.G.C. Guidebook, University of Maine, Orono, p. 99-125.

Wones, D.R., 1976, Granitic intrusives of the Penobscot Bay region, Maine, and their structural setting; in Pajari, G.E., Jr., ed., Field guide to the geology and plutonic rocks of southwestern New Brunswick and the Penobscot Bay area of Maine: I.G.C.P. Canadian Plutonics Study Group, Project Caledonian Orogen, v. 1, p. 39-69.

Wones, D.R., 1978, Norumbega fault zone, Maine: U.S. Geological Survey Summary of Technical Report VIII; National Earthquake Hazards Reduction Program, p. 108-111.

Wones, D.R., 1980, Contributions of crystallography, mineralogy, and petrology to the geology of the Lucerne pluton, Hancock County, Maine: American Mineralogist, v. 65, p. 411-437.

Wones, D.R., and Stewart, D.B., 1976, Middle Paleozoic regional right-lateral strike-slip faults in central coastal Maine (abs.): Geological Society of America, Abstracts with Programs, v 8, p. 304.

Zartman, R.E., and Gallego, M.D., 1979, USGS(D)-BUB-8 (Sample 139), USGS(D)-BUB-9 (Sample 140), USGS(D)-BUB-10 (Sample 141), and USGS(D)-ORA-301 (Sample 142); in Marvin, R.F., and Dobson, S.W., eds., Radiometric ages: Compilation B, U.S. Geological Survey: Isochron West, The Bulletin of Isotopic Geochronology, no. 26, p. 18-19.

Zen, E., 1983, Exotic terranes in the New England Appalachians-limits, candidates, and ages: A speculative essay: Geological Society of America Memoir, no. 158, p. 55-81.

Zietz, I., Haworth, R.T., Williams, H., and Daniels, D.L., compilers, 1980, Magnetic anomaly map of the Appalachian Orogen: contribuition no. 15, I.G.C.P., Project no. 27, Appalachian-Caledonides Orogen, scale 1:1,000,000.

APPENDIX: STRATIGRAPHY OF PASSAGASSAWAKEAG AND BUCKSPORT TERRANE BOUNDARY ZONE

Copeland Formation

The Copeland Formation (Trefethen, 1950; Wing, 1957) is composed of interlayered beds of bluish-gray pelitic schist and quartzite. The type locality is at Copeland Hill in the northwest portion of the study area (Plate 1). The Copeland Formation crops out in an arcuate, belt-like pattern which extends from the Norumbega Fault Zone in the northwest to the southwest corner of the study area where it pinches out. The width of the belt ranges from 3.5 km in the north to 2.5 km in the south. The original thickness of the Copeland Formation is unknown because its contacts are poorly constrained and multiple folding events have deformed it.

The Copeland Formation has been correlated on the basis of similar lithologies (Wones, 1976; Loiselle and Wones, 1983) with the Hogback Formation (Perkins and Smith, 1925) and Appleton Ridge Formation (Bickel, 1976) in the Belfast area (area immediately southwest of the Mount Waldo pluton, Fig. 1b) and with the Cape Elizabeth Formation of the the Casco Bay Group (Katz, 1917; Hussey, 1968, 1985) in the Sheepscot Bay area (Fig. 1b) (Table 1). The Appleton Ridge Formation has been assigned a 455 ± 25 Ma age from Rb/Sr whole-rock isochron data (Brookins, 1976). The Cape Elizabeth Formation has been assigned a 485 ± 30 Ma age from Rb/Sr whole rock isochron data (Brookins and Hussey, 1978), and stratigraphic relationships suggest that it is Late Precambrian to Ordovician in age (Hussey, 1968, 1985). These lithologic correlations are rather tenuous and the assignment of a Cambrian to Ordovician age to the Copeland Formation is tentative.

Pelites of the Copeland Formation are predominantly composed of medium-grained biotite, muscovite, and quartz. Accessory staurolite, andalusite, and sillimanite may also occur near stocks of Stricklen Ridge granite. Quartzites contain minor amounts of biotite and muscovite. Minor plagioclase (An_{21-28}), tourmaline, apatite, ilmenite, and garnet occur in both pelites and quartzites.

The pelites and quartzites are interlayered on a scale ranging from a few centimeters to tens of meters (Fig. 3a). Compositional grading of the layers from quartzite to pelite on individual outcrops (Fig. 3a) and across the unit as a whole is interpreted as bedding. Quartzites are predominant on Deer Hill and the southeast margin of Blood Mountain (Plate 1) where they comprise 75-90% of the outcrop. Farther to the west, such as on Orcutt Mountain and the northwest margin of Blood Mountain, pelites comprise approximately 75% of the outcrop.

Veins, lenses, and centimeter-scale boudins of quartz that parallel bedding and foliation are prevalent in the pelites. Quartz and quartz + feldspar veins are especially common within ~0.5 km of the contact with the Rider Bluff member and Bucksport Formation. Green amphibolite layers concordant to the pelite and quartzite layering are typically 10 to 20 cm thick but cannot be traced along strike for more than a few meters. The lensoid character of the amphibolite layers suggests that they are boudins of originally more continuous mafic layers.

The contact between the Copeland and the Passagassawakeag Formations is not exposed in the study area. It is not known whether the contact is conformable, unconformable (Stewart and Wones, 1974), or tectonic. The relative structural position between the two units is also unknown.

Rider Bluff member

The Rider Bluff member (informal useage by Stewart and Wones, 1974; Wones, 1976) of the Copeland Formation is a green, finely-laminated (millimeter-scale) pelitic siltstone. The type locality is on Rider Bluff in the northern portion of the study area

(Plate 1). The Rider Bluff member crops out as a sinuous, discontinuous belt along the eastern margin of the Copeland Formation. The width of the outcrop ranges from 2.0 km at Rider Bluff to 0.2-0.8 km further to the south. It is not known if this range in outcrop width is related to changes in bedding orientation, unit thickness, and/or deformation. The original thickness of the Rider Bluff member is unknown because its contacts are poorly constrained and because multiple folding events have deformed it.

In thin section, the Rider Bluff member is predominantly composed of chlorite, quartz, and plagioclase. The laminations are defined by alternating chlorite- and quartz-rich laminations. Minor epidote, muscovite, magnetite, garnet, tourmaline, and pyrite may also occur. Biotite, garnet, and albite occur as abundant porphyroblasts 1-3 mm across.

Bedding in the Rider Bluff member is difficult to recognize but may be represented by magnetite- or garnet-rich layers. Magnetite-rich layers contain 1-5% euhedral, 1-2 mm diameter magnetite octahedra. One anomalous outcrop on the southern tip of Long Lake (Plate 1) contains 25% magnetite. Garnet-rich layers contain 5-10% euhedral, 3-5 mm diameter, amber-colored garnets. The magnetite- and garnet-rich layers generally parallel the fine laminations, and contacts between these layers and the surrounding schist are diffuse. Ubiquitous quartz lenses and boudins are parallel to and folded with the laminations and comprise approximately 5% of any outcrop.

The presence of magnetite- and/or garnet-rich layers and biotite and albite porphyroblasts in the Rider Bluff distinguishes it from the Copeland and Bucksport Formations. In the absence of these layers, Rider Bluff is distinguished from the Bucksport Formation by the presence of abundant quartz lenses and boudins and the absence of carbonate, and is distinguished from the Copeland Formation by the presence of millimeter-scale laminations and the absence of interlayered pelitic schist and quartzite.

Magnetic anomaly maps of the area show a magnetic high of 300-500 nanoteslas. This anomaly displays a map pattern that generally coincides with the outcrop pattern of the Rider Bluff member (Zietz and others, 1980; Stewart and others, 1986). Magnetic anomalies over the Rider Bluff member in the northern portion of the study area (e.g. Rider Bluff, Plate 1) are as high as 700 nanoteslas. These anomalies are probably the result of the magnetite present in the Rider Bluff member.

The Rider Bluff member is assigned to the Copeland Formation (Wones, unpublished data) because it is lithologically more similar to the Copeland Formation than to any other unit. Kaszuba and Wones (1985) interpreted the Rider Bluff member as ductilely deformed Copeland Formation. Subsequent work revealed that the two units are lithologically distinct where undeformed, but that ductilely deformed Rider Bluff member is almost indistinguishable from deformed Copeland Formation. No fossils have been found in the Rider Bluff member, and no radiometric dating has been attempted. The contact between the Rider Bluff member and the Copeland Formation to the west and the Bucksport Formation to the east is not exposed.

Stricklen Ridge granite

The area on Fig. 2 and Plate 1 showing the extent of Stricklen Ridge granite (informal useage by Wones, 1974, 1976; Stewart and Wones, 1974) outlines the occurrence of a two-mica, garnet-bearing leucogranite that intruded the Copeland and Formation and Rider Bluff member as dikes, sills, and very small stocks. The regional stratigraphy is traceable through the granite terrane. Overall the granite comprises less than one-eighth of the total map area outlined as Stricklen Ridge granite. Within the Copeland Formation, two areas of 1-2 km^2 extent have been delineated where Stricklen Ridge granite comprises greater than 50% of the exposure (Fig. 2; Plate 1; Table 10). Within these stocks there are only a few places where granite comprises greater than 90% of the

Table 10. Estimated modal percentage by area of different rock types exposed in a representative outcrop mapped as a Stricklen Ridge granite stock. Outcrop is located at UTM grid coordinate 4943.0N, 521.55E on Plate 1 and at #SR-52 on Fig. 21. Mode was determined by a 1 m grid spacing of a horizontal pavement approximately 200 m² in area. First data column includes the percentage of outcrop not exposed, the second column excludes this area from the totals. Modal analyses (volume percent) of the three granite varieties are listed in Table 11.

coarse-grained granite	54.5%	71.0%
fine-grained granite	2.5%	3.0%
tonalite	3.5%	4.5%
Copeland Formation	16.5%	21.5%
not exposed	23.0%	—
total	100.0%	100.0%

exposure. The granite was named by Wones (unpublished data) for exposures of one of these stocks on Stricklen Ridge (Plate 1). A third stock-like body, < 0.5 km^2 in extent, occurs in the Passagassawakeag Formation (Stewart and Wones, 1974). Dikes of Stricklen Ridge granite have been assigned a 412 ± 14 Ma age based on concordant U-Pb data from zircons (Zartman and Gallego, 1979).

The Stricklen Ridge granite is a compositionally restricted (Pitcher, 1979) monzogranite in the IUGS classification system (Streckeisen, 1973) (Fig. 22). Biotite-rich tonalite (Fig. 22; Table 11) dikes locally occur in small amounts (Table 10) in Stricklen Ridge granite outcrops. These tonalite dikes cut Stricklen Ridge granite and are intruded by pegmatite. No tonalite is reported in the Penobscot Bay area. The Winterport granite (Trefethen, 1944) occurs just north of the Mount Waldo pluton (Fig. 1b) (Wones, unpublished data) and displays the same field relationships as the tonalite, but it is described as a mafic-rich granodiorite (Stewart and Wones, 1974; Wones, 1976).

Feldspars and quartz range in size up to ~5 mm in diameter (i.e. seriate texture, Wones, 1980). The crystallization sequence, as interpreted from crystallinity, inclusion relationships, and grain to grain contacts, is uniform throughout the granite terrane (Fig 23). Despite its compositional restriction, the granite displays variations in kinds and abundance of accessory minerals (Fig. 22; Table 11) and texture (Fig. 24a). Aplites, tourmaline-bearing pegmatites, and miarolitic cavaties are abundant, suggesting vapor saturation of the melt (Jahns and Tuttle, 1963; Jahns and Burnham, 1969; Krauskopf, 1979).

K-feldspar is usually subhedral to anhedral, perthitic microcline (Or_{90-95}, Ab_{5-10}), but sometimes it is found to occur as orthoclase. K-feldspar porphyroclasts in mylonites developed in Stricklen Ridge granites sometimes occur as asymmetric cores of perthitic orthoclase mantled by optically continuous microcline (Fig. 24b). Zoned K-feldspars

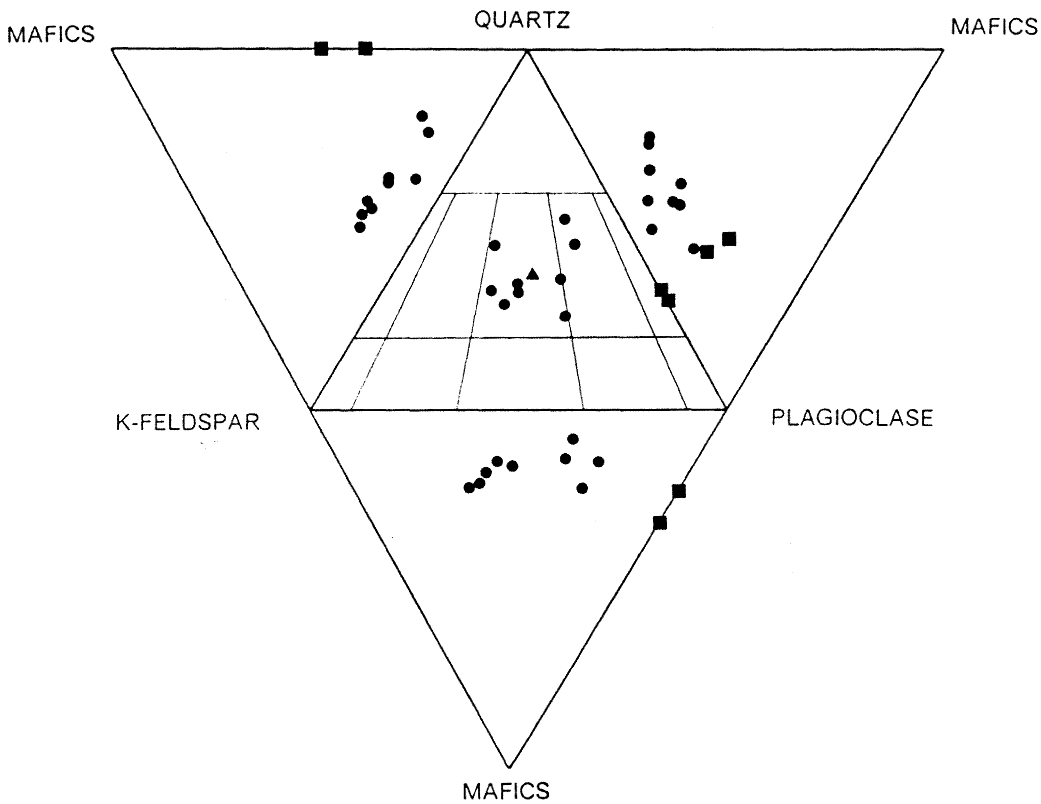

Figure 22. Modal analyses of Stricklen Ridge granite. Solid circle, granite; solid square, tonalite; solid triangle, sample of Carl and others (1984) used in normative analysis plotted in Fig. 20.

Table 11. Modal data (by volume) of representative samples of Stricklen Ridge granite. Minimum 1000 points counted per thin section. Chlorite, hematite, ilmenite, and epidote are secondary minerals associated with the recrystallization of biotite. Secondary muscovite associated with the recrystallization of muscovite and plagioclase. Abbreviations: tr, trace amounts (less than detected by point count grid); np, not present. Sample locations plotted in Fig. 21.

	1	2	3	4	5	6	7
Quartz	40.3	40.6	24.4	42.2	34.0	28.9	26.1
K-feldspar	29.1	30.1	np	13.9	21.7	34.9	35.5
Plagioclase	18.6	16.8	52.4	35.8	39.2	24.0	27.9
Biotite	1.5	0.3	21.4	np	0.2	1.8	5.5
Muscovite	9.2	9.5	np	7.2	2.6	5.7	0.7
Garnet	np	np	np	np	0.8	4.2	np
Apatite	tr	0.3	0.3	tr	tr	tr	0.4
Chlorite	1.1	1.5	0.5	np	0.6	0.5	2.0
Hematite & Ilmenite	0.2	tr	0.1	np	tr	tr	0.1
Epidote	np	np	np	np	np	np	0.1
Secondary Muscovite	tr	0.9	0.9	0.9	0.8	tr	1.6
Total	100.0	100.0	100.0	100.0	99.9	100.0	99.9

1. Coarse-grained granite of Table I-1, #SR-52D.
2. Fine-grained granite of Table I-1, #SR-52G.
3. Tonalite of Table I-1, #SR-52C.
4, 5, 6. Granite near stock on Stricklen Ridge (UTM grid no. 4949.2N, 523.3E, Plate 1), #SR-9C, 9D, and 9E (respectively).
7. Granite near shear zone (UTM grid no. 4946.1N, 523.6E, Plate 1), #SR-2G.

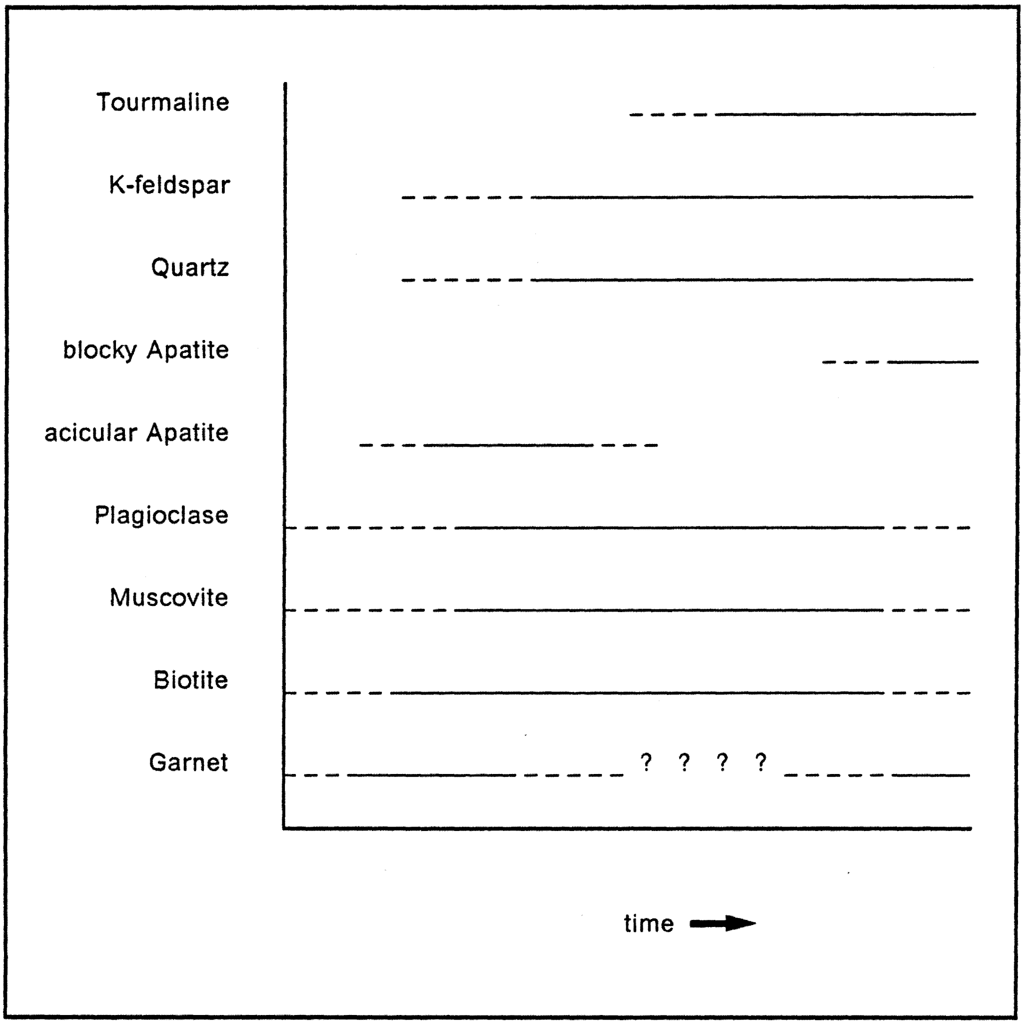

Fig. 23. Inferred crystallization sequence in Stricklen Ridge granites.

Figure 24. Textures of Stricklen Ridge granite. a. slab of Stricklen Ridge granite displaying textural variation. b. K-feldspar porphyroclast in Stricklen Ridge granite mylonite. Core of orthoclase (O) is mantled microcline (M). Crossed nikols. Scale bar = 100 μm. c. plagioclase inclusions (arrowheads) in perthite (P). Crossed nikols. Scale bar = 1.0 mm.

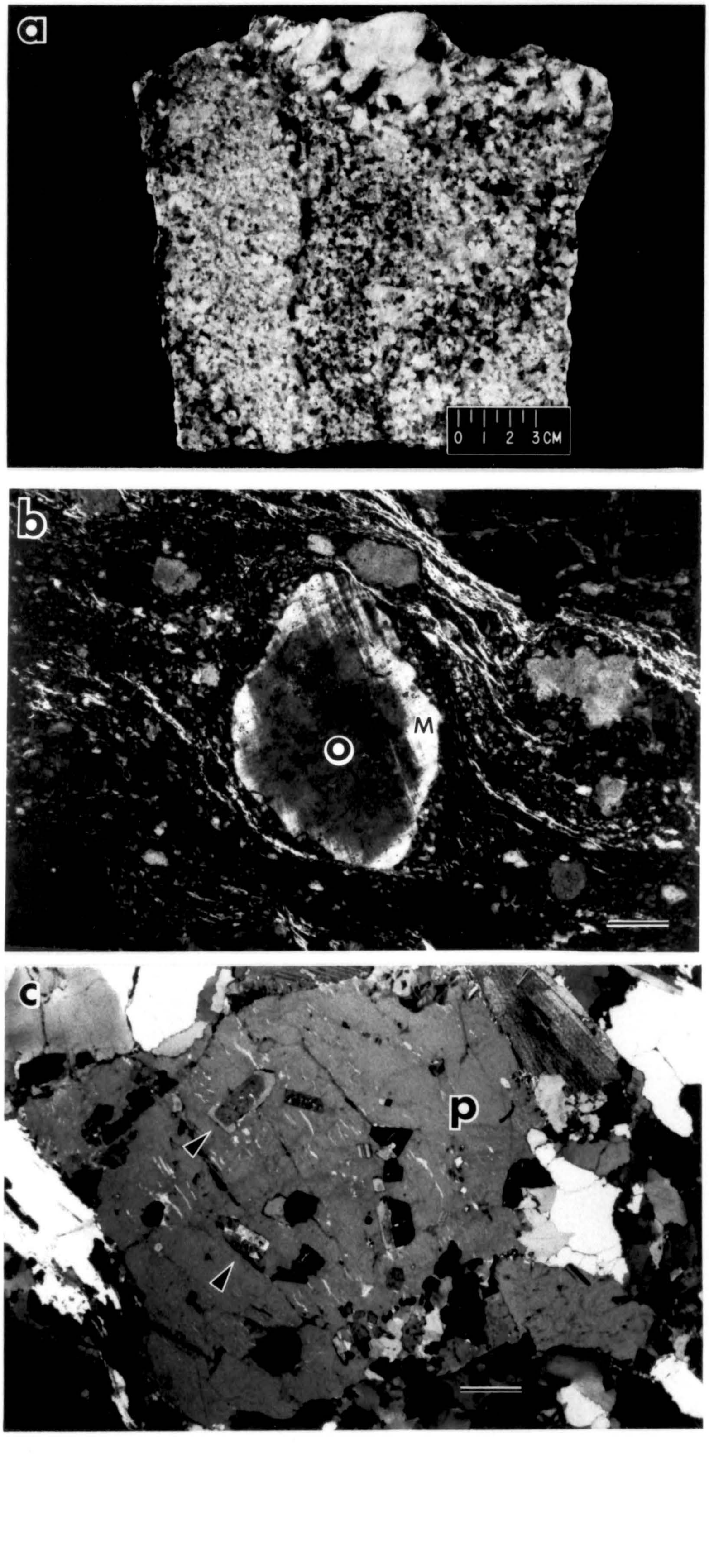
a
0 1 2 3CM
b
o
M
c
p

are not observed in undeformed granites, suggesting that the zoning is related to processes occurring during ductile deformation of the granites.

Plagioclase is subhedral and uniform in composition (An_{10-17}). Compositional zoning in plagioclase is prevalent, but no systematic zoning pattern is observed. K-feldspar sometimes surrounds and replaces plagioclase as anhedral grains. This replacement may be related to fluid/rock interaction during late-stage crystallization of the granite of to one of the post-granite deformational episodes. Plagioclase also occurs as 0.1-0.25 mm diameter, altered (sericite), subhedral inclusions in perthite (Fig. 24c). These inclusions are mantled by 10-50 μm thick rinds of unaltered feldspar (Fig 24c). Microprobe analyses of plagioclase inclusions in one perthite crystal (Or_{90-92}, Ab_{10-8}) shows that the inclusions are zoned (not systematically) and range in composition from 90% to 99% albite while the clear rims are 99% albite. Optical measurements on other plagioclase inclusions are consistent with these data. The plagioclase inclusions may represent early-crystallized magmatic plagioclase armored by and included within perthite, xenocrysts incorporated into the melt during movement or emplacement, or restite (White and Chappell, 1977) preserved from melting in the source region. However, inclusions representing early-crystallized magmatic plagioclase should be richer in anorthite component than non-included plagioclase.

Gravity data collected from the Penobscot Bay area (Kane and Bromery, 1966; Sweeney, 1974, 1976) indicates a north-south-trending, elongate anomaly trough over the study area. Two- and three-dimensional models of this data (Sweeney, 1974, 1976) suggest that the anomaly represents Stricklen Ridge granite as a discrete body at depth. Two-dimensional models (Sweeney, 1974, 1976) suggest that the southern portion of the body is equant in shape with vertical sides. Its dimensions range from 3.5 km wide and 3.0 km thick to 2.0 km wide and 3.5 km thick depending on the backround densities chosen. To the north, the body becomes triangle-shaped with a maximum thickness of 1.5 km and a western contact that dips steeply inward (east). Three-dimensional models

(Sweeney, 1974, 1976) suggest that the Stricklen Ridge granite is a north-south-trending body ~3.0 km thick, 1.5 to 3.0 km wide, and more than 11 km long with a total volume of approximately 100 km^3. Contacts on the east side are subvertical while those on the west side dip inward (east) towards the body.

In Sweeney's (1974, 1976) gravity models, a difference of approximately 0.01 g/cm^3 between granite and backround densities results in a thickness change of approximately 1 km for the subsurface granite bodies, but the models depend on density data from only two samples (Sweeney, 1976, p. 245). While the exact dimensions depicted in Sweeney's (1976) models may be debatable, the data strongly suggest that the Stricklen Ridge granite occurs as a discrete body just below the surface of the study area. The abundance of aplites, tourmaline-bearing pegmatites, and miarolitic cavaties; the variation in texture; and the occurrence of sills, dikes, and very small stocks rather than one homogeneous expanse of granite in the study area are consistent with it being the roof zone of a granitic pluton.

Bucksport Formation

The Bucksport Formation (Trefethen, 1950; Wing, 1957) is a greenschist facies calcareous siltstone. The unit is named for exposures located in the Silver Lake area outside of the study area (~4 km southwest of the study area and ~4 km north of the town of Bucksport). It crops out in the study area as an irregularly-shaped belt (0.6-3.5 km wide) east of the Rider Bluff member and west of the Lucerne pluton (Plate 1) and directly adjacent to the Copeland Formation in the southwest portion of the study area. The original thickness of the unit in the study area is unknown because it is not well exposed and its contacts are poorly constrained.

The siltstones of the Bucksport Formation contain finely-laminated (1-2 mm thick) carbonate-bearing beds (0.5 to several meters thick). The laminations are defined by the alternation of quartz- and mica-rich siltstone containing fine- to very fine-grained quartz, white mica, chlorite, calcite, ilmenite, and plagioclase. Accessory biotite, calcic amphibole, tourmaline, titanite, and epidote may also occur. Interlayered with the calcareous siltstones (which comprise approximately 95% of any outcrop) are sulfide-bearing pelitic siltstone beds (several centimeters to 0.5 m thick) which weather to a rusty color. The pelites are compositionally and texturally similar to the calcite-bearing beds but are coarser-grained, contain less quartz and more phyllosilicate, and contain no sphene or amphibole and little or no carbonate.

In the northern portion of the study area, quartz veins commonly occur as lenses and boudins parallel to the laminations, although cross-cutting veins do occur. Occasional composite quartz + calcite veins also occur. The quartz veins are far less common in the southern portion of the study area. This distribution of quartz veins within the Bucksport Formation may be related to proximity to the Norumbega Fault Zone.

The Bucksport Formation is lithologically similar to the Silurian Vassalboro Formation and has been correlated with it (Stewart and Wones, 1974; Wones, 1976, 1980; Osberg, 1980; Loiselle and Wones, 1983; Gates and others, 1984; Hussey, 1984) (Table 1). No fossils are found within the Bucksport Formation, and nowhere can it be traced directly into the Vassalboro Formation. Age correlations are based strictly on lithologic similarities across the Norumbega Fault Zone. The Late Silurian to Early Devonian Flume Ridge Formation (Ruitenberg, 1967; Ruitenberg and Ludman, 1978), part of the Fredericton Trough, has also been correlated with the Bucksport Formation based on lithologic similarities (Wones, 1980; Ludman, 1981) (Fig. 1; Table 1). The Bucksport Formation as mapped by Bickel (1976) in the Belfast area (immediately southwest of the Mount Waldo pluton, Fig. 1) was distinguished by Wones (unpublished data) as a different unit from Bucksport Formation as defined by Wing (1957) in the type locality north of the town of Bucksport.

Mafic rock

One outcrop of a fine-grained, porphyritic mafic rock occurs in the study area (roadcut at UTM grid coordinate 4941.75N, 522.0E, see Plate 1). No contacts are exposed between it and the country rock, and it is massive except for brittle fractures and faults.

In thin section, the rock is composed of 60% euhedral bytownite and 40% anhedral, interstitial orthopyroxene which displays a subophitic texture. The rock is a norite in the IUGS classification system (Streckeisen, 1973). Bytownite occurs as 0.5-2.5 mm long laths (aspect ratio ~4:1) that are randomly oriented. Larger laths display normal, continuous zoning from ~An_{90} cores to An_{80} rims. Fibrous green amphibole, brown biotite, and magnetite occur as alteration products of orthopyroxene and what is interpreted to be matrix. Matrix is completely altered, but orthopyroxene is relatively pristine.

The porphyritic texture, composition, and lack of metamorphism and ductile deformation suggest the norite intruded the country rock as a dike or sill after ductile deformation. Mesozoic mafic dike swarms are common in the Sheepscot Bay area (Fig. 1b) (Hussey, 1985), and this rock probably represents one such dike.

The vita has been removed from the scanned document

EXPLANATION

Metasedimentary Rocks

DSb — Bucksport Formation (Trefethen, 1950; Wing, 1957). Silurian (?) to Devonian (?). Grey- to green-weathering calcareous siltstone. Intercalated beds of sulfidic pelite common.

OЄc, OЄcr — Copeland Formation (Trefethen, 1950; Wing, 1957). Precambrian (?) to Ordovician (?). OCc, grey-weathering, interlayered pelite and quartzite. OCcr, Rider Bluff member. Thinly-laminated, pelitic, chlorite-rich siltstone. Contains garnet and magnetite in alternating layers.

pЄp — Passagassawakeag Formation (Bickel, 1976). Precambrian (?). Quartz-feldspar-biotite gneiss intercalated with biotite schist. Commonly contains sillimanite and garnet.

Plutonic Rocks

Dl — Lucerne Pluton (Wones, 1980). White-weathering, coarse-grained, seriate granite. Two feldspars, biotite-bearing. Rare aplites and quartz-tourmaline veins. Zircon Pb/Pb age of 380±4 Ma (Zartman and Gallego, 1979).

SDsr — Stricklen Ridge granite stock (Wones, unpublished data). Garnet-bearing, two-mica granite, pegmatite, and aplite that comprise 50%-90% of outcrop. Concordant U/Pb zircon age of 412±14 Ma (Zartman and Gallego, 1979).

SDsrc, SDsrr — extent of Stricklen Ridge granite. Copeland Formation (SDsrc) and Rider Bluff member (SDsrr) intruded by dikes and sills of Stricklen Ridge granite. Granite comprises <50% of outcrop.

Contacts

- known
- approximate
- very approximate
- inferred from Wones (1980)

Faults

- brittle
- ductile, dextral
- ductile, sinistral

Symbols

- 59 — strike and dip of inclined, vertical bedding
- 45, 12 — strike and dip of inclined axial surface and bearing and plunge of associated inclined hinge of small-scale F_1 fold
- 34 — strike and dip of inclined S_1 foliation
- 55, 65 — strike and dip of inclined axial surface and bearing and plunge of associated inclined hinge of small-scale F_2 fold
- 21 — bearing and plunge of inclined L_2 mineral lineation and crenulation axis
- 69 — strike and dip of inclined, vertical S_3 mylonitic foliation in metasedimentary rock
- 79 — strike and dip of inclined S_3 mylonitic foliation in plutonic rock
- 77, 76, 79 — strike and dip of inclined, vertical axial surface and bearing and plunge of associated inclined hinge of small-scale F_4 fold
- 56 — bearing and plunge of inclined L_4 mineral lineation and crenulation axis
- 66 — strike and dip of inclined brittle joint in metasedimentary rock
- 75 — strike and dip of inclined brittle joint in plutonic rock
- massive plutonic rock (no fabric observed)

mapped by: John P. Kaszuba, 1984, 1985
assisted by: Steve Ela
Joe Jurinski

Plate 1. Bedrock geologic map of a portion of the Brewer Lake 7 1/2 minute quadrangle